Universitetet i Stavanger

FACULTY OF SCIENCE AND TECHNOLOGY

MASTER'S THESIS

Study programme/specialisation: Petroleum Engineering / Well Engineering	Spring semester, 2019 Open
Author: Parham Barazesh	P.Barazesh ..... (signature of author)
Programme coordinator: Supervisor(s): Tore Flåtten	
Title of master's thesis: Numerical simulation of temperature-dependent flow dynamics in drilling operations	
Credits:30	
Keywords: Flow dynamics The Riemann problem Numerical simulation Isothermal Euler model Full Euler model MATLAB Weakly implicit mixture flux model X-Force scheme	Number of pages: 102 Stavanger, 06/15/2019

Abstract

This thesis is a description of the research and improvements on solving hyperbolic conservation laws by defining a hybrid explicit/implicit numerical scheme. Former researches have been done by (Evje and Flåtten 2005) on the weakly implicit mixture flux method (WIMF) for the isothermal two-phase flow model. The research consists of proposing a semi-implicit numerical scheme for a two-phase flow system by defining a hybrid model incorporating the advection upstream splitting method (AUSMD) to develop an implicit scheme conjugated with an upwind explicit flux. While the WIMF scheme can demonstrate precise resolution of the moving discontinuity, it is bounded by a CFL condition restricting the timestep and grid sizes for numerical simulation (Evje and Flåtten 2005).

The aim of the current research is to formulate and systematically code a numerical scheme named X-Force predictor-corrector, as a contribution to previous works of (Evje and Flåtten 2005) and (Evje, Flåtten et al. 2008). The new research has been done on a hybrid scheme consisting of pressure-based and density-based steps to traverse from Isothermal Euler model in the previous works to full Euler model by associating energy equations. The material stated in the thesis is based on unpublished work by Tore Flåtten and Trygve Wangensteen in a collaboration for TechnipFMC with respect to their FlowManager process surveillance software.

Acknowledgment

I would like to give my sincere appreciations to Tore Flåtten, my supervisor at the University of Stavanger for his great support and endeavor. He showed me the route for acquiring a thorough understanding of the current research. Despite far distance, he was available all the time and helped me with a great enthusiasm to get motivated on every single step in the research. Also, I appreciate my family for their spiritual support and my friend Hamed Sahebi for his excellent collaboration in our research tasks and sharing the knowledge.

Table of Contents

List of Tables

List of figures

1 Introduction

The work of this master thesis is dedicated to developing a numerical scheme to solve a set of hyperbolic differential equations (Full Euler equations) with a specific case of Riemann initial conditions. Concurrent studies are done by (Sahebi 2019) to solve the equations analytically and the results are compared for a more accurate understanding of the mathematical and physical perspectives. The general form for a conservation law could be written as the following formula:

$$\frac{\partial u}{\partial t} + \frac{\partial f(u)}{\partial x} = 0 \qquad (1.1)$$
$$u(x,0) = \phi(x)$$

where $u(x,t)$ is the vector of conserved quantities including density, momentum and energy, $f(u)$ indicates the flux passing the control volume of concern and $\phi(x)$ is the initial condition. In our case we have a Riemann problem in the form:

$$\phi(x) = \begin{cases} u_L \ , & x \leq 0 \\ u_R \ , & x > 0 \end{cases} \qquad (1.2)$$

The Riemann problem is a specific initial value problem for conservation equations concerning constant values at left and right boundaries with a single discontinuity in the middle. The main focus of the solution is on the discontinuity and we observe shockwaves and rarefaction waves in an infinitesimal amount of time in the domain of interest. In terms of physics, The Riemann problem could be described by the behaviour of fluids in a control volume separated by a membrane whose removal would cause shock waves or rarefaction waves to propagate. The Riemann problem is a fundamental phenomenon for understanding Euler equations since all the physical properties could be illustrated as characteristics making the Riemann problem convenient to be used in numerical simulation and CFD analysis.

According to (LeVeque 2002) and (Toro 2013), Finite Volume Methods are used to analyze and assess partial differential equations through algebraic equations. FVM form the basis of computational flow dynamics. The physics of the flow dynamics could be written in the form of partial differential equations referred to as conservation laws, ensuring that mass, momentum

and energy are conserved. A conservation law describes the change of the amount of the physical property is equal to the difference between inflow and outflow of the control volume.

1.1 Staggered and collocated schemes

Numerical schemes can be classified as staggered or collocated (non-staggered) schemes. In staggered schemes, variables such as pressure and density are calculated at the cell centers of the control volume while velocity and momentum are situated at cell interfaces. Staggered schemes have been used in flow simulators with a focus on structured grids. Despite the disadvantage of the complexity of analysis due to this notion that variables are stored in different locations in the control volume, staggered schemes provide good reasons to relinquish the discretization error leading to checkerboard pattern in the solution referred to odd-even decoupling and was used in the classical CFD. For the matter of complexity and hardship of observing variables, the collocated grid system is vastly used in flow simulators, which all the variables are stored at the same location in the control volume, however, staggered systems are more suitable with high-pressure gradient and multiphase flows. (Meier, Alves et al. 1999) (Harlow and Welch 1965). Figure 1 shows the grid structure of staggered and collocated with this note that f is the function of interest and $F_i^k = \frac{\partial^k f}{\partial x^k}$ denotes the k-th derivative approximation of f at x_i (Reis, Tasso et al. 2015).

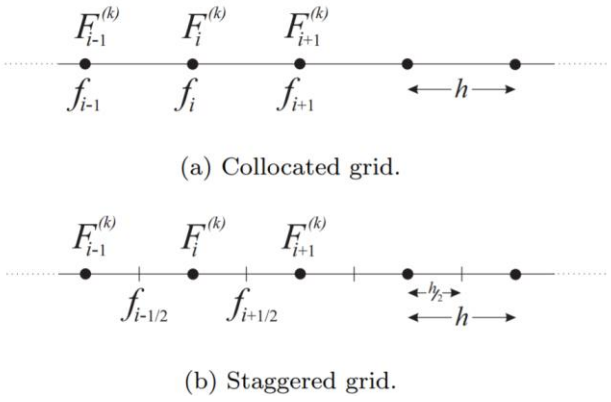

Figure 1: Staggered vs Collocated grids(Reis, Tasso et al. 2015)

1.2 Literature review and previous works

Two-phase flow model analysis has been an interesting topic in flow dynamics for several decades and various researches have been done by several authors (Wallis 1969, Ransom and Hicks 1988, Andrianov and Warnecke 2004, Zeidan, Romenski et al. 2007, Zeidan 2011).

AUSMD recognized as Advection Upwind Splitting Method was first proposed by Wada and Liou as a contribution to Van Leer and Hiinel flux splitting method. Van Leer method was used as most prosperous scheme consolidating ideal compressible flows with shocks until the mid-90s. The scheme was developed based on the Lagrangian scheme unravelling Godunov's method. (Van Leer 1979). AUSMD was developed to eliminate the effect of numerical dissipation on the contact discontinuity as it was in Van Leer model in order to achieve high resolution, considering enthalpy conservation and numerical stability in capturing strong shock waves.

Following the previous researches on two-phase flow, Evje and Flåtten, proposed Weakly Implicit Mixture Flux model (WIMF) to solve hyperbolic set of differential equations by using AUSMD on a combination of a robust implicit flux and an upwind explicit flux to a hybrid model in order to obtain high level of accuracy and stability while allowing CFL condition to be violated.

One of the most important examples of a system of hyperbolic equations is the isothermal Euler model which consists of mass and momentum conservation equations given by:

$$\frac{\partial \rho}{\partial t} + \frac{\partial m}{\partial x} = 0 \tag{1.3}$$

$$\frac{\partial m}{\partial t} + \frac{\partial \left(\frac{m^2}{\rho} + p(\rho) \right)}{\partial x} = 0 \tag{1.4}$$

where ρ, m and $p(\rho)$ represent density, momentum and pressure, respectively

Splitting the convective flux into its wave decomposition could be considered as a possible method to deal with the large discrepancy between wave velocities by solving the fast waves and slow waves through implicit and explicit schemes respectively. A flux hybridization technique is used to integrate upwind resolution in a central pressure-based numerical scheme. This will lead to a precise resolution in slow waves without getting interrupted by stability issues connected to fast waves to achieve higher efficiency, accuracy and robustness compared to fully explicit and implicit approaches. The hybrid scheme described could be naturally derived through approximate Riemann solvers (Evje, Flåtten et al. 2006).

Above all else, their model was designed to solve the isothermal two-fluid model and the need to solve the energy conservation law is still unaddressed. This is the aim of the current master thesis.

1.3 Motivation

Deliberating the concept of staggered and collocated schemes, the motivation for the thesis is to create a link between these two types of schemes based on the work done by Evje and Flåtten. Also, we consider the effect of energy conservation law in the Full Euler model. Within staggered and collocated schemes, we can also separate between pressure-based and density-based schemes. In the density-based numerical scheme, we perform the calculation for density as a conserved property, while in a pressure-based scheme, we solve the equations for pressure and thermodynamic variables leading to a non-conservative method. Traditionally the advantage of using pressure-based schemes is that we ensure a good level of stability, but the lack of conservation results in mass leakage as we do not move mass when calculating pressure. The numerical scheme of the thesis is a hybrid pressure-based/density-based scheme in a consistent way to get the advantages of both methods. We consider pressure-based numerical calculations in the predictor step and density-based calculations in the corrector step. In fact, the motivation is to merge both schemes to get accuracy, stability and robustness while we are adding the effect of energy conservation into the model.

1.4 Thesis structure

The contents of this master thesis are presented in 4 chapters. In chapter 1 an overview and introduction of the thesis are briefly described. The former research in solving the hyperbolic conservation laws and application of staggered and collocated schemes is discussed. The motivation of this thesis and contributions to the previous works is also mentioned.

In chapter 2 the theory behind hyperbolic conservation laws is described in steps to pave the way to understand the theory. We start with a general definition of the hyperbolic conservation laws, the CFL condition and stability requirements, characteristic lines followed by a discussion about the Riemann problem. The Finite Volume Methods are mentioned with exact and approximate Riemann solvers in the Godunov method and the Roe method. Afterwards linear hyperbolic equations are discussed with the simplest case of the Advection equation. The

analytical solution and the attempts to solve the equation numerically are discussed. Then we head towards nonlinearities and solve the inviscid Burgers equation, analytically and numerically. And eventually, the Euler system is discussed.

In chapter 3, we discuss the current research on the WIMF scheme and the unpublished work on an X-Force predictor-corrector scheme to solve the full Euler model. The formulation process and the derived calculations are also discussed.

In chapter 4 the result of the WIMF scheme with the new contributions is discussed. Two different validations are used to verify the formulated numerical scheme. First, we have verified the results with research done by (Sahebi 2019) on a concurrent master thesis and secondly, we have validated the solution with Toro's five test problem (Toro 2013). The conclusions and future prospects to develop the current research are also mentioned.

2 Theory of hyperbolic conservation laws

In the theory section, we discuss the calculations needed to solve the full Euler model as a system of nonlinear hyperbolic equations. Because of the complexity of the calculation, we plan to build up the way gradually by defining the hyperbolic equations and try to write the computer code to solve them with different numerical schemes and compare the results. Here we consider the advection equation as a linear hyperbolic equation, the inviscid Burgers equation as a nonlinear hyperbolic equation. Then we focus on the system of equations deliberating Isothermal Euler model and finally, we spread our work on the full Euler model.

2.1 Hyperbolic conservation laws

Conservations laws are physical laws stating that a quantity such as mass, momentum, energy, electric charge, etc. is conserved. Conservation laws deal with the mathematical equation of the following form formulating variation of conserved quantities over time.

$$\frac{\partial}{\partial t}u + \nabla f = 0 \tag{2.1}$$

where f denotes the function of the flux indicating the amount of the conserved quantity passing any surface in the vector field at a specific time.

And from calculus we note that the divergence of the flux function would be:

$$\nabla f = \frac{\partial f_1}{\partial x_1} + \frac{\partial f_2}{\partial x_2} + \frac{\partial f_3}{\partial x_3} \tag{2.2}$$

By considering a fixed region $\Omega \in R^3$ total mass accumulated in Ω will be:

$$\int_{\Omega} u(x,t)dv \tag{2.3}$$

Utilizing conservation laws and divergence theories we can write the integral form of the equation as follows:

$$\frac{d}{dt}\int_{\Omega} u(x,t)dv = \int_{\Omega}\frac{\partial}{\partial t}u(x,t)dv = -\int \nabla f\, dv = -\int_{\Sigma} f n d\Sigma \tag{2.4}$$

With Σ as the boundary of our region Ω and $f.n$ shows the inner vector product of f with the unit normal to the surface Σ. The above equation shows no mass is created or destroyed and mass variation inside the control volume is only dependent on mass flow in or out. (Meyers 2011)

The Conservation laws equation could be written as a quasilinear form for one-dimensional flow as equation (1.1) which could be rewritten as:

$$u_t + A(u)u_x = 0 \tag{2.5}$$

where

$$A(u) = \frac{\partial f(u)}{\partial u} \tag{2.6}$$

is known as the Jacobian matrix of the system. If the Jacobian matrix $A(u)$ has n real, distinct eigenvalues $\lambda_1(u) < \lambda_2(u) < \cdots < \lambda_n(u)$, the system of conservation laws is called hyperbolic.

2.2 The CFL condition and stability

In order to investigate how accurate is the numerical computation with regards to our flux function, we should note that the solution for any numerical simulation must converge to the true solution of the differential equation when our grid size and time steps tend to be zero. This means that while time grows the error should not grow leading to a divergence so we cannot trust the solution. To numerically study the convergence, the CFL condition is introduced and named after Courant, Friedrichs and Lewy who suggested such condition at the same time. The CFL condition should satisfy every numerical computation as a necessity of convergence. Note that being satisfied with the CFL condition does not guaranty convergence but it should be checked for every explicit discretization. If the Courant number is equal to 1 then we are barely satisfying the CFL

condition and in the case that Courant number is equal to 0.5 we satisfy the CFL condition with a margin of 50%.

Let's consider the advection equation $u_t + au_x = 0$ as a simple example and visualize it in the time-grid considering both time and space are discrete:

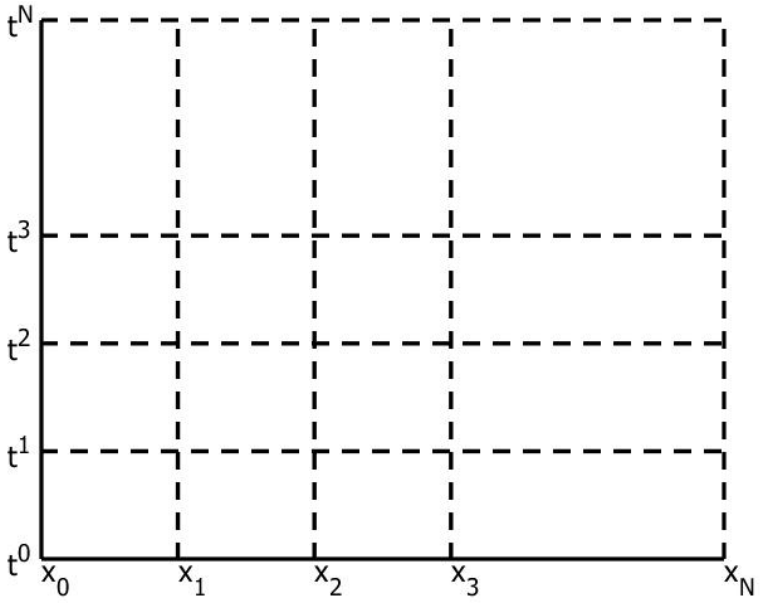

Figure 2: sketch of general grid discretization

Considering the behaviour of the solution of the transport equation we know that the solution will move towards the right or left if velocity is positive or negative respectively. Hence in the space-time plot, we have a diagonal move in the contour of the solution as shown below. Slant lines show the position of a single location on the wave such as peak or valley.

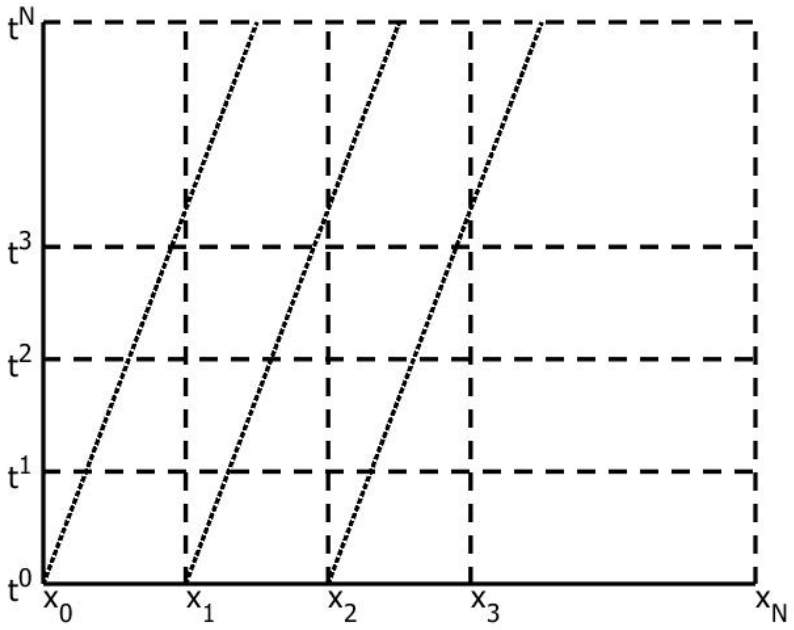

Figure 3: movement of single points on a wave

As we have mentioned we consider the advection equation for simplicity. In this case, the speed of the movement depends on a, which is mathematically the slope of the slant lines. Hence the bigger the magnitude of a the shallower the slanted lines are. Now having a look at the numerical discretization with considering upwind difference we note:

$$\frac{\partial u}{\partial x}|i \cong \frac{u_i - u_{i-1}}{\Delta x} \qquad 2.7$$

$$\frac{\partial u}{\partial t}|n \cong \frac{u^{n+1} - u^n}{\Delta t} \qquad 2.8$$

Then the discretization would result in:

$$\frac{u_i^{n+1} - u_i^n}{\Delta t} + a\frac{u_i^n - u_{i-1}^n}{\Delta x} = 0 \qquad 2.9$$

Redirecting to the contour graph we show the points illustrating the variables in the numerical discretized equation that we need to solve at each timestep. CFL condition says that we must use a small timestep so the slope of the diagonal line connecting the grid points must be shallower than the slope of wave movement. In more details, the slanted lines are not only showing the solution contour and wave movement, but it also shows the analytical domain of influence and domain of dependence of the solution in the coverage area in below. The grid point connecting lines also demonstrate the numerical domain of dependence in the area covering below.

CFL condition simply says that the numerical domain of dependence should cover the analytical domain of dependence which is also sometimes referred to as the physical or real domain of dependence, this puts a severe restriction on the size of grids and timesteps.

The slope of the numerical domain of dependence is: $\frac{\Delta t}{\Delta x}$

The slope of the physical domain of dependence is: $\frac{1}{a}$

Considering CFL condition we should have:

$$\left|\frac{\Delta t}{\Delta x}\right| \leq \left|\frac{1}{a}\right|$$

$$\Delta t \leq \frac{\Delta x}{|a|} \tag{2.10}$$

The Courant number for a linear equation is defined as:

$$CFL = \frac{\Delta t}{\Delta x}\,|a| \tag{2.11}$$

And for nonlinear equations we would have:

$$CFL = \Delta t \max\left(\frac{|a|}{\Delta x}\right) \tag{2.12}$$

2.3 Characteristic lines in conservation laws:

To analyze the behaviour of the conservation laws we can consider how the solution behaves in the smooth regions away from shockwaves and then analyze the behaviour of the shockwaves. Consider the simplest case of the scalar conservation law in equation (1.1).

Applying chain rule, we will get the primitive form as:

$$\frac{\partial u}{\partial t}+\frac{\partial f}{\partial u}\frac{\partial u}{\partial x}=0 \qquad 2.13$$

By applying a linear combination of the derivative in two different directions we have coordinate transform to F as:

$$\frac{\partial u}{\partial F}=\frac{\partial u}{\partial t}+\frac{\partial f}{\partial u}\frac{\partial u}{\partial x} \qquad 2.14$$

$$if\ \frac{\partial t}{\partial F}=1\ and\ \frac{\partial x}{\partial F}=\frac{df}{du}$$

Since $\frac{\partial t}{\partial F}=1$ we conclude that direction changes, in the same way, increasing t would result in increasing F. Also from $\frac{\partial x}{\partial F}=\frac{df}{du}$ we conclude changes in x are in the same way as F if $\frac{df}{du}>0$ and they change in the reverse direction if $\frac{df}{du}<0$. So the F would be exactly aligned with the characteristic line directions with the slope of $\frac{1}{\frac{df}{du}}=\frac{du}{df}$.

Concerning the partial differential equation we have, which is equal to 0 we conclude that u will not change along the characteristic lines so we can plot the characteristic lines as contour lines in the x-t. so basically characteristic lines are the lines that can form a total derivative showing the left and right side of the differential equation.

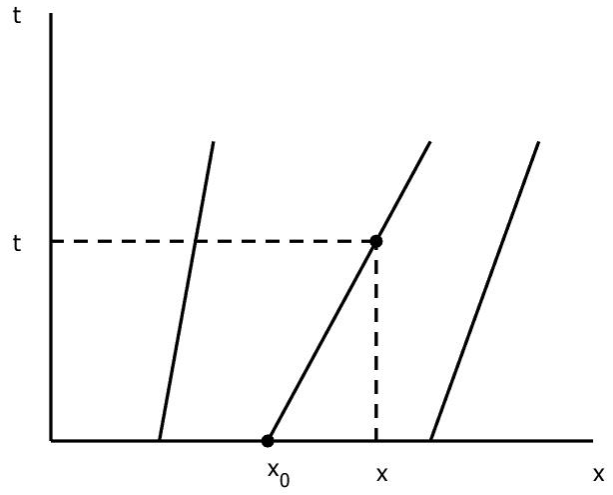

Figure 4: Typical characteristic lines for a hyperbolic conservation law (Toro 2013)

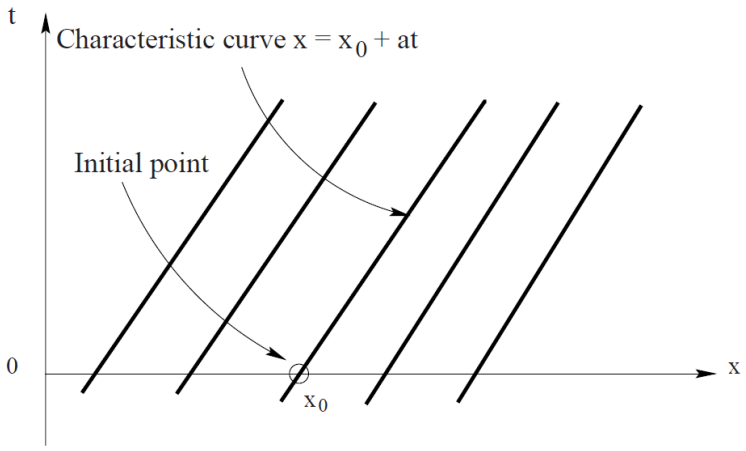

Figure 5: characteristic lines for the linear advection equation for positive wave velocity of a and initial position x_0 (Toro 2013)

2.4 The Riemann problem

Riemann problem is a specific initial condition problem conjugated with conservation laws, concerning constant values at boundaries with a single discontinuity in the middle and often solved for an infinitesimal time around the discontinuity. In multiphase flow studies, it deals with a flow of two immiscible fluids with different densities. The Riemann problem helps understand the conservation equations as we can see shock waves and rarefaction waves as characteristics. The general formulation for a Riemann initial condition is given by:

$$u_0(x) = \begin{cases} U_L & , \quad x \leq 0 \\ U_R & , \quad x > 0 \end{cases} \qquad 2.15$$

The notion which is of high interest is that Riemann problem deals with sharp discontinuities at a specific point. Therefore, numerical methods such as finite elements will not be able to represent sharp discontinuities as they use smooth fields. Riemann solvers are numerical techniques developed to handle sharp discontinuities and proposed by several scholars. Here we discuss the Godunov method and the Roe method as examples of exact and approximate Riemann solvers respectively.

2.5 Finite volume methods for conservation laws

Considering finite volume methods in one dimension, we divide the domain into finite volumes or grid cells and focus on calculating the approximation of the flux q. We update the values on each grid over timesteps.

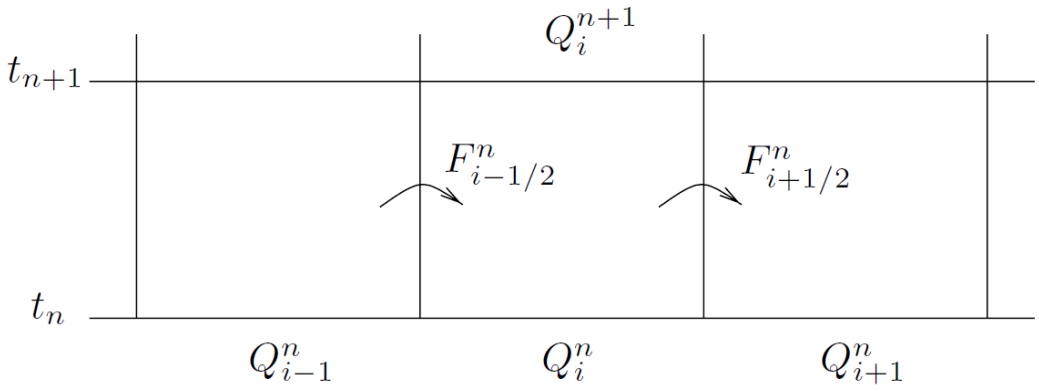

Figure 6: finite volume method illustrating cell average updates from fluxes at the cell interface (LeVeque 2002)

Illustrated by figure 6, Q_i^n indicates the approximated average value over the ith grid at timestep n and its value would be calculated as:

$$Q_i^n = \frac{1}{\Delta x} \int_{x_{i-\frac{1}{2}}}^{x_{i+\frac{1}{2}}} q(x, t_n) dx \qquad 2.16$$

where Δx represents the length interval or each cell.

We note the basic integral form of conservation laws as:

$$\frac{d}{dt}\int_{x_1}^{x_2} q(x,t)dx = F_1(t) - F_2(t) \qquad 2.17$$

where $F_1(t)$ and $F_2(t)$ show the fluxes into and out of the system

By approximating the flux q over a timestep we calculate average flux F equation as:

$$F^n_{j-\frac{1}{2}} \approx \frac{1}{\Delta t}\int_{t^n}^{t^{n+1}} f\left(q\left(x_{i-\frac{1}{2}}\right)\right)dt \qquad 2.18$$

$$F^n_{j+\frac{1}{2}} \approx \frac{1}{\Delta t}\int_{t^n}^{t^{n+1}} f\left(q\left(x_{i+\frac{1}{2}}\right)\right)dt$$

Then the approximation equation 2.16 would result in a basic numerical form of conservation equation:

$$Q_i^{n+1} = Q_i^n - \frac{\Delta t}{\Delta x}\left(F^n_{j+\frac{1}{2}} - F^n_{i-\frac{1}{2}}\right) \qquad 2.19$$

2.5.1 The Godunov method

Concerning figure 6, a general one-dimensional framework of finite volume method is illustrated. We split the line into N cells each of which having width of Δx, the center position of x_i and center walls of $x_{i\pm\frac{1}{2}}$. we investigate a set of discrete unknowns:

$$Q_i^n = \frac{1}{\Delta x}\int_{x_{i-\frac{1}{2}}}^{x_{i+\frac{1}{2}}} q(t^n,x)dx \qquad 2.20$$

where $x_{i-\frac{1}{2}} = x_{low} + \left(i-\frac{1}{2}\right)\Delta x$ and $t^n = n\Delta t$ construct set of point for the hyperbolic problem $u_t + \left(f(u)\right)_x = 0$

Integrating the hyperbolic problem over the control volume of interest in the interval of $x_{i-\frac{1}{2}}$ and $x_{i+\frac{1}{2}}$, a method of lines formulation for the spatial cell average is achieved:

$$\frac{\partial}{\partial t}Q_i(t) = -\frac{1}{\Delta x}\left(f\left(u\left(t,x_{i+\frac{1}{2}}\right)\right) - f\left(u\left(t,x_{i-\frac{1}{2}}\right)\right)\right) \qquad 2.21$$

Integrating the above formula over a time interval of t^n and t^{n+1} results in the exact update formulation:

$$Q_i^{n+1} = Q_i^n - \frac{1}{\Delta x}\int_{t^n}^{t^{n+1}} \left(f\left(u\left(t, x_{i+\frac{1}{2}}\right)\right) - f\left(u\left(t, x_{i-\frac{1}{2}}\right)\right)\right) dt \quad 2.22$$

In the Godunov method, we replace the time integrals with a forward Euler method.

$$\int_{t^n}^{t^{n+1}} \left(f\left(u\left(t, x_{i-\frac{1}{2}}\right)\right)\right) dt \cong \Delta t f^{\downarrow}(Q_{i-1}^n - Q_i^n) \quad 2.23$$

Which leads to the update formula for Q_i^n.

In the equation above $f^{\downarrow}(u_L, u_R) = f(u_L)\ if\ u_L = u_R$

The most basic form of full Godunov scheme would be in the following form:

$$Q_i^{n+1} = Q_i^n - \lambda\left(f^*_{i+\frac{1}{2}} - f^*_{i-\frac{1}{2}}\right) \quad 2.24$$

where $\lambda = \frac{\Delta t}{\Delta x}\ and\ f^*_{i-\frac{1}{2}} = f^{\downarrow}(Q_{i-1}^n, Q_i^n)$

(Годунов 1959, LeVeque 2002)

2.5.2 The Roe method

The Roe solver is an approximate Riemann solver developed based on Godunov scheme. Roe solver estimates the Godunov flux $F_{i+\frac{1}{2}}$ at U_i and U_{i+1} cell edges. Concerning equation1, Roe proposed $\tilde{A}(u_i, u_{i+1})$, a constant matrix between two cells to approximate Jacobian matrix $A(u)$ and then solve the conservation law as the following form:

$$\begin{cases} u_t + \tilde{A}u_x = 0 \\ u(x,0) = \phi(x) = \begin{cases} u_L & , \quad x \leq 0 \\ u_R & , \quad x > 0 \end{cases} \end{cases} \tag{2.25}$$

It should be noted that the following properties should be checked for Roe matrix:

- Roe matrix should be diagonalizable or non-defective, in order to ensure it has real eigenvalues, so the linear system is hyperbolic and the approximate solution of the Riemann problem has the same characteristics as the actual problem while it is possible to solve the equation using wave structure.
- Roe matrix should be consistent with the exact Jacobian.

$$\tilde{A}(u,u) = A(u) \tag{2.26}$$

- Roe matrix should satisfy conservation across discontinuities.

$$F_{i+1} - F_i = \tilde{A}(u_{i+1} - u_i) \tag{2.27}$$

2.6 The Advection equation

Transport equation which is sometimes referred to convection-diffusion equation is the simplest form of the linear hyperbolic equation which forms the basis of most of the commonly used transportation models such as transport of physical properties of an incompressible fluid flowing in the pipeline. Let's consider a wave u moving with constant velocity a in the direction from left to the right.

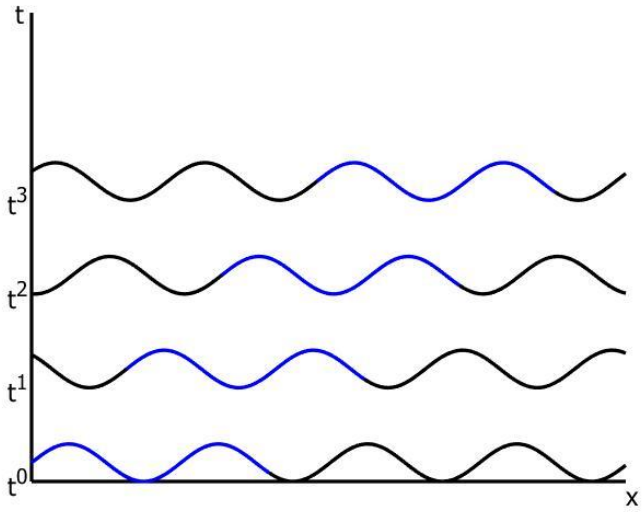

Figure 7: general solution of the linear advection equation in 2D illustrating wave movement with constant velocity

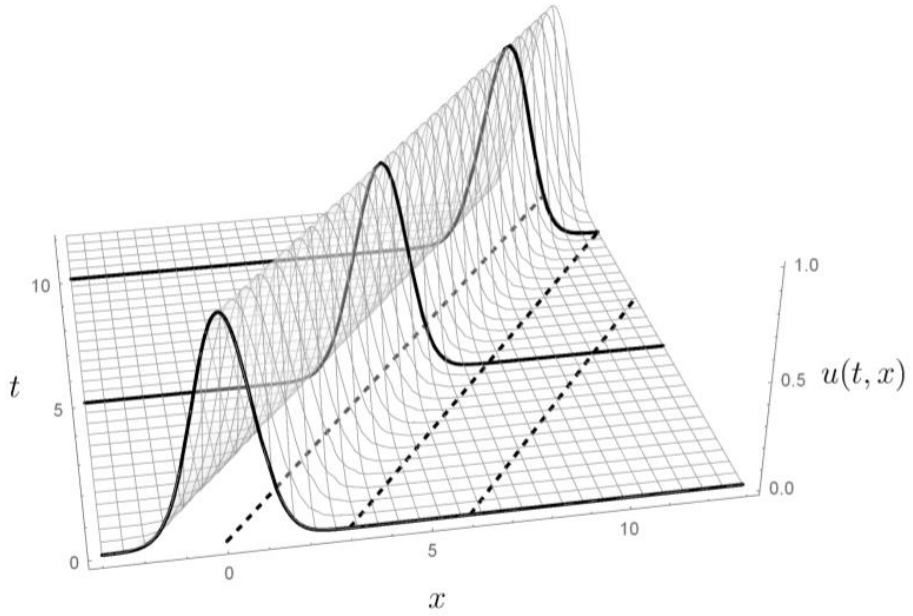

Figure 8: Solution of the linear advection equation in 3D illustrating wave movement in the x-t plane (Novozhilov)

Considering the transport of the wave it could be illustrated that shape of the wave is not changing, hence u is constant along some specific parallel lines in the x-t plane which are called characteristic lines having the following equation:

$$x = at + x_0 \qquad 2.28$$

where a is wave speed $\frac{\Delta x}{\Delta t}$, and x_0 is constant.

Deliberating consistency of wave shape along the characteristic lines, the directional derivative of u along the lines would be zero and then we can derive transport equation with a dot product as:

$$(a, 1).(u_x, u_t) = 0 \qquad 2.29$$

$$u_t + a u_x = 0 \qquad 2.30$$

What this equation says is nothing, but the entire initial condition of u would simply move along the x-axis with the velocity of a, no matter what the initial condition is. In the case we have considering the discontinuity as an initial condition, then the discontinuity will move. The solution of the linear advection equation is constant along characteristic lines and is shown in the following figure in different cases of positive (figure. A) and negative (figure. B) moving velocities. (LeVeque 2002)

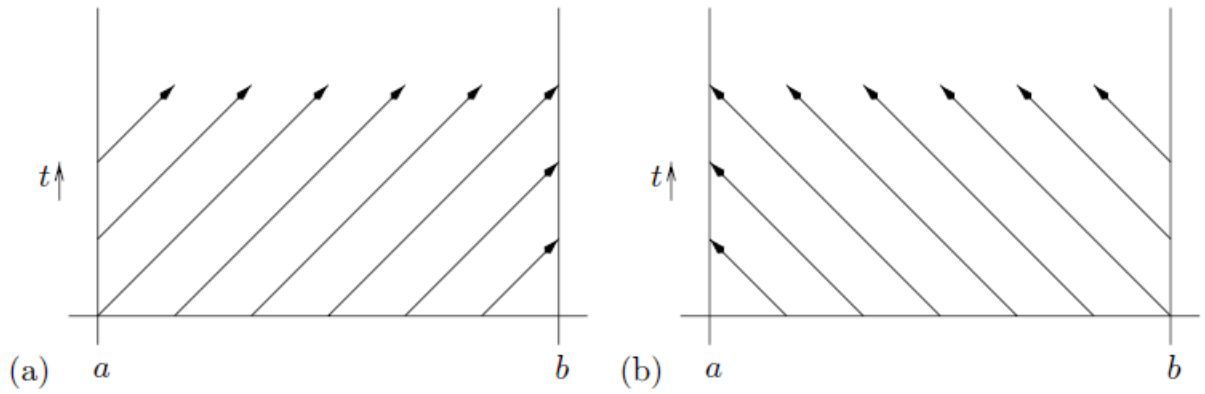

Figure 9: Characteristic lines for the linear advection equation for positive and negative wave velocity on the interval [a,b] (LeVeque 2002)

2.7 The Riemann problem for the advection equation

Consider the advection equation:

$$u_t + a u_x = 0 \tag{2.31}$$

$$u(x, t=0) = u_0(x) = \begin{cases} U_L & , \quad x \leq 0 \\ U_R & , \quad x > 0 \end{cases} \tag{2.32}$$

As we know the analytical solution for the linear advection equation is in the form of:

$$u(x,t) = u_0(x - at) = \begin{cases} U_L & , \quad x - at \leq 0 \\ U_R & , \quad x - at > 0 \end{cases} \tag{2.33}$$

Deliberating the physical behaviour of the advection equation, we know that the initial data are propagated with a velocity of a. Riemann initial condition makes the solution to take the value of U_L in the left section and U_R in the right section. Numerical discretization of the linear advection equation with Riemann initial condition with $U_L = 1 \; and \; U_R = 0$ over 11 grid cells and 10 timesteps is derived explicitly and implicitly and coded with MATLAB. the results in 2D and 3D are shown in the following sections.

2.7.1 Explicit scheme Riemann solver

The explicit Lax-Friedrichs scheme is formulated for the linear advection equation as follows with the computer code to plot the solution is 2D and 3D.

$$u(n+1, j) = \frac{1}{2}(u(n, j+1) + u(n, j-1)) - \frac{1}{2} a\gamma (u(n, j+1) - u(n, j-1)) \tag{2.34}$$

where $\gamma = \frac{\Delta x}{\Delta t}$

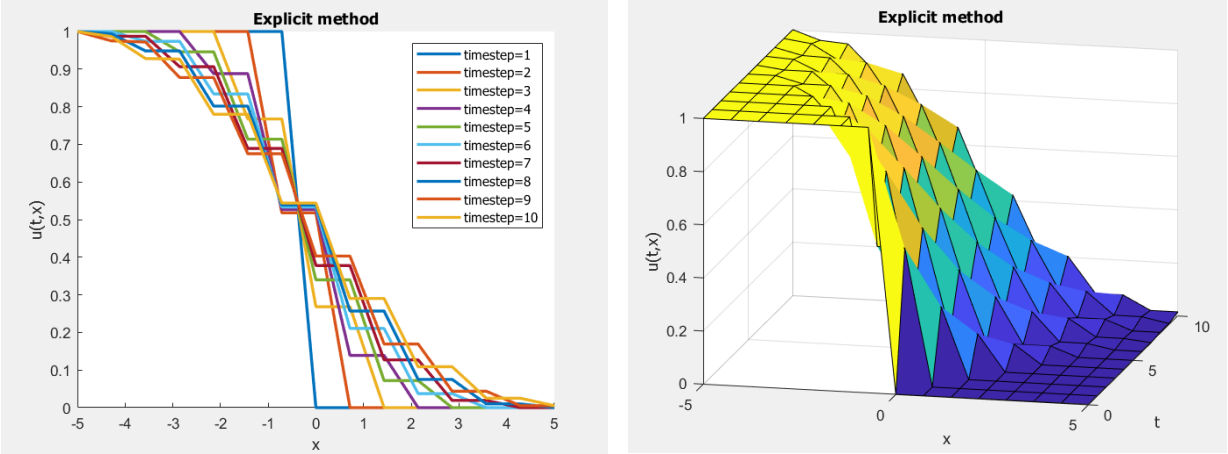

Figure 10: Solution of Riemann problem for the linear advection equation for $U_L = 1$ and $U_R = 0$ with the explicit scheme in 2D and 3D

As we have seen we have smearing out of the solution with we do the simulation with a sharp discontinuity, that is a fact of numerical diffusion. The reason for that is quite intuitive. if we solve the Riemann problem in terms of finite volume our sharp discontinuity will move along the grid cells arising over timesteps. Then we average the solution forming a new discontinuity moving and do it again and again. The finite volume averaging process will necessarily introduce numerical diffusion and smearing. It should be noted that lots of these numerical methods can be derived in many ways generating same results, but Lax-Friedrichs scheme is the most natural way of thinking about the finite difference by simply approximating the derivative and put it in the equation interpreting it as a Riemann solver.

2.7.2 Implicit scheme Riemann solver

As we discussed, when we solve the Riemann problem numerically, we cannot avoid numerical diffusion. There are many ways of thinking about that but it all boils down to the basic idea that there is no way you can discretize a set of equations without losing information about the full solution. It is naturally intuitive but if we want to have stability, we should have diffusion. In order to minimize the diffusion, the only way is to have oscillation in the scheme since we don't know where discontinuity is. Numerical scheme formulation for the linear advection equation based on the Lax-Friedrichs scheme is given by:

$$u(n+1,j) = \frac{1}{2}(u(n+1,j+1) + u(n+1,j-1)) - \frac{1}{2}a\gamma(u(n+1,j+1) - u(n+1,j-1)) \quad 2.35$$

where $\gamma = \frac{\Delta x}{\Delta t}$

To solve the implicit scheme for the linear advection equation the following matrix calculation should be done in each timestep:

$$A = \begin{pmatrix} 1-\frac{1}{2}\gamma & \frac{1}{2}\gamma & 0 & 0 & 0 & 0 & 0 & 0 & 0 & 0 & 0 \\ -\frac{1}{2}\gamma & 1 & \frac{1}{2}\gamma & 0 & 0 & 0 & 0 & 0 & 0 & 0 & 0 \\ 0 & -\frac{1}{2}\gamma & 1 & \frac{1}{2}\gamma & 0 & 0 & 0 & 0 & 0 & 0 & 0 \\ 0 & 0 & -\frac{1}{2}\gamma & 1 & \frac{1}{2}\gamma & 0 & 0 & 0 & 0 & 0 & 0 \\ \dots & \dots & \dots & \dots & \dots & \dots & \dots & \dots & \dots & \dots & \dots \\ 0 & 0 & 0 & 0 & 0 & 0 & 0 & 0 & -\frac{1}{2}\gamma & 1 & \frac{1}{2}\gamma \\ 0 & 0 & 0 & 0 & 0 & 0 & 0 & 0 & 0 & -\frac{1}{2}\gamma & 1+\frac{1}{2}\gamma \end{pmatrix} \quad 2.36$$

$$B = \begin{pmatrix} \frac{1}{2}u(n,1)+\frac{1}{2}u(n,2) \\ \frac{1}{2}u(n,1)+\frac{1}{2}u(n,3) \\ \frac{1}{2}u(n,2)+\frac{1}{2}u(n,4) \\ \frac{1}{2}u(n,3)+\frac{1}{2}u(n,5) \\ \dots \\ \frac{1}{2}u(n,N-2)+\frac{1}{2}u(n,N) \\ \frac{1}{2}u(n,N-1)+\frac{1}{2}u(n,N) \end{pmatrix} \quad 2.37$$

$$X = \begin{pmatrix} UL \\ u(n+1,2) \\ u(n+1,3) \\ u(n+1,4) \\ u(n+1,5) \\ \dots \\ u(n+1,N-1) \\ u(n+1,N) \end{pmatrix} \quad 2.38$$

$$AX = B \quad 2.39$$

The results are plotted:

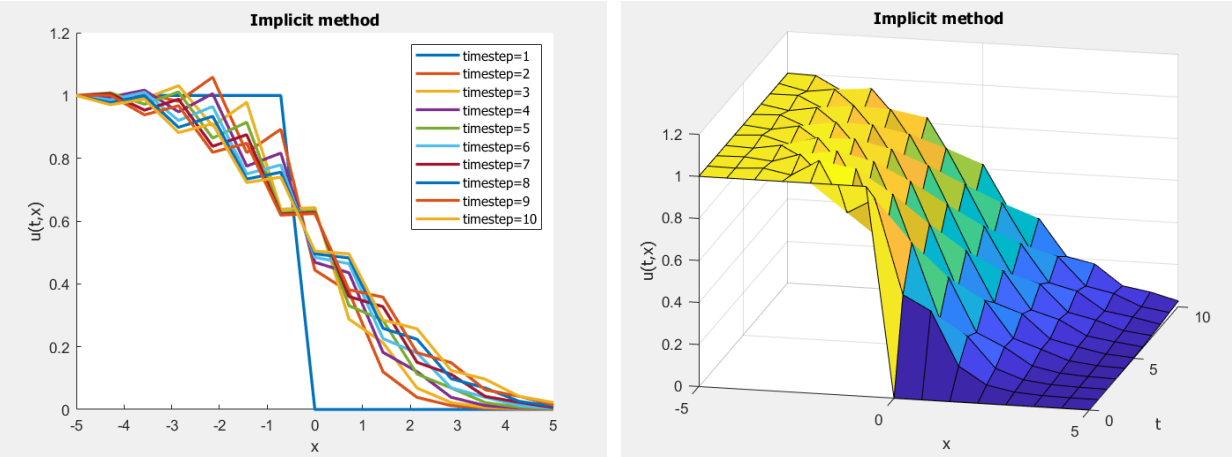

Figure 11: Solution of Riemann problem for the linear advection equation for $U_L = 1$ and $U_R = 0$ with the implicit scheme in 2D and 3D

2.8 Nonlinearities and shock formation

In the general case of nonlinear conservation laws, the Jacobian matrix A depends on the state $u(x,t)$. Then we perceive a change in solution profile in time in conclusion results in a shock formation at a finite time and new waves may be created with the loss of regularity.

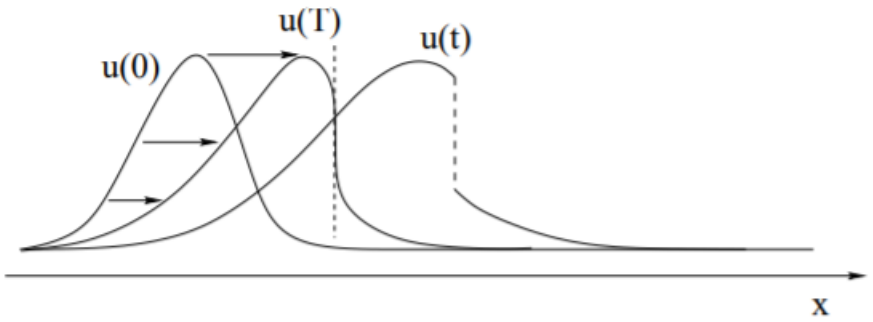

Figure 12: Solution profile for a nonlinear equation illustrating wave propagation depending on u (Bressan 2013)

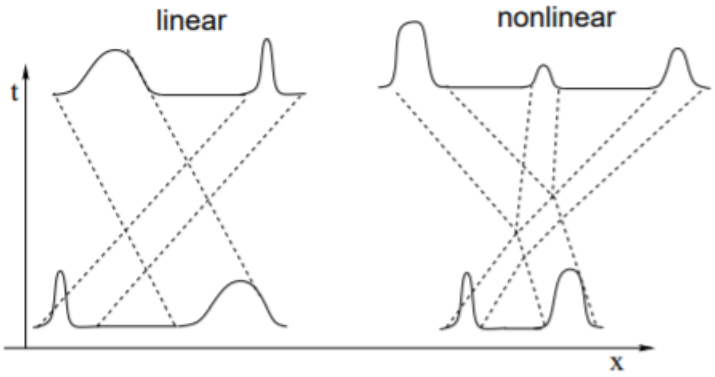

Figure 13: Solution of linear and nonlinear hyperbolic systems illustrating superposition of travelling waves in a linear equation and nontrivial interaction of waves for the nonlinear equation (Bressan 2013)

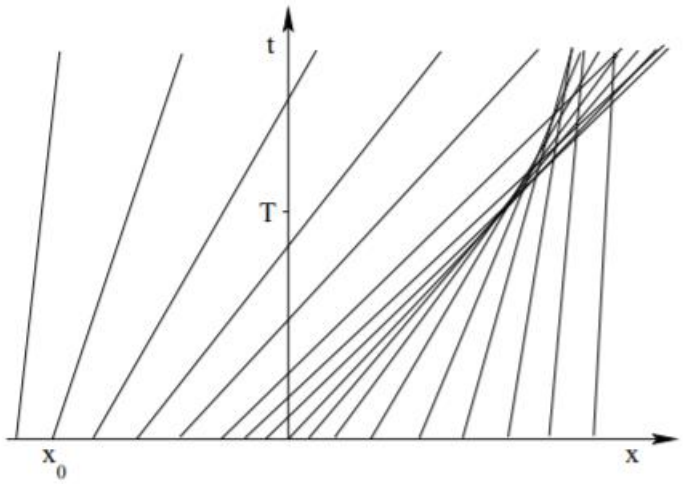

Figure 14: Shock production at specific time T (Bressan 2013)

A shockwave with regards to the mathematical definition is a compressional discontinuity in an infinitesimal amount of time conjugated with a propagating disturbance carrying energy. They are irreversible discontinuities with dramatic changes in properties such as pressure, density and temperature in a very thin layer of about $10^{-7}m$ long, which can occur in a supersonic flow field, externally (such as shockwaves expelling from fighter jets in specific air conditions) or internally in pipes and nozzles. Unlike shockwaves, rarefaction waves are conjugated with decreasing the density of the properties being expanded over time.

Concerning the shockwaves and rarefaction waves over an infinitesimal amount of time, we can consider constant values right in the boundaries of the discontinuity in a microscopic view ignoring the variation from a macroscopic prospect.

2.9 The Riemann problem for the inviscid Burgers equation

Burgers equation could be derived from equation (1.1) with a specific flux function as follows:

$$f(U) = \frac{1}{2}U^2 \tag{2.40}$$

Here we have a nonlinear hyperbolic equation since we don't have constant velocity and the flux is transported with a varying velocity as a function of U, making the discontinuity spreading in different ways based on left and right boundaries.

Being a conservation law indicates that what flows in each cell is equal to what flows out, so flow is conserved and just moves from one cell to the other. We now try to solve Burgers equation numerically using different schemes and compare the results together and develop a general combined scheme. Also, the analytical solution is stated.

2.9.1 Analytical solution

The first order quasi-linear PDE is in the following form:

$$a(x,t,u)u_x + b(x,t,u)u_y = f(x,t,u) \tag{2.41}$$

where the coefficients are dependent on u.

If we can determine two linearly independent first integrals of the form $h(x,t,u)=c_1$ and $j(x,t,u)=c_2$ with c_1 and c_2 as constants, the equation could be solved in the method of characteristics, similar to semi-linear equations. First, we form a differential type of the equation in the form:

$$\frac{dx}{a(x,t,u)}=\frac{dt}{b(x,t,u)}=\frac{du}{f(x,t,u)} \qquad 2.42$$

The general solution to the PDE can be written in the implicit form of:

$$j(x,t,u)=F(h(x,t,u)) \qquad 2.43$$

where F is an arbitrary differentiable function.

The inviscid Burgers equation in fluid mechanics and gas dynamics is a homogeneous quasi-linear PDE with $a=u, b=1, f=0$, the form of the equation will be like:

$$uu_x+bu_t=f \qquad 2.44$$
$$u(x,0)=\varphi(x)$$

If $f=0$ we have the inviscid flow and we can conclude that du is constant.

$$u=c_1 \qquad 2.45$$

where c_1 is a constant

now if we combine the equation to form an ODE we can obtain:

$$\frac{dx}{dy}=u=c_1 \qquad 2.46$$

$$x=c_1t+c_2 \qquad 2.47$$

where c_2 is another constant.

Combining the equations, we have:

$$x - ut = c_2 \quad (2.48)$$

Now we have found c_1 and c_2 which will lead us to find h and j. If we combine them with a differentiable function F as described, we will have:

$$c_1 = F(c_2) \quad (2.49)$$

$$u = F(x - ut) \quad (2.50)$$

Now we found the solution form for the equation and we need to find F based on the Initial Condition we have. Applying the initial conditions, we get:

$$u(x, 0) = \varphi(x) \quad (2.51)$$
$$= F(x - u\,.\,0) = F(x)$$
$$\varphi = F$$

Therefore, the solution to the Cauchy problem associated with the Burgers equation is:

$$u(x, y) = \varphi(x - ut) \quad (2.52)$$

In the specific case of the Riemann problem, we could have:

$$\varphi(x, t) = \begin{cases} 0 & , \quad x \leq 0 \\ 1 & , \quad x > 0 \end{cases} \quad (2.53)$$

then the result would be:

$$u(x,t) = \begin{cases} 0 & , \quad x \leq ut \\ 1 & , \quad x > ut \end{cases} \qquad 2.54$$

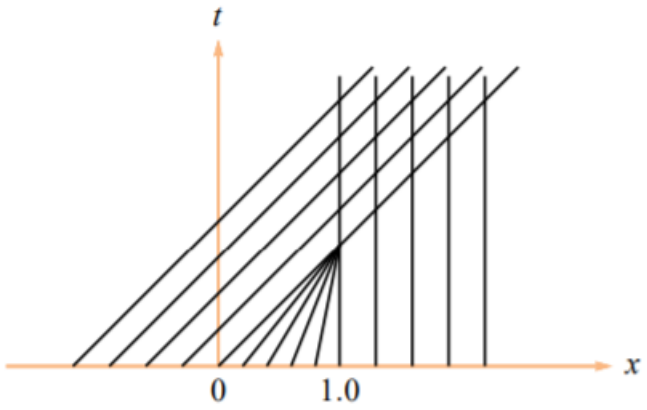

Figure 15: Characteristic lines for the inviscid Burgers equation (Salih 2015)

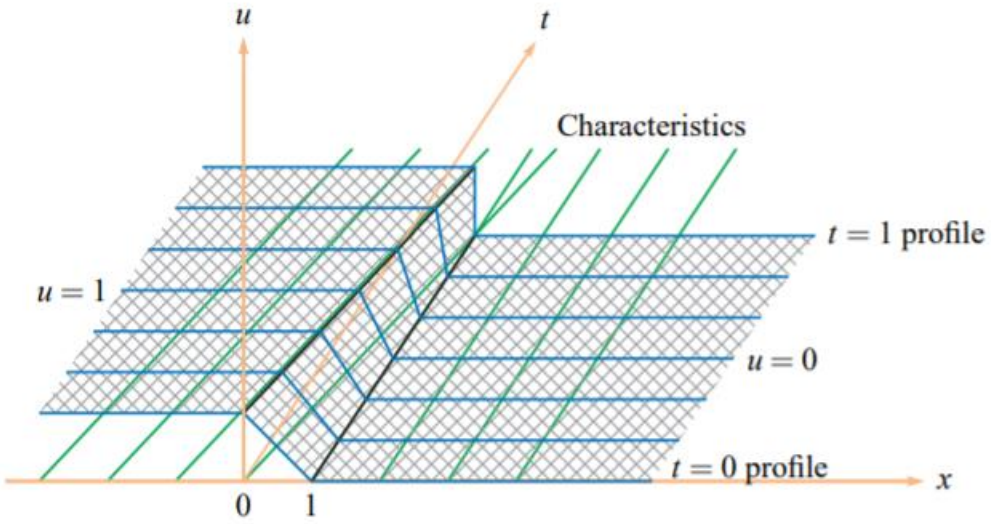

Figure 16: Solution surface for inviscid Burgers equation (Salih 2015)

2.9.2 Numerical solution

To derive the numerical solution for the Burgers equation we take into consideration the Lax-Friedrichs and upwind scheme and try to compare them in explicit form and find a combined manual scheme.

2.9.2.1 An unstable flux

Having a general form of conservation laws in equation 2.19 if we use simple arithmetic average flux function as a particular case:

$$F_{i+\frac{1}{2}} = \frac{1}{2}\left(f(Q_i^n) + f(Q_{i+1}^n)\right) \qquad 2.55$$

equation 2.19 would be written as:

$$Q_i^{n+1} = Q_i^n - \frac{\Delta t}{2\Delta x}\left(f(Q_{i+1}^n) - f(Q_{i-1}^n)\right) \qquad 2.56$$

It should be noted that equation 2.56 could not be used as it is generally unstable for hyperbolic problems even if we choose relatively low timestep to ensure CFL condition. (LeVeque 2002)

2.9.2.2 Lax-Friedrichs scheme

Lax-Friedrichs scheme is similar to the unstable flux mentioned in equation 2.56 method with the use of the flux average in adjacent nodes instead of the flux in the cell center. Therefore, the classical formulation would be:

$$U_j^{n+1} = \frac{1}{2}\left(U_{j+1}^n + U_{j-1}^n\right) - \frac{\gamma}{2}\left(f(U_{j+1}^n) - f\left(U_{j-1}^n\right)\right) \qquad 2.57$$

2.9.2.3 Upwind scheme

The upwind scheme gives us the highest accuracy for solving numerical schemes when the solution depends only on the neighbouring points. Considering Burgers equation 2.13 and 2.40

We know that the wave speed will be equal to $a = \frac{\partial f}{\partial U}$

If we consider the upwind scheme we would have:

$$a_{j+\frac{1}{2}} = \frac{f\left(U_{j+1}\right) - f\left(U_j\right)}{U_{j+1} - U_j} \qquad 2.58$$

$$if\ U_{j+1} = U_j \rightarrow a_{j+\frac{1}{2}} = U_j$$

If $a_{j+\frac{1}{2}} >= 0$ It means flow direction is from left to right

If $a_{j+\frac{1}{2}} < 0$ it means flow direction is from right to left

And the upwind scheme for Burgers equation could be written as:

$$U_j^{n+1} = U_j^n - \frac{\Delta t}{\Delta t}\left(F_{j+\frac{1}{2}} - F_{j-\frac{1}{2}}\right) \qquad 2.59$$

where:

$$F_{j+\frac{1}{2}} = \begin{cases} f(U_j) & if \quad a_{j+\frac{1}{2}} \geq 0 \\ f(U_{j+1}) & if \quad a_{j+\frac{1}{2}} < 0 \end{cases} \qquad 2.60$$

The inviscid Burgers equation is solved using Riemann solver with regards to Lax-Friedrichs and upwind schemes for different left and right boundaries and the following results are obtained:

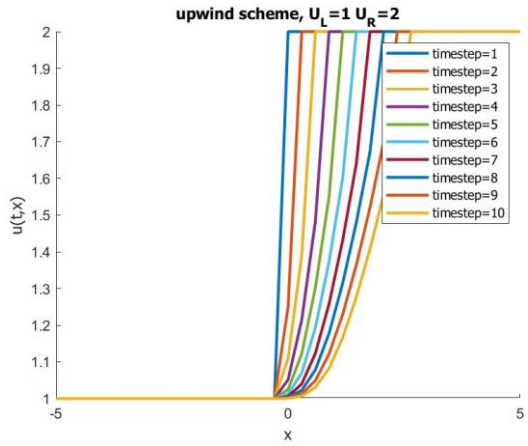

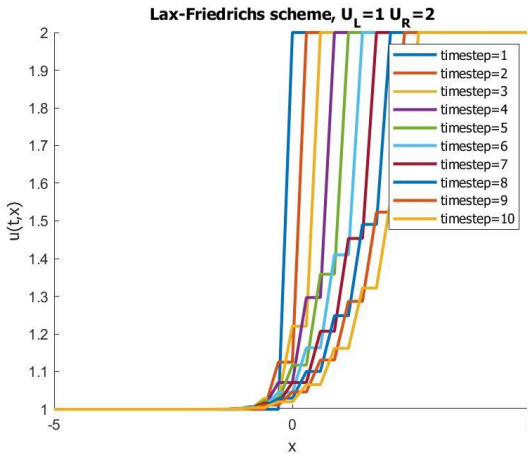

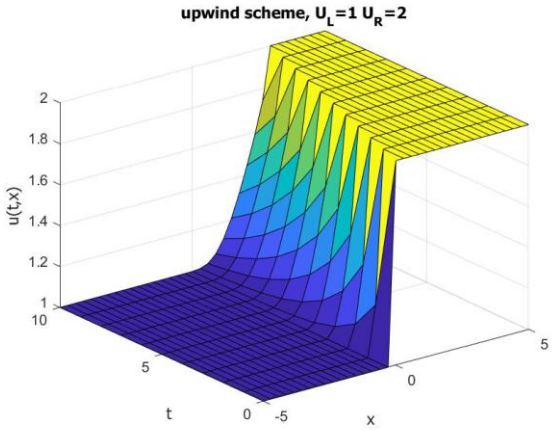
upwind scheme, U_L=1 U_R=2
u(t,x)
t
x

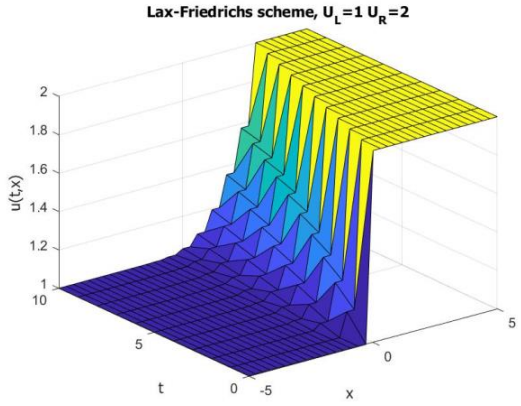
Lax-Friedrichs scheme, U_L=1 U_R=2
u(t,x)
t
x

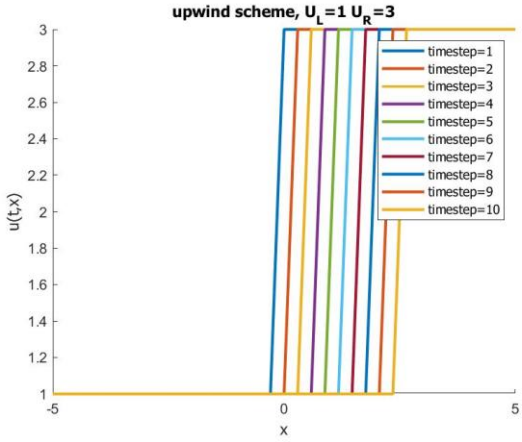
upwind scheme, U_L=1 U_R=3
u(t,x)
x
timestep=1
timestep=2
timestep=3
timestep=4
timestep=5
timestep=6
timestep=7
timestep=8
timestep=9
timestep=10

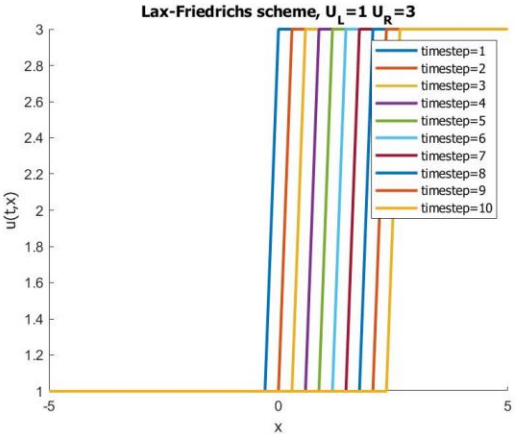
Lax-Friedrichs scheme, U_L=1 U_R=3
u(t,x)
x
timestep=1
timestep=2
timestep=3
timestep=4
timestep=5
timestep=6
timestep=7
timestep=8
timestep=9
timestep=10

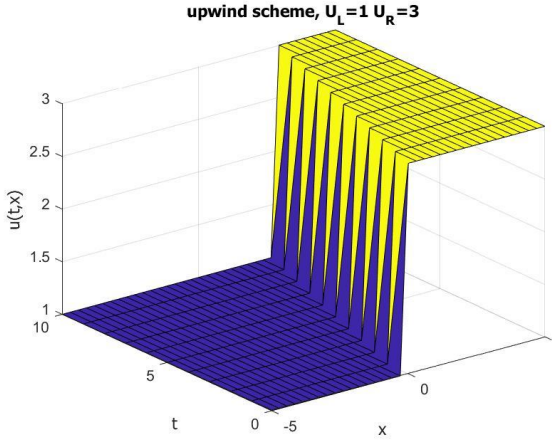
upwind scheme, U_L=1 U_R=3
u(t,x)
t
x

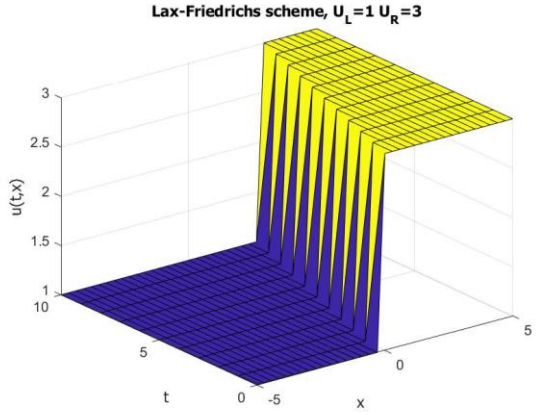
Lax-Friedrichs scheme, U_L=1 U_R=3
u(t,x)
t
x

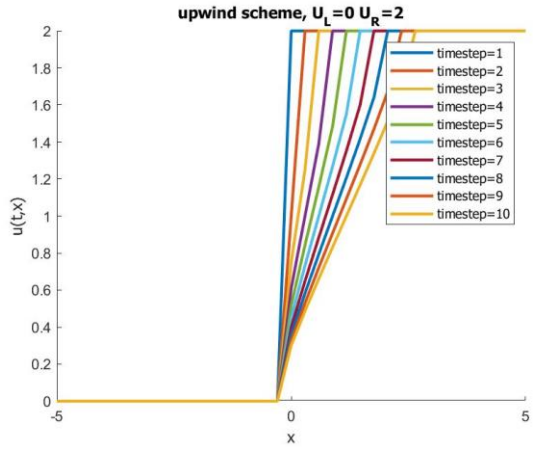
upwind scheme, U_L=0 U_R=2
u(t,x)
x
timestep=1
timestep=2
timestep=3
timestep=4
timestep=5
timestep=6
timestep=7
timestep=8
timestep=9
timestep=10

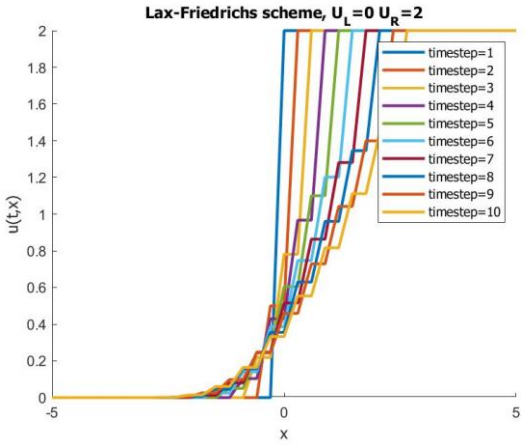
Lax-Friedrichs scheme, U_L=0 U_R=2
u(t,x)
x
timestep=1
timestep=2
timestep=3
timestep=4
timestep=5
timestep=6
timestep=7
timestep=8
timestep=9
timestep=10

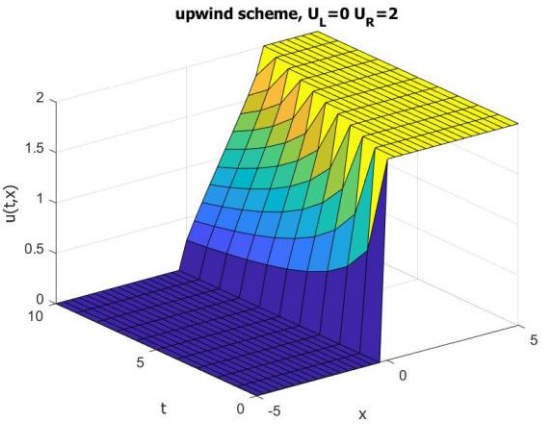
upwind scheme, U_L=0 U_R=2
u(t,x)
t
x

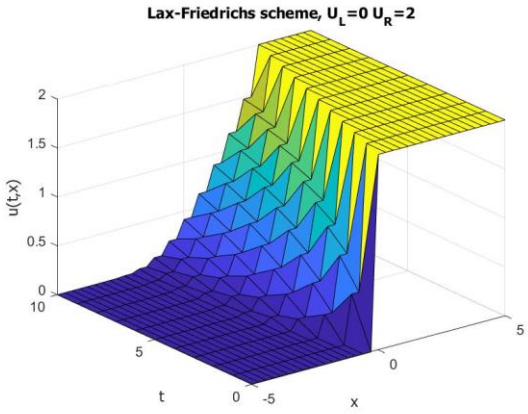
Lax-Friedrichs scheme, U_L=0 U_R=2
u(t,x)
t
x

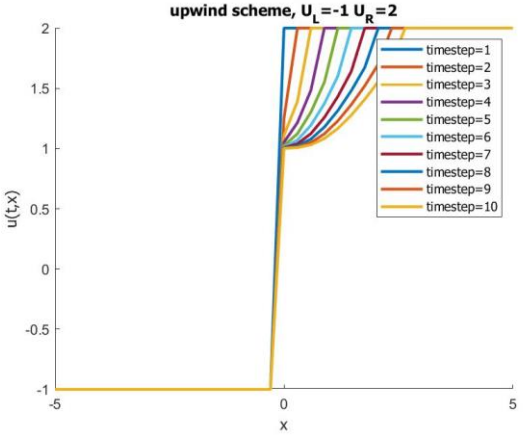
upwind scheme, U_L=-1 U_R=2
u(t,x)
x
timestep=1
timestep=2
timestep=3
timestep=4
timestep=5
timestep=6
timestep=7
timestep=8
timestep=9
timestep=10

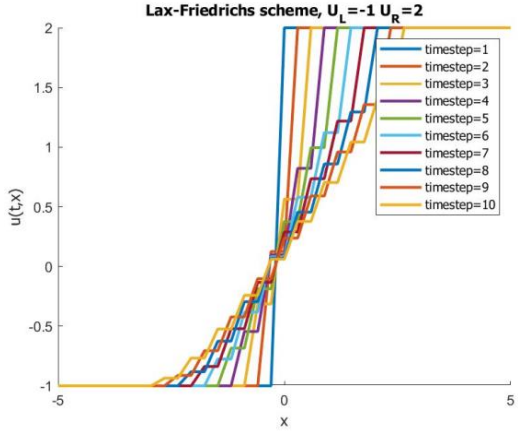
Lax-Friedrichs scheme, U_L=-1 U_R=2
u(t,x)
x
timestep=1
timestep=2
timestep=3
timestep=4
timestep=5
timestep=6
timestep=7
timestep=8
timestep=9
timestep=10

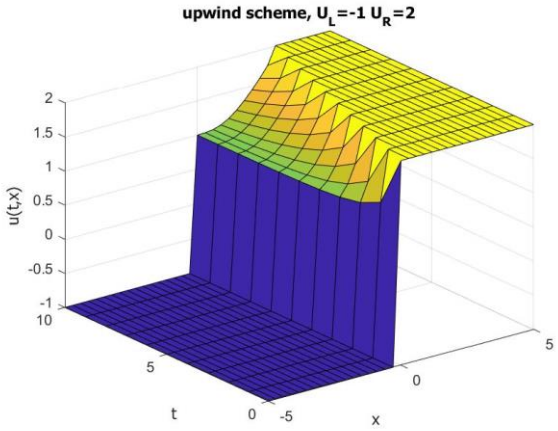
upwind scheme, U_L=-1 U_R=2
u(t,x)
t
x

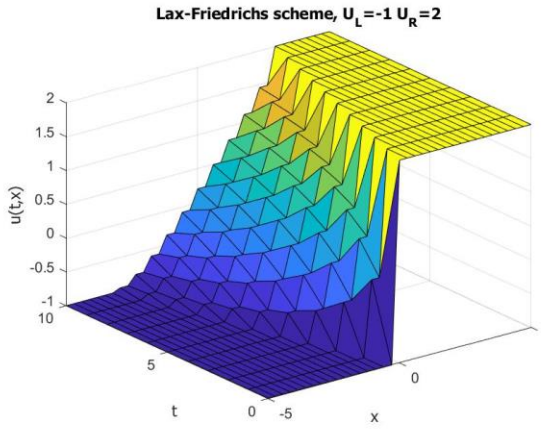
Lax-Friedrichs scheme, U_L=-1 U_R=2
u(t,x)
t
x

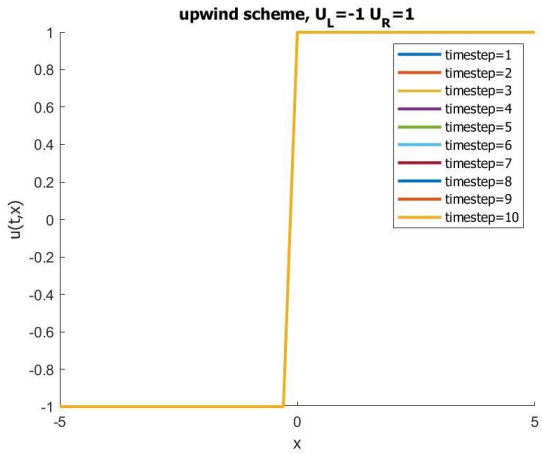
upwind scheme, U_L=-1 U_R=1
timestep=1
timestep=2
timestep=3
timestep=4
timestep=5
timestep=6
timestep=7
timestep=8
timestep=9
timestep=10
u(t,x)
x

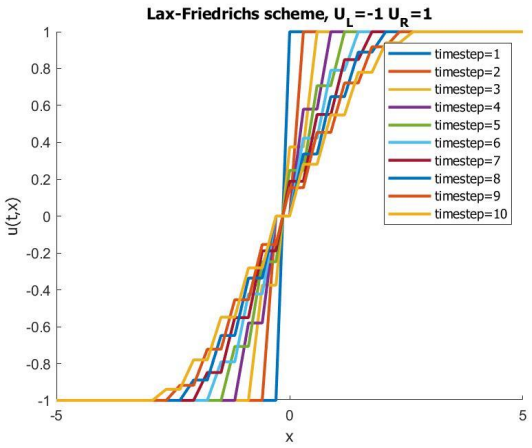
Lax-Friedrichs scheme, U_L=-1 U_R=1
timestep=1
timestep=2
timestep=3
timestep=4
timestep=5
timestep=6
timestep=7
timestep=8
timestep=9
timestep=10
u(t,x)
x

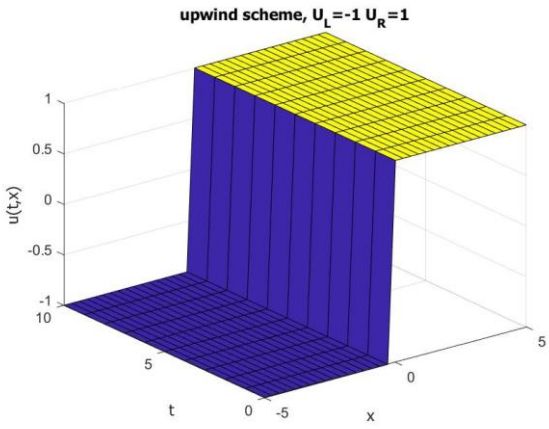
upwind scheme, U_L=-1 U_R=1
u(t,x)
t
x

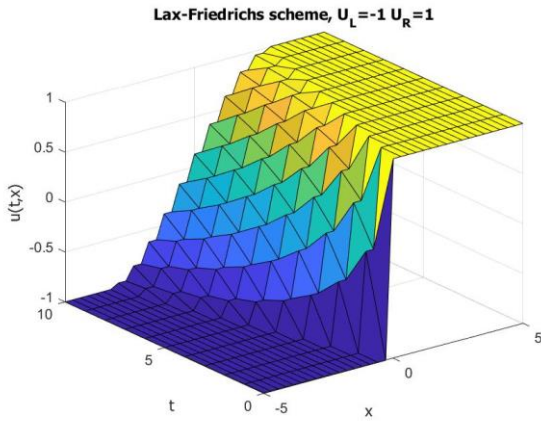
Lax-Friedrichs scheme, U_L=-1 U_R=1
u(t,x)
t
x

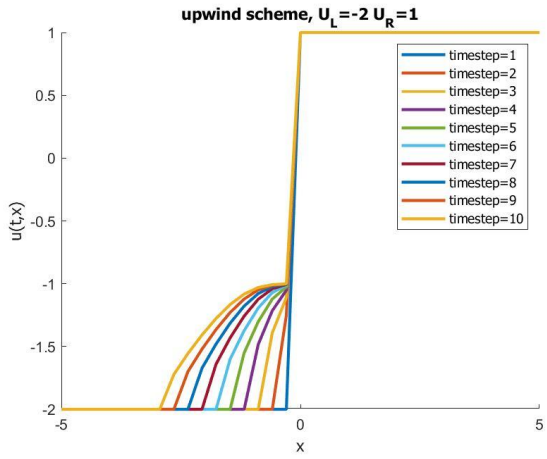
upwind scheme, U_L=-2 U_R=1
u(t,x)
x
timestep=1
timestep=2
timestep=3
timestep=4
timestep=5
timestep=6
timestep=7
timestep=8
timestep=9
timestep=10

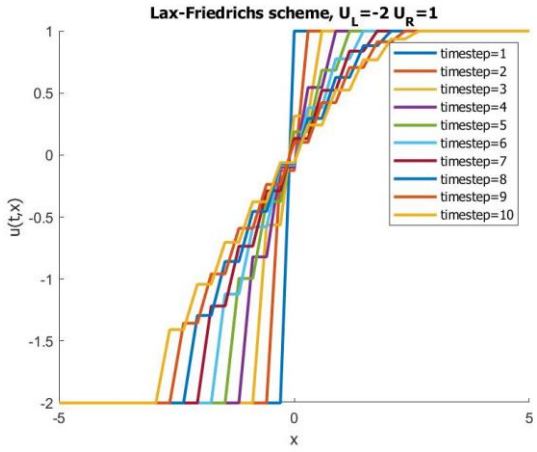
Lax-Friedrichs scheme, U_L=-2 U_R=1
u(t,x)
x
timestep=1
timestep=2
timestep=3
timestep=4
timestep=5
timestep=6
timestep=7
timestep=8
timestep=9
timestep=10

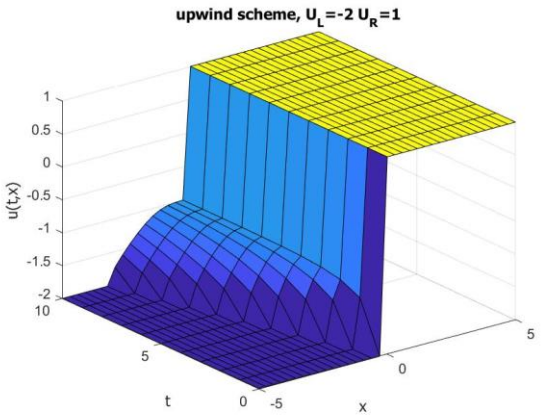
upwind scheme, U_L=-2 U_R=1
u(t,x)
t
x

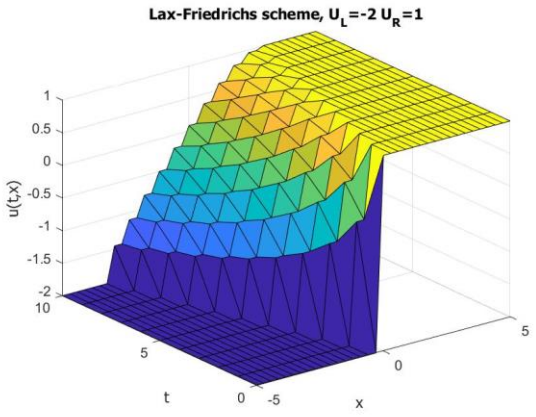
Lax-Friedrichs scheme, U_L=-2 U_R=1
u(t,x)
t
x

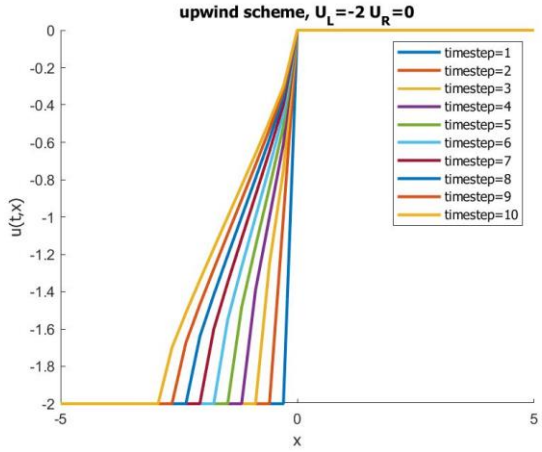
upwind scheme, U_L=-2 U_R=0
u(t,x)
x
timestep=1
timestep=2
timestep=3
timestep=4
timestep=5
timestep=6
timestep=7
timestep=8
timestep=9
timestep=10

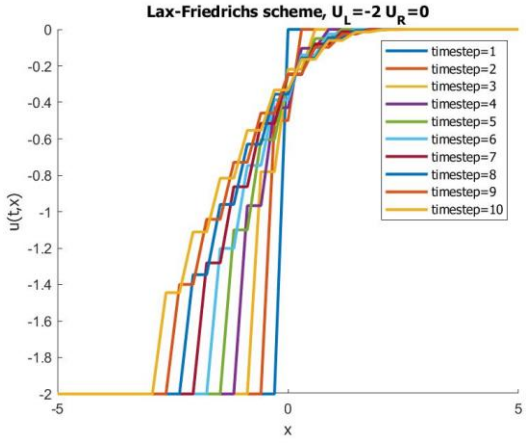
Lax-Friedrichs scheme, U_L=-2 U_R=0
u(t,x)
x
timestep=1
timestep=2
timestep=3
timestep=4
timestep=5
timestep=6
timestep=7
timestep=8
timestep=9
timestep=10

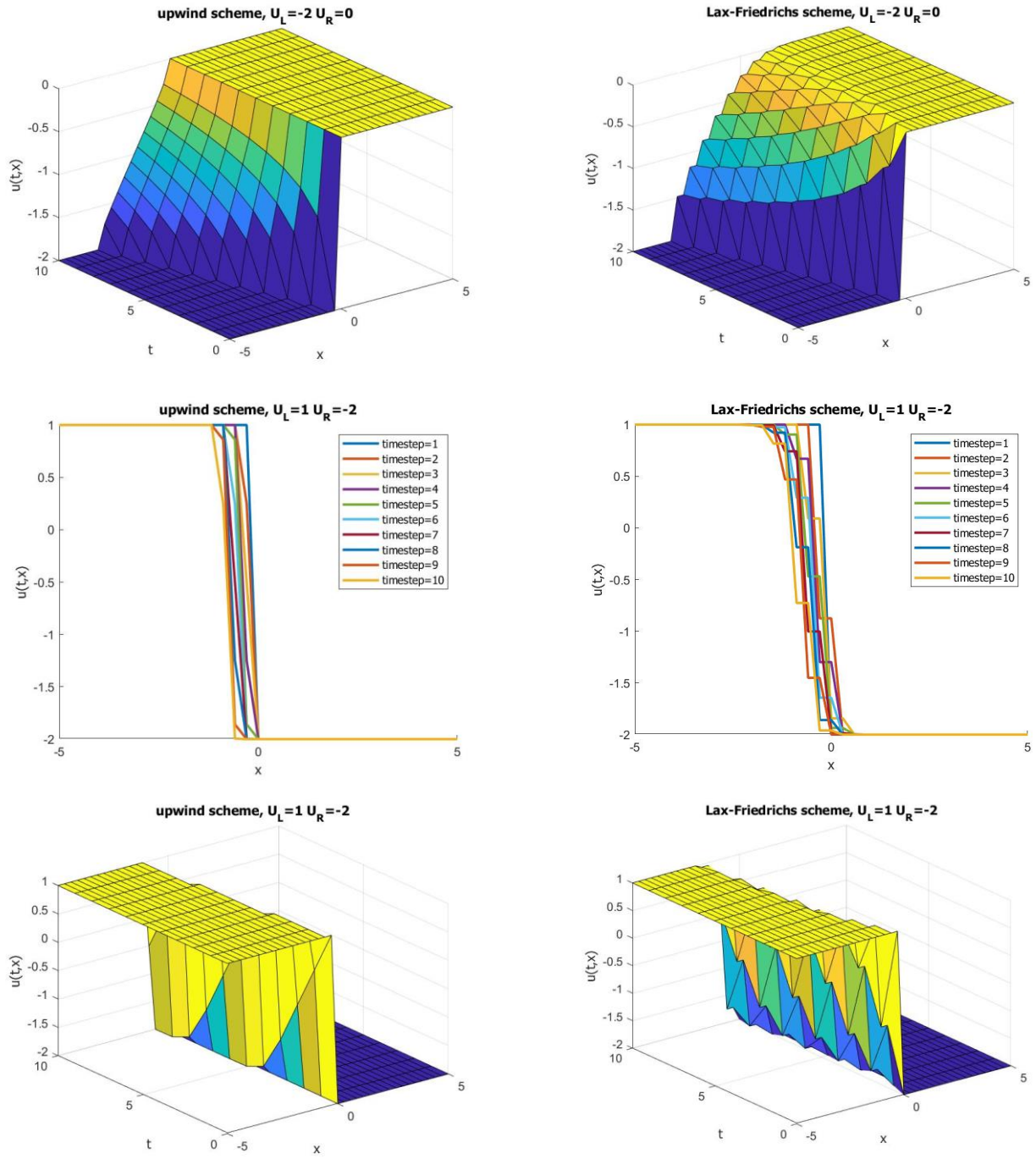

Figure 17: Numerical solution of the Riemann problem for the inviscid Burgers equation with different left and right boundaries with $\Delta t = 0.1, \Delta x = 0.2$ at $t = 1$, A comparison between Lax-Friedrichs and upwind schemes in 2D and 3D

As it could be vividly illustrated from the figures, we can identify inaccurate results from the upwind scheme in case we have changes in sign of the left and right boundaries while the Godunov scheme always produces the correct solution projected on the grid. Also, we can

determine 4 different cases satisfying Godunov numerical scheme for the solution based on the boundary values which are described below:

Case1:

$$U_L > 0 \; and \; U_R > 0:$$

We note that after infinitesimal time, the solution will move towards right no matter the middle part is a discontinuity or an expansion. Then the solution after infinitesimal time will be

$$f_{(i+1/2)} = f(U_L) \qquad 2.61$$

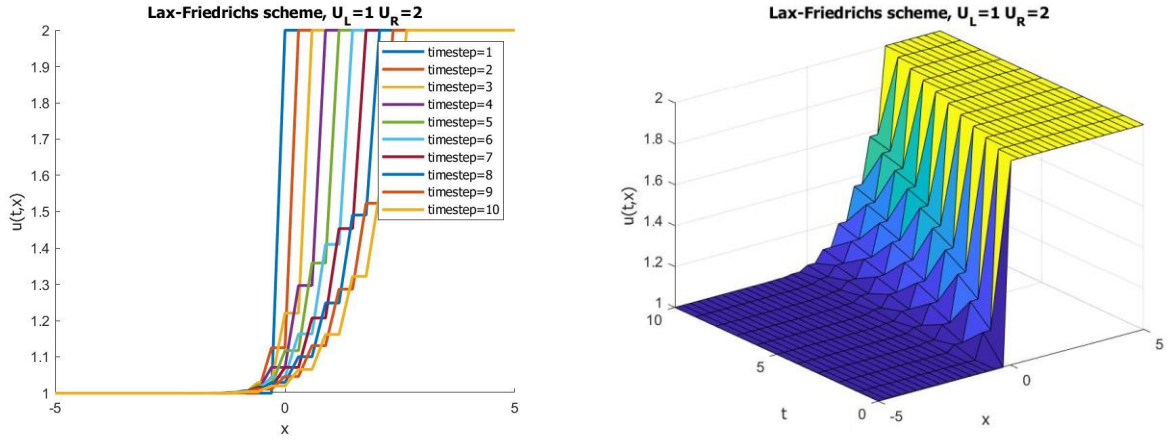

Figure 18: Numerical solution of the Riemann problem for the inviscid Burgers equation for case $0 < U_L < U_R$

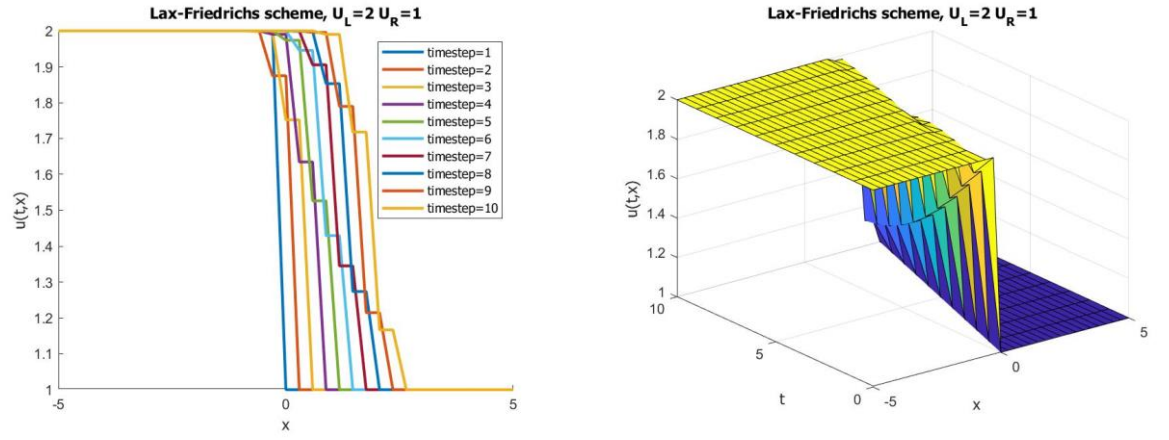

Figure 19: Numerical solution of the Riemann problem for the inviscid Burgers equation for case $0 < U_R < U_L$

Case 2:

$$U_L < 0 \; and \; U_R < 0$$

In this case, the solution will move toward left and we have:

$$f_{(i+1/2)} = f(U_R) \qquad 2.62$$

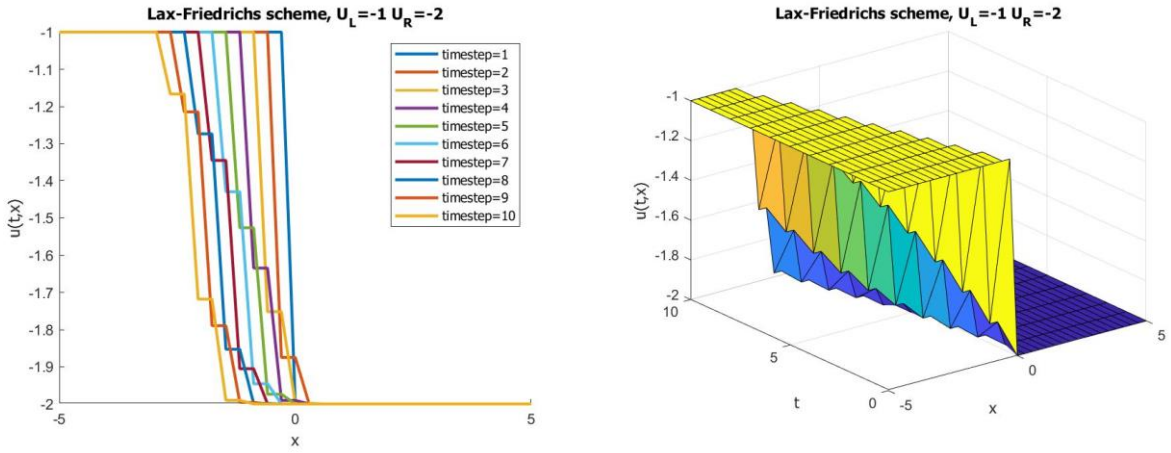

Figure 20: Numerical solution of the Riemann problem for the inviscid Burgers equation for the case $U_R < U_L < 0$

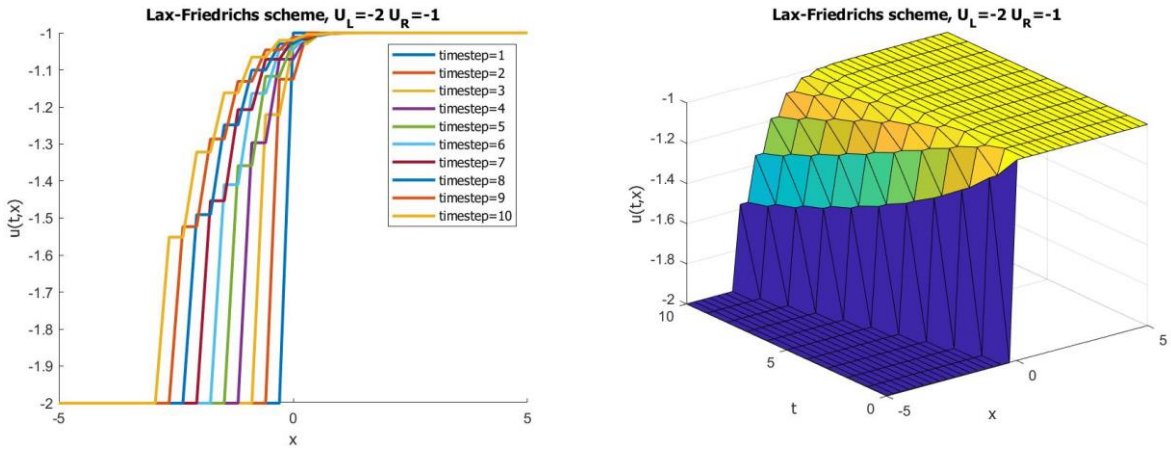

Figure 21: Numerical solution of the Riemann problem for the inviscid Burgers equation for the case $U_L < U_R < 0$

Case 3:

$$U_L < 0 < U_R$$

In this case, after infinitesimal time, the solution spreads. Then the value of the solution at the interface after infinitesimal time in the characteristic lines could be illustrated in a general graph of the following structure:

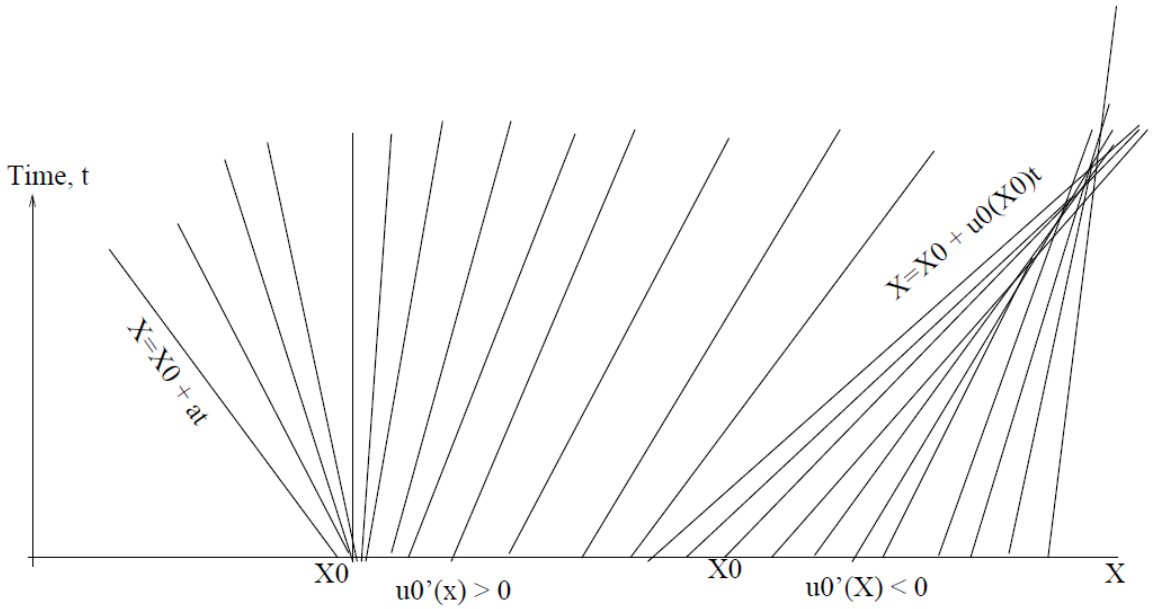

Figure 22: Characteristic lines for Burgers equation illustrating divergence and convergence of the lines based on the slope of the lines. $u_0(x)' < 0$ leads to convergence and $u_0(x)' > 0$ leads to divergence (Khouider 2008)

Above is the graph of $f(u)$ versus x at different times. at the infinitesimal time, we have a vertical line in the interface. The slope of the value of the solution in the vertical line would be $\frac{df}{du}$ which for Burgers equation from equation 2.40 we have:

$$\frac{df}{du} = u \tag{2.63}$$

The vertical line is corresponding to the value of the solution where the characteristics stay straight.

$$\frac{df}{du} = u = 0 \tag{2.64}$$

Then in this case, after infinitesimal time wave expands over 0 at the center.

$$f_{i+\frac{1}{2}} = 0 \tag{2.65}$$

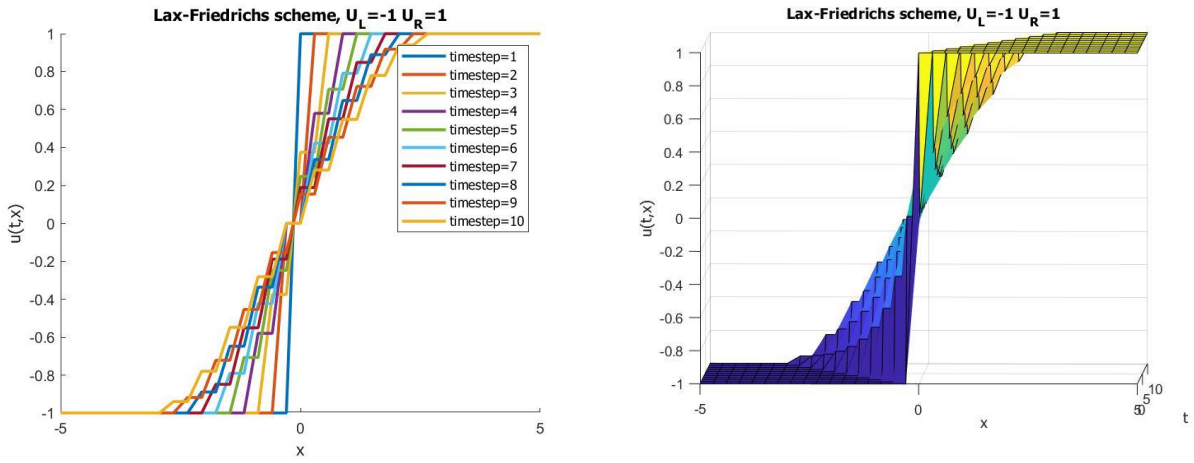

Figure 23: Numerical solution of the Riemann problem for the inviscid Burgers equation for the case $U_L < 0 < U_R$

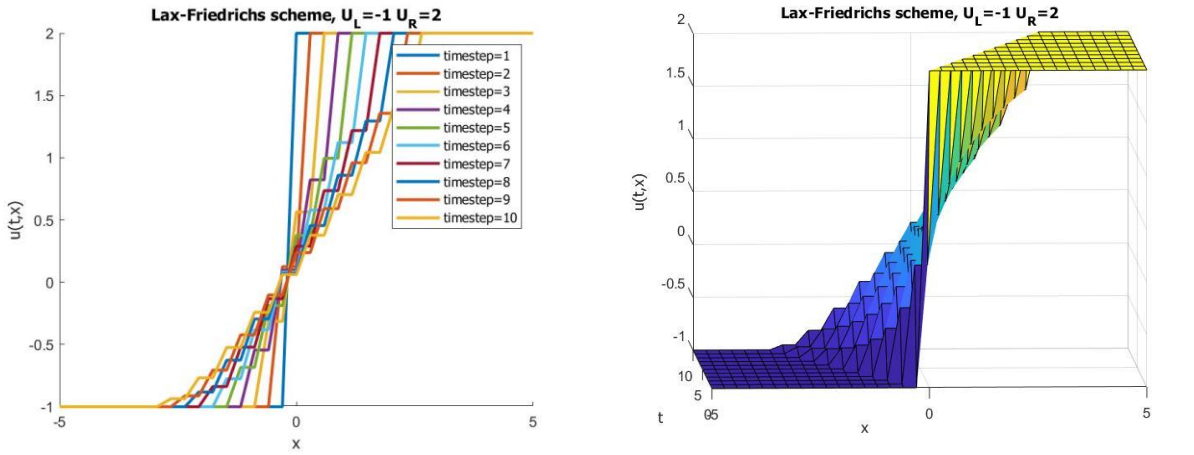

Figure 24: Numerical solution of the Riemann problem for the inviscid Burgers equation for the case $U_L < 0 < U_R$.

Note that despite unsymmetrical boundary values, the solution still expands over 0.

Case 4:

$$U_R < 0 < U_L$$

In this case, we have a shock instead of expansion and the shock moves in direction of df/du. Then:

$$f_{i+\frac{1}{2}} = \begin{cases} f(U_L) & , \ \dfrac{U_L + U_R}{2} > 0 \\ f(U_R) & , \ \dfrac{U_L + U_R}{2} < 0 \end{cases} \qquad 2.66$$

Here $\frac{U_L+U_R}{2}$ is shock wave speed and for the case of greater than 0 the wave will go to the right and the case of less than zero it will go to the left.

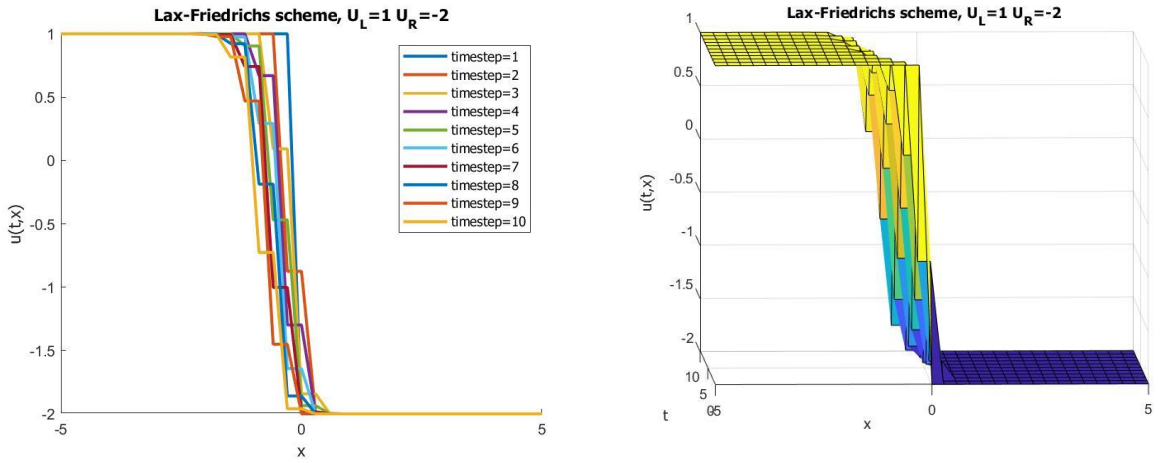

Figure 25: Numerical solution of the Riemann problem for the inviscid Burgers equation for the case $U_R < 0 < U_L$ and $\frac{U_L+U_R}{2} < 0$

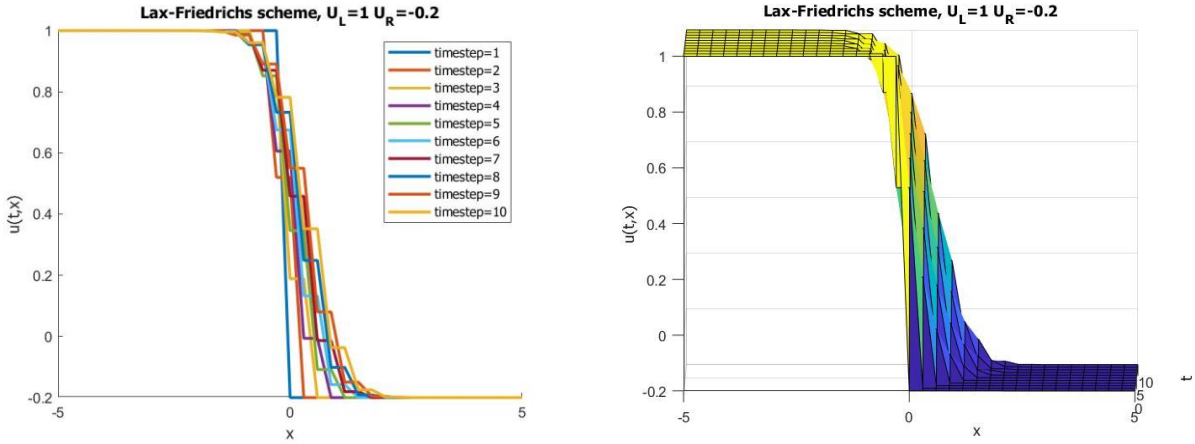

Figure 26: Numerical solution of the Riemann problem for the inviscid Burgers equation for the case $U_R < 0 < U_L$ and $\frac{U_L+U_R}{2} > 0$

2.9.2.4 Equivalent Lax-Friedrichs scheme

In this section, we define an equivalent formulation for the Lax-Friedrichs method and show that they are mathematically equivalent.

The numerical formulation for the equivalent Lax-Friedrichs scheme has the following form:

$$U_j^{n+1} = U_j^n - \frac{\Delta t}{\Delta x}\left(F_{j+\frac{1}{2}} - F_{j-\frac{1}{2}}\right) \tag{2.67}$$

where

$$F_{j+\frac{1}{2}} = \frac{1}{2}\left(f\left(U_j^n\right) + f\left(U_{j+1}^n\right)\right) - \frac{1}{2}\frac{\Delta x}{\Delta t}\left(U_{j+1}^n - U_j^n\right) \tag{2.68}$$

Consider a general flux function $f(U)$. Following the equivalent Lax-Friedrichs scheme formulation for calculating U_j^{n+1} mentioned in equation 2.67 we do have:

$$\begin{aligned} F_{j+\frac{1}{2}} - F_{j-\frac{1}{2}} = {} & \frac{1}{2}\left(f\left(U_j^n\right) + f\left(U_{j+1}^n\right)\right) - \frac{1}{2}\frac{\Delta x}{\Delta t}\left(U_{j+1}^n - U_j^n\right) \\ & - \frac{1}{2}\left(f\left(U_{j-1}^n\right) + f\left(U_j^n\right)\right) - \frac{1}{2}\frac{\Delta x}{\Delta t}\left(U_j^n - U_{j-1}^n\right) \end{aligned} \tag{2.69}$$

$$\gamma = \frac{\Delta t}{\Delta x} \tag{2.70}$$

Rewriting equation 2.69 we would have:

$$F_{j+\frac{1}{2}} - F_{j-\frac{1}{2}} = \frac{1}{2}\left(f(U_{j+1}^n) - f\left(U_{j-1}^n\right)\right) - \frac{1}{2}\frac{1}{\gamma}(U_{j+1}^n - U_j^n - U_j^n + U_{j-1}^n) \tag{2.71}$$

$$= \frac{1}{2}\left(f(U_{j+1}^n) - f\left(U_{j-1}^n\right)\right) - \frac{1}{2}\frac{1}{\gamma}\left(U_{j+1}^n - 2U_j^n + U_{j-1}^n\right) \rightarrow \times(-\gamma)$$

$$= -\frac{\gamma}{2}\left(f(U_{j+1}^n) - f\left(U_{j-1}^n\right)\right) + \frac{1}{2}\left(U_{j+1}^n - 2U_j^n + U_{j-1}^n\right) \rightarrow +U_j^n$$

$$U_j^{n+1} = -\frac{\gamma}{2}\left(f(U_{j+1}^n) - f\left(U_{j-1}^n\right)\right) + \frac{1}{2}\left(U_{j+1}^n + U_{j-1}^n\right)$$

As it has been derived equivalent Lax-Friedrichs scheme is the same as the Lax-Friedrichs scheme and this has been proved mathematically for any flux function.

2.9.2.5 Equivalent upwind scheme

In this section, we introduce an equivalent upwind scheme and show that it is mathematically equivalent to the classical upwind scheme in section 2.3.2.2.

By rewriting equation 2.67 we do have:

$$F_{j+\frac{1}{2}} = \frac{1}{2}\left(f\left(U_j^n\right) + f\left(U_{j+1}^n\right)\right) - \frac{1}{2}\left|a_{j+\frac{1}{2}}\right|\left(U_{j+1}^n - U_j^n\right) \tag{2.72}$$

$$a_{j+\frac{1}{2}} = \frac{f\left(U_{j+1}^n\right) - f\left(U_j^n\right)}{U_{j+1}^n - U_j^n} \tag{2.73}$$

Consider a general flux function $f(U)$ we want to show that equivalent upwind scheme is the same as the standard upwind scheme.

If $a_{j+\frac{1}{2}} \geq 0$ we have:

$$\begin{aligned} F_{j+\frac{1}{2}} &= \frac{1}{2}\left(f\left(U_j^n\right) + f\left(U_{j+1}^n\right)\right) - \frac{1}{2}\left(\frac{f\left(U_{j+1}^n\right) - f\left(U_j^n\right)}{U_{j+1} - U_j}\right)\left(U_{j+1}^n - U_j^n\right) \\ &= \frac{1}{2}\left(f\left(U_j^n\right) + f\left(U_{j+1}^n\right)\right) - \frac{1}{2}\left(f\left(U_{j+1}^n\right) - f\left(U_j^n\right)\right) \\ &= \frac{1}{2}\left(2f\left(U_j^n\right)\right) \\ &= f\left(U_j^n\right) \end{aligned} \tag{2.74}$$

If $a_{j+\frac{1}{2}} < 0$ we have:

$$\begin{aligned} F_{j+\frac{1}{2}} &= \frac{1}{2}\left(f\left(U_j^n\right) + f\left(U_{j+1}^n\right)\right) + \frac{1}{2}\left(\frac{f\left(U_{j+1}^n\right) - f\left(U_j^n\right)}{U_{j+1} - U_j}\right)\left(U_{j+1}^n - U_j^n\right) \\ &= \frac{1}{2}\left(f\left(U_j^n\right) + f\left(U_{j+1}^n\right)\right) + \frac{1}{2}\left(f\left(U_{j+1}^n\right) - f\left(U_j^n\right)\right) \\ &= \frac{1}{2}\left(2f\left(U_{j+1}^n\right)\right) \end{aligned} \tag{2.75}$$

$$= f\left(U_{j+1}^{n}\right)$$

If $a_{j-\frac{1}{2}} \geq 0$ we have:

$$F_{j-\frac{1}{2}} = \frac{1}{2}\left(f\left(U_{j-1}^{n}\right) + f\left(U_{j}^{n}\right)\right) - \frac{1}{2}\left(\frac{f\left(U_{j}^{n}\right) - f\left(U_{j-1}^{n}\right)}{U_j - U_{j-1}}\right)\left(U_{j}^{n} - U_{j-1}^{n}\right) \quad 2.76$$

$$= \frac{1}{2}\left(f\left(U_{j-1}^{n}\right) + f\left(U_{j}^{n}\right)\right) - \frac{1}{2}\left(f\left(U_{j}^{n}\right) - f\left(U_{j-1}^{n}\right)\right)$$

$$= \frac{1}{2}\left(2f\left(U_{j-1}^{n}\right)\right)$$

$$= f\left(U_{j-1}^{n}\right)$$

If $a_{j-\frac{1}{2}} < 0$ we have:

$$F_{j-\frac{1}{2}} = \frac{1}{2}\left(f\left(U_{j-1}^{n}\right) + f\left(U_{j}^{n}\right)\right) + \frac{1}{2}\left(\frac{f\left(U_{j}^{n}\right) - f\left(U_{j-1}^{n}\right)}{U_j - U_{j-1}}\right)\left(U_{j}^{n} - U_{j-1}^{n}\right) \quad 2.77$$

$$= \frac{1}{2}\left(f\left(U_{j-1}^{n}\right) + f\left(U_{j}^{n}\right)\right) + \frac{1}{2}\left(f\left(U_{j}^{n}\right) - f\left(U_{j-1}^{n}\right)\right)$$

$$= \frac{1}{2}\left(2f\left(U_{j}^{n}\right)\right)$$

$$= f\left(U_{j}^{n}\right)$$

As mentioned above, we have proved that our equivalent upwind scheme is equal to the standard upwind scheme for any flux function.

2.9.2.6 General formulation

Deliberating the former analysis of Lax-Friedrichs and upwind scheme and their equivalent formulations, we see that these two schemes could be written in a common framework which is as follows:

Equivalent Lax-Friedrichs scheme has the same formulation as equation 2.59 with following flux functions:

$$F_{j+\frac{1}{2}} = \frac{1}{2}\left(f\left(U_j^n\right) + f\left(U_{j+1}^n\right)\right) - \frac{1}{2}\frac{\Delta x}{\Delta t}\left(U_{j+1}^n - U_j^n\right) \quad 2.78$$

$$F_{j-\frac{1}{2}} = \frac{1}{2}\left(f\left(U_{j-1}^n\right) + f\left(U_j^n\right)\right) - \frac{1}{2}\frac{\Delta x}{\Delta t}\left(U_j^n - U_{j-1}^n\right) \quad 2.79$$

The equivalent upwind scheme could be reformatted to equation 2.59 with the following flux functions:

$$F_{j+\frac{1}{2}} = \frac{1}{2}\left(f\left(U_j^n\right) + f\left(U_{j+1}^n\right)\right) - \frac{1}{2}\left|a_{j+\frac{1}{2}}\right|\left(U_{j+1}^n - U_j^n\right) \quad 2.80$$

$$a_{j+\frac{1}{2}} = \frac{f\left(U_{j+1}^n\right) - f\left(U_j^n\right)}{U_{j+1}^n - U_j^n}$$

We have shown before that equivalent Lax-Friedrichs scheme and equivalent upwind scheme are equal to Lax-Friedrichs and upwind schemes, respectively. From the structure of the schemes, we can find a common pattern leading to generate a new general scheme for both Lax-Friedrichs and upwind schemes, letting us generalize Lax-Friedrichs and upwind schemes in a unified framework. Considering equation 2.59 and the flux functions for equivalent Lax-Friedrichs and equivalent upwind schemes in equations 2.68 and 2.72, the unified flux function to be used in equation 2.59 is introduced below:

$$F_{j+\frac{1}{2}} = \frac{1}{2}\left(f\left(U_j^n\right) + f\left(U_{j+1}^n\right)\right) - \frac{1}{2}\frac{\Delta x}{\Delta t}Q_{j+\frac{1}{2}}\left(U_{j+1}^n - U_j^n\right) \quad 2.81$$

$$Q_{j+\frac{1}{2}} = \begin{cases} 1 \; for \; Lax - Friedrich \; scheme \\ \dfrac{\Delta t}{\Delta x}\left|a_{j+\frac{1}{2}}\right| \; for \; upwind \; scheme \end{cases} \quad 2.82$$

$$a_{j+\frac{1}{2}} = \frac{f\left(U_{j+1}^n\right) - f\left(U_j^n\right)}{U_{j+1}^n - U_j^n} \quad 2.83$$

Regarding the new scheme, we can redefine the CFL condition as having a stable scheme in case of

$$Q_{upwind} < Q_{Lax-Friedrich}$$

Then we will have:

$$\frac{\Delta t}{\Delta x}|a| < 1 \qquad 2.84$$

It should be noted that we are free to apply a continuum of schemes between Lax-Friedrichs and upwind by choosing Q between $Q_{Lax-Friedrich}$ and Q_{upwind} and create a stable scheme.

2.10 The Euler equation

The conservation equation demonstrates transport of physical extensive quantities such as mass, momentum and energy in a mathematical way. The equation can be described in the integral form or derivative form in terms of flux integral or divergence operator respectively. A flux j represents the amount of a physical quantity q flowing through a surface in unit area per unit time.

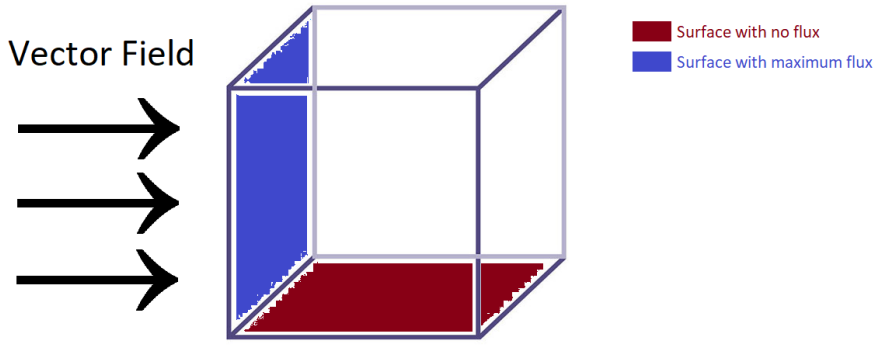

Figure 27: Diagram of a vector field and flux passing surfaces

Through the divergence theorem, the differential form of the conservation equation without source and sink term can be written as:

$$\frac{\partial q}{\partial t} + \nabla.\mathrm{j} = 0 \qquad 2.85$$

where q represents the quantity,

and j is the flux of q

Using the vector definition, mass flux could be simply derived from the density of the quantity and velocity of the vector field as:

$$\text{Mass flux} = \rho . u \tag{2.86}$$

The corresponding equation in the differential form will be:

$$\frac{\partial \rho}{\partial t} + \frac{\partial (\rho u)}{\partial x} = 0 \tag{2.87}$$

Concerning that the velocity u used in the equations is deduced from a macroscopic point of view of gas molecules and the gas has an average velocity over the particles near the point of concern. So, the advective flux ρu^2 shows the macroscopic momentum flux of gas molecules flowing with constant velocity. This could not be happening in reality as we know a gas flow over the absolute zero temperature, consists of molecules moving and colliding each other even if there is no fluid flow. Therefore, a contribution should be added to the advective flux to demonstrate the effect of pressure. In general, the pressure is added to the advective momentum flux to obtain total momentum flux as:

$$\text{Momentum flux} = \rho u^2 + p \tag{2.88}$$

The corresponding equation in differential form would be:

$$\frac{\partial (\rho u)}{\partial t} + \frac{\partial (\rho u^2 + p)}{\partial x} = 0 \tag{2.89}$$

Total energy E is formulated as the summation of internal energy and kinetic energy:

$$E = \frac{1}{2}\rho u^2 + \rho e \tag{2.90}$$

where e is internal energy per unit mass referred to as specific internal energy.

We attempt to mathematically derive an expression for $\frac{\partial E}{\partial t}$

$$\frac{\partial E}{\partial t} = \frac{\partial}{\partial t}\left(\frac{1}{2}\rho u^2 + \rho e\right) \tag{2.91}$$

$$d\left(\frac{1}{2}\rho u^2\right) = \frac{1}{2}d(\rho u.u) = \frac{1}{2}ud(\rho u) + \frac{1}{2}\rho u du$$

$$d(\rho u) = \rho du + ud\rho \rightarrow du = \frac{d(\rho u) - ud\rho}{\rho}$$

$$d\left(\frac{1}{2}\rho u^2\right) = \frac{1}{2}ud(\rho u) + \frac{1}{2}\rho u\frac{d(\rho u) - ud\rho}{\rho}$$

$$= \frac{1}{2}ud(\rho u) + \frac{1}{2}ud(\rho u) - \frac{1}{2}u^2 d\rho$$

$$= ud(\rho u) - \frac{1}{2}u^2 d\rho$$

$$\frac{\partial}{\partial t}\left(\frac{1}{2}\rho u^2\right) = u\frac{\partial(\rho u)}{\partial t} - \frac{1}{2}u^2\frac{\partial \rho}{\partial t} \tag{2.92}$$

concerning equations 2.87 and 2.89 we have:

$$\frac{\partial(\rho u)}{\partial t} = -\frac{\partial}{\partial x}(\rho u^2 + p) \tag{2.93}$$

$$\frac{\partial \rho}{\partial t} = -\frac{\partial(\rho u)}{\partial x} \tag{2.94}$$

Combining equations 2.93 and 2.94 with equation 2.92 we can obtain:

$$\frac{\partial}{\partial t}\left(\frac{1}{2}\rho u^2\right) = -u\frac{\partial}{\partial x}(\rho u^2 + p) + \frac{1}{2}u^2\frac{\partial(\rho u)}{\partial x} \quad 2.95$$

$$\frac{\partial}{\partial t}\left(\frac{1}{2}\rho u^2\right) + u\frac{\partial}{\partial x}(\rho u^2 + p) - \frac{1}{2}u^2\frac{\partial(\rho u)}{\partial x} = 0$$

$$\frac{\partial}{\partial t}\left(\frac{1}{2}\rho u^2\right) + u\frac{\partial}{\partial x}(\rho u^2) - \frac{1}{2}u^2\frac{\partial(\rho u)}{\partial x} + u\frac{\partial p}{\partial x} = 0$$

$$u\frac{\partial}{\partial x}(\rho u^2) - \frac{1}{2}u^2\frac{\partial}{\partial x}(\rho u) = u^2\frac{\partial}{\partial x}(\rho u) + \rho u^2\frac{\partial u}{\partial x} - \frac{1}{2}u^2\frac{\partial}{\partial x}(\rho u)$$

$$= \frac{1}{2}u^2\frac{\partial}{\partial x}(\rho u) + \rho u^2.\frac{\partial u}{\partial x}$$

$$= \frac{1}{2}u^2\frac{\partial}{\partial x}(\rho u) + \frac{1}{2}\rho u\frac{\partial}{\partial x}(u^2)$$

$$= \frac{\partial}{\partial x}(\frac{1}{2}\rho u^3)$$

Finally, we will have:

$$\frac{\partial}{\partial t}\left(\frac{1}{2}\rho u^2\right) + \frac{\partial}{\partial x}(\frac{1}{2}\rho u^3) + u\frac{\partial p}{\partial x} = 0 \quad 2.96$$

For internal energy we note:

$$de = \frac{p}{\rho^2}d\rho + Tds \quad 2.97$$

$$I = \rho e \quad 2.98$$

$$dI = \rho de + ed\rho + \rho Tds \quad 2.99$$

$$= \frac{p}{\rho} + ed\rho + \rho Tds$$

$$= \left(e + \frac{p}{\rho}\right)d\rho + \rho Tds$$

$$\frac{\partial I}{\partial t} = \left(e + \frac{p}{\rho}\right)\frac{\partial \rho}{\partial t} + \rho T \frac{\partial s}{\partial t} \qquad 2.100$$

We know from entropy conservation equation that:

$$\frac{\partial s}{\partial t} + v\frac{\partial s}{\partial x} = 0 \qquad 2.101$$

Substituting equations 2.100 and 2.101 into equations 2.87 and 2.89, we have:

$$\frac{\partial I}{\partial t} = -\left(e + \frac{p}{\rho}\right)\frac{\partial}{\partial x}(\rho u) - \rho T v \frac{ds}{dx} \qquad 2.102$$

$$\frac{\partial(\rho e)}{\partial t} + \left(e + \frac{p}{\rho}\right)\frac{\partial}{\partial x}(\rho u) + \rho T v \frac{ds}{dx} = 0$$

$$\frac{\partial(\rho e)}{\partial t} + e\frac{\partial}{\partial x}(\rho u) + p\frac{\partial u}{\partial x} + \rho u \frac{\partial e}{\partial x} = 0$$

$$\frac{\partial(\rho e)}{\partial t} + \frac{\partial}{\partial x}(\rho e u) + p\frac{\partial u}{\partial x} = 0$$

By adding the derived equations 2.96 and 2.100 we have:

$$\frac{\partial}{\partial t}\left(\frac{1}{2}\rho u^2\right) + \frac{\partial}{\partial x}\left(\frac{1}{2}\rho u^3\right) + u\frac{\partial p}{\partial x} + \frac{\partial(\rho e)}{\partial t} + \frac{\partial}{\partial x}(\rho e u) + p\frac{\partial u}{\partial x} = 0 \qquad 2.103$$

$$\frac{\partial E}{\partial t} + \frac{\partial}{\partial x}\left(\frac{1}{2}\rho u^3\right) + u\frac{\partial p}{\partial x} + \frac{\partial}{\partial x}(\rho e u) + p\frac{\partial u}{\partial x} = 0$$

$$\frac{\partial E}{\partial t} + \frac{\partial}{\partial x}\left(\frac{1}{2}\rho u^3\right) + \frac{\partial}{\partial x}(\rho e u) + \frac{\partial(pv)}{\partial x} = 0$$

$$\frac{\partial E}{\partial t} + \frac{\partial}{\partial x}\left(\frac{1}{2}\rho u^3 + \rho e u + p u\right) = 0$$

$$\frac{\partial E}{\partial t} + \frac{\partial}{\partial x}\left(u\left(\frac{1}{2}\rho u^2 + \rho e + p\right)\right) = 0$$

And in the final form we obtain the energy conservation law equation in differential form:

$$\frac{\partial E}{\partial t} + \frac{\partial}{\partial x}\big(u(E + p)\big) = 0 \qquad 2.104$$

The Euler equation is a set of quasilinear hyperbolic equations of mass, momentum and energy conservation laws which is derived by linearization of the continuity equation for mass, momentum and energy fluxes and results in the following matrix equation:

$$\begin{pmatrix} \rho \\ \rho u \\ E \end{pmatrix}_t + \begin{pmatrix} \rho u \\ \rho u^2 + p \\ u(E+p) \end{pmatrix}_x = 0 \qquad 2.105$$

where ρ is density, proportional to mass if the volume is unchanged,

P is pressure,

ρu is momentum,

and E represents total energy,

Euler model is a very strong and most basic model for fluid dynamics because it deals with mass, momentum and energy conservation laws and they are all basic physical characteristics expressed in conservation equations. It should be noted that we remove the effect of viscosity because of simplicity and naturally less effect of viscosity on the solution of the 1D model of our choice.

3 Numerical simulation

3.1 WIMF scheme

In 2005 Evje and Flåtten proposed Weakly Implicit Mixture Flux Model (WIMF) for two-phase flow in order to keep a high level of accuracy, stability and robustness while allowing CFL criterion to be violated. The model consists of a set of hyperbolic conservation laws considering the constant velocity of the flow along characteristic lines. Typically, explicit methods are used for such a case. Explicit schemes are simpler and more flexible in the treatment of complex pipe networks. However, a well-known disadvantage of the explicit methods is a dependency on the Courant number and stability issue (Evje and Flåtten 2005).

$$\frac{\Delta x}{\Delta t} \geq |\lambda\_\max| \tag{3.1}$$

which λ_{max} is the largest eigenvalue of the system.

For two-phase flow model, we have four eigenvalues which depends on sonic waves and volume fraction waves knowing this fact that sonic waves are much faster than volume fraction waves. This may lead to serious issues with the computational efficiency of explicit schemes. So, involving some implicit methods would be convenient to fix the issue, by coupling some variables throughout the computational domain. This may result in two different approaches referred to as weakly implicit and strongly implicit. In weakly implicit approach, a weaker CFL condition should be satisfied for volume fraction waves but the original CFL criterion may be violated. This approach has been first studied by (Faille and Heintzé 1999) and (Masella, Tran et al. 1998). In strongly implicit no CFL condition applies for stability (Evje and Flåtten 2005).

The mixture flux method proposed by Evje and Flåtten incorporates physical variables such as pressure and volume fractions into the calculation. These variables are dependent on conservative variables and the approach is proposed in order to combine diffusive and non-dissipative fluxes. In mixture flux method, pressure evolution equation is derived and solved at cell interfaces. Then implicit mass fluxes are calculated according to pressure calculation and the implicit fluxes are merged with upwind fluxes to form a hybrid scheme (Evje and Flåtten 2005).

As a result of the introduced scheme referred to as WIMF-AUSMD, accuracy, efficiency and resolution robustness connected to sonic and volume fraction waves on collocated grids are concluded while allowing CFL criterion to be violated. (Evje and Flåtten 2005). The derived equations of WIMF scheme are discussed in section 3.8.

3.2 X-Force scheme

In the research done recently, we have formulated X-Force scheme for the full Euler model and developed the code to numerically simulate the model for a Riemann problem. Considering the system of conservation laws of equation 1.1, the scheme is proposed by (Evje, Flåtten et al. 2008) on the general formulation of equation 2.67. Further researches have been done to involve a conservative version of the pressure-based method where pressure is solved on staggered grids similar to the classical CFD methods. The contents of this section are mainly derived from (Flåtten 2019).

The X-Force scheme is based on splitting the flux as:

$$F(u) = G(u) + H(u) \tag{3.2}$$

In case of splitting the flux to $G(u) = H(u) = \frac{1}{2}F(u)$, The Force scheme would be derived (Toro 2013) and in the case of $G(u) = F(u), H(u) = 0$, the modified Lax-Friedrichs scheme is recovered (Tadmor 1984). We select $G(u)$ as the convective flux and $H(u)$ as the pressure flux leading to build a natural pressure-momentum coupling to develop a linearly implicit formulation with simpler development progress.

3.2.1 Scheme formulation – Explicit

According to (Evje, Flåtten et al. 2008), the final formulation of the proposed scheme is:

$$\begin{aligned} U_j^{n+1} = {} & \frac{1}{4}\left(U_{j-1}^n + 2U_j^n + U_{j+1}^n\right) - \frac{\Delta t}{2\Delta x}\left(F\left(U_{j+1}^n\right) - F\left(U_{j-1}^n\right)\right) \\ & + \left(\frac{\Delta t}{\Delta x}\right)^2 \hat{C}_{j+\frac{1}{2}}\left(G\left(U_{j+1}^n\right) - G\left(U_j^n\right)\right) \\ & - \left(\frac{\Delta t}{\Delta x}\right)^2 \hat{C}_{j-\frac{1}{2}}\left(G\left(U_j^n\right) - G\left(U_{j-1}^n\right)\right) \end{aligned} \tag{3.3}$$

where

$$C = \frac{\partial H}{\partial u} \tag{3.4}$$

and $\hat{C}$ corresponds to the cell average:

$$\hat{C}_{j+\frac{1}{2}} = \hat{C}\left(U_j^n, U_{j+1}^n\right) \tag{3.5}$$

The scheme could also be written in an equivalent form as equation 2.67 where:

$$F_{j+\frac{1}{2}} = \frac{1}{2}\left(F\left(U_j^n\right) + F\left(U_{j+1}^n\right)\right) - \frac{1}{2}\frac{\Delta x}{\Delta t} Q_{j+\frac{1}{2}}\left(U_{j+1}^n - U_j^n\right) \tag{3.6}$$

$Q_{j+\frac{1}{2}}$ is the viscosity matrix and could be written in the form of:

$$Q_{j+\frac{1}{2}} = \frac{1}{2} I - 2\left(\frac{\Delta t}{\Delta x}\right)^2 \hat{C}_{j+\frac{1}{2}} \hat{B}_{j+\frac{1}{2}} \tag{3.7}$$

where

$$B = \frac{\partial G}{\partial u} \tag{3.8}$$

and $\hat{B}$ is the Roe average of the Jacobian of G and could be simply derived as:

$$\hat{B}_{j+\frac{1}{2}}\left(U_{j+1}^n - U_j^n\right) = G\left(U_{j+1}^n\right) - G\left(U_j^n\right) \tag{3.9}$$

With respect to flux splitting, the scheme could be written in an alternative way as:

$$\tilde{U}_{j+\frac{1}{2}} = \frac{1}{2}\left(U_j^n + U_{j+1}^n\right) - \frac{\Delta t}{\Delta x}\left(G\left(U_{j+1}^n\right) - G\left(U_j^n\right)\right) \tag{3.10}$$

$$U_j^{n+1} = \frac{1}{2}\left(\widetilde{U}_{j-\frac{1}{2}} + \widetilde{U}_{j+\frac{1}{2}}\right) - \frac{\Delta t}{\Delta x}\left(H_{j+\frac{1}{2}} - H_{j-\frac{1}{2}}\right) \quad 3.11$$

where

$$H_{j+\frac{1}{2}} = \frac{1}{2}\left(H\left(U_j^n\right) + H\left(U_{j+1}^n\right)\right) - \frac{\Delta t}{\Delta x}\hat{C}_{j+\frac{1}{2}}\hat{B}_{j+\frac{1}{2}}\left(U_{j+1}^n - U_j^n\right) \quad 3.12$$

3.2.2 Scheme formulation – Implicit

The implicit formulation could be derived simply by considering the next timestep (n+1) in the numerical discretization instead of the current timestep (n). The formulation then would be in the following form:

$$\widetilde{U}_{j+\frac{1}{2}} = \frac{1}{2}\left(U_j^n + U_{j+1}^n\right) - \frac{\Delta t}{\Delta x}\left(G\left(U_{j+1}^{n+1}\right) - G\left(U_j^{n+1}\right)\right) \quad 3.13$$

$$U_j^{n+1} = \frac{1}{2}\left(\widetilde{U}_{j-\frac{1}{2}} + \widetilde{U}_{j+\frac{1}{2}}\right) - \frac{\Delta t}{\Delta x}\left(H_{j+\frac{1}{2}} - H_{j-\frac{1}{2}}\right) \quad 3.14$$

where

$$H_{j+\frac{1}{2}} = \frac{1}{2}\left(H\left(U_j^n\right) + H\left(U_{j+1}^n\right)\right) - \frac{\Delta t}{\Delta x}\hat{C}_{j+\frac{1}{2}}\hat{B}_{j+\frac{1}{2}}\left(U_{j+1}^{n+1} - U_j^{n+1}\right) \quad 3.15$$

We note that the equations should be solved as a coupled system.

3.2.3 Isothermal Euler model

The isothermal Euler model could be written as a system of mass and momentum conservation equations 1.3 and 1.4 with the pressure given as

$$p = a^2\rho \quad , \quad a = constant \quad 3.16$$

Given equation 3.3 the explicit scheme can be derived directly from the equation and the implicit scheme would be in the following form:

$$\rho_j^{n+1} = \frac{1}{4}\left(\rho_{j-1}^n + 2\rho_j^n + \rho_{j+1}^n\right) - \frac{\Delta t}{2\Delta x}\left((\rho v)_{j+1}^{n+1} - (\rho v)_{j-1}^{n+1}\right) \quad 3.17$$

$$\tilde{p}_{j+\frac{1}{2}} = \frac{1}{2}\left(p_j^n + p_{j+1}^n\right) - \frac{\Delta t}{\Delta x}a^2\left((\rho v)_{j+1}^{n+1} - (\rho v)_j^{n+1}\right) \quad 3.18$$

$$(\rho v)_j^{n+1} = \frac{1}{4}\left((\rho v)_{j-1}^n + 2(\rho v)_j^n + (\rho v)_{j+1}^n\right) - \frac{\Delta t}{2\Delta x}\left((\rho v^2)_{j+1}^{n+1} - (\rho v^2)_{j-1}^{n+1}\right) - \frac{\Delta t}{\Delta x}\left(\tilde{p}_{j+\frac{1}{2}} - \tilde{p}_{j-\frac{1}{2}}\right) \quad 3.19$$

It should be noted that the scheme above is linear in the mass flux but nonlinearly implicit in the convective momentum flux. To get a linear flux discretization in the implicit form we will substitute $(\rho v^2)_j^{n+1}$ with $(\rho v^2)_j^n$.

3.3 Pressure-Velocity coupling

In this section, we acquire a conservative scheme using a two-step method referred to as predictor-corrector as an alternative formulation of the X-Force scheme. Using the predictor-corrector version of X-Force scheme it is plausible to linearize the equations directly.

3.3.1 Pressure evolution equation

From the conservation of mass equation 1.1 and equation 3.16 we derive the pressure evolution equation:

$$\frac{\partial \rho}{\partial t} + \frac{\rho \partial (v) + v\partial \rho}{\partial x} = 0 \quad , \quad \partial \rho = a^2 \partial p \quad 3.20$$

$$\frac{1}{a^2}\frac{\partial p}{\partial t} + \rho\frac{\partial v}{\partial x} + \frac{v}{a^2}\frac{\partial p}{\partial x} = 0$$

$$\frac{\partial p}{\partial t} + \rho a^2\frac{\partial v}{\partial x} + v\frac{\partial \rho}{\partial x} = 0$$

3.3.2 Velocity evolution equation

Similar to the pressure evolution equation we can derive the equation of velocity evolution from the momentum conservation equation:

$$\frac{\partial(\rho v)}{\partial t}+\frac{\partial}{\partial x}(\rho v.v+p)=0 \qquad 3.21$$

$$\frac{\rho\partial v+v\partial\rho}{\partial t}+\frac{v\partial(\rho v)+\rho v\partial v}{\partial x}+\frac{\partial p}{\partial x}=0$$

$$\rho\frac{\partial v}{\partial t}+\rho v\frac{\partial v}{\partial x}+\frac{\partial p}{\partial x}+v\left(\frac{\partial\rho}{\partial t}+\frac{\partial(\rho v)}{\partial x}\right)=0$$

$$\rho\frac{\partial v}{\partial t}+\rho v\frac{\partial v}{\partial x}+\frac{\partial p}{\partial x}=0$$

$$\frac{\partial v}{\partial t}+v\frac{\partial v}{\partial x}+\frac{1}{\rho}\frac{\partial p}{\partial x}=0$$

3.4 Non-conservative formulation

Following the general non-conservative system in the form of equation 2.5 we split the Jacobian matrix into two different matrices corresponding to convective and pressure fluxes, similar to equation 3.2:

$$A(u)=B(u)+C(u) \qquad 3.22$$

where $B(u)$ and $C(u)$ point to $G(u)$ flux and $H(u)$ flux respectively as we have discussed them in section 3.2. Cell averages would also be defined as:

$$\hat{B}_{j+\frac{1}{2}}=\hat{B}\left(U_j^n,U_{j+1}^n\right) \qquad 3.23$$

$$\hat{C}_{j+\frac{1}{2}}=\hat{C}\left(U_j^n,U_{j+1}^n\right) \qquad 3.24$$

3.4.1 Scheme formulation - Explicit

Following equations 3.10 and 3.11 a two-step method could be written for the non-conservative formulation:

$$\widetilde{U}_{j+\frac{1}{2}} = \frac{1}{2}\left(U_j^n + U_{j+1}^n\right) - \frac{\Delta t}{\Delta x}\hat{B}_{j+\frac{1}{2}}\left(U_{j+1}^n - U_j^n\right) \quad 3.25$$

$$U_j^{n+1} = \frac{1}{2}\left(\widetilde{U}_{j-\frac{1}{2}} + \widetilde{U}_{j+\frac{1}{2}}\right) - \frac{\Delta t}{\Delta x}\left(\hat{C}_{j+\frac{1}{2}}\left(\widetilde{U}_{j+\frac{1}{2}} - U_j^n\right) + \hat{C}_{j-\frac{1}{2}}\left(U_j^n - \widetilde{U}_{j-\frac{1}{2}}\right)\right) \quad 3.26$$

3.4.2 Scheme formulation – Implicit

Similar to section 3.3.2, the implicit formulation is derived as the following coupled equations:

$$\widetilde{U}_{j+\frac{1}{2}} = \frac{1}{2}\left(U_j^n + U_{j+1}^n\right) - \frac{\Delta t}{\Delta x}\hat{B}_{j+\frac{1}{2}}\left(U_{j+1}^{n+1} - U_j^{n+1}\right) \quad 3.27$$

$$U_j^{n+1} = \frac{1}{2}\left(\widetilde{U}_{j-\frac{1}{2}} + \widetilde{U}_{j+\frac{1}{2}}\right) - \frac{\Delta t}{\Delta x}\left(\hat{C}_{j+\frac{1}{2}}\left(\widetilde{U}_{j+\frac{1}{2}} - U_j^n\right) + \hat{C}_{j-\frac{1}{2}}\left(U_j^n - \widetilde{U}_{j-\frac{1}{2}}\right)\right) \quad 3.28$$

3.5 Predictor-Corrector approach

In the predictor-corrector approach of X-Force scheme, we linearize the scheme in a different set of variables $w(u)$ in order to solve the problem incorporating variables u, through a conservative prospect. Concerning equation 2.5 the conservation equation could be written for $w(u)$ as:

$$\frac{\partial w}{\partial t} + M(w)\frac{\partial w}{\partial x} = 0 \quad 3.29$$

where

$$M\left(w(u)\right) = \frac{\partial w}{\partial u}A(u)\frac{\partial u}{\partial w} \quad 3.30$$

Similar to 3.28 we split the Jacobian matrix as:

$$M = R + T \quad 3.31$$

where

$$R = \frac{\partial w}{\partial u} B \frac{\partial u}{\partial w} \qquad 3.32$$

$$T = \frac{\partial w}{\partial u} C \frac{\partial u}{\partial w}$$

Similar to equations 3.27 and 3.28 we solve equation 3.29 with respect to the new state variable $\widetilde{W}_j^n$ and write the predictor and use the state variable as input to the implicit fluxes to obtain corrector steps:

3.5.1 Predictor step

$$\widetilde{W}_{j+\frac{1}{2}} = \frac{1}{2}\left(W_j^n + W_{j+1}^n\right) - \frac{\Delta t}{\Delta x}\hat{R}_{j+\frac{1}{2}}\left(W_{j+1}^{n+1} - W_j^{n+1}\right) \qquad 3.33$$

$$\widetilde{W}_j^{n+1} = \frac{1}{2}\left(\widetilde{W}_{j-\frac{1}{2}} + \widetilde{W}_{j+\frac{1}{2}}\right) - \frac{\Delta t}{\Delta x}\left(\hat{T}_{j+\frac{1}{2}}\left(\widetilde{W}_{j+\frac{1}{2}} - W_j^n\right) + \tilde{T}_{j-\frac{1}{2}}\left(W_j^n - \widetilde{W}_{j-\frac{1}{2}}\right)\right) \qquad 3.34$$

3.5.2 Corrector step

3.5.2.1 Conservative form

$$\widetilde{U}_{j+\frac{1}{2}} = \frac{1}{2}\left(U_j^n + U_{j+1}^n\right) - \frac{\Delta t}{\Delta x}\left(G\left(\widetilde{U}_{j+1}^{n+1}\right) - G\left(\widetilde{U}_j^{n+1}\right)\right) \qquad 3.35$$

$$U_j^{n+1} = \frac{1}{2}\left(\widetilde{U}_{j-\frac{1}{2}} + \widetilde{U}_{j+\frac{1}{2}}\right) - \frac{\Delta t}{\Delta x}\left(H_{j+\frac{1}{2}} - H_{j-\frac{1}{2}}\right) \qquad 3.36$$

$$H_{j+\frac{1}{2}} = H\left(\widetilde{W}_{j+\frac{1}{2}}\right) \qquad 3.37$$

3.5.2.2 Non-conservative form

$$\widetilde{U}_{j+\frac{1}{2}} = \frac{1}{2}\left(U_j^n + U_{j+1}^n\right) - \frac{\Delta t}{\Delta x}\hat{B}_{j+\frac{1}{2}}\left(\widetilde{U}_{j+1}^{n+1} - \widetilde{U}_j^{n+1}\right) \qquad 3.38$$

$$U_j^{n+1} = \frac{1}{2}\left(\widetilde{U}_{j-\frac{1}{2}} + \widetilde{U}_{j+\frac{1}{2}}\right) - \frac{\Delta t}{\Delta x}\left(\hat{C}_{j+\frac{1}{2}}\left(\widetilde{U}_{j+\frac{1}{2}} - U_j^n\right) + \hat{C}_{j-\frac{1}{2}}\left(U_j^n - \widetilde{U}_{j-\frac{1}{2}}\right)\right) \quad 3.39$$

3.6 Application of Predictor-Corrector approach on Isothermal Euler model

Concerning the Isothermal Euler model, we can rewrite the equations in terms of primitive variables as follows:

$$w = \begin{pmatrix} p \\ v \end{pmatrix} \quad 3.40$$

$$\frac{\partial u}{\partial w} = \begin{pmatrix} a^{-2} & 0 \\ v.a^{-2} & \rho \end{pmatrix} \quad 3.41$$

$$\frac{\partial w}{\partial u} = \begin{pmatrix} a^2 & 0 \\ \frac{-v}{\rho} & 1/\rho \end{pmatrix} \quad 3.42$$

Then we can calculate R and T matrices from equation 3.32:

$$R = \begin{pmatrix} v & \rho a^2 \\ 0 & v \end{pmatrix} \quad 3.43$$

$$T = \begin{pmatrix} 0 & 0 \\ \frac{1}{\rho} & 0 \end{pmatrix}$$

Finally, the predictor step for Isothermal Euler model would be derived as:

$$p_j^{n+1} = \frac{1}{2}\left(p_{j-\frac{1}{2}}^{n+1} + p_{j+\frac{1}{2}}^{n+1}\right) \quad 3.44$$

where

$$\tilde{p}_{j+\frac{1}{2}} = \frac{1}{2}\left(p_j^n + p_{j+1}^n\right) - \frac{\Delta t}{\Delta x} v_{j+\frac{1}{2}}^n \left(\tilde{p}_{j+1}^{n+1} - \tilde{p}_j^{n+1}\right) - \frac{\Delta t}{\Delta x}[\rho a^2]_{j+\frac{1}{2}}^n \left(\tilde{v}_{j+1}^{n+1} - \tilde{v}_j^{n+1}\right) \quad 3.45$$

$$\tilde{p}_{j-\frac{1}{2}} = \frac{1}{2}\left(p_{j-1}^{n} + p_{j}^{n}\right) - \frac{\Delta t}{\Delta x} v_{j-\frac{1}{2}}^{n}\left(\tilde{p}_{j}^{n+1} - \tilde{p}_{j-1}^{n+1}\right) - \frac{\Delta t}{\Delta x}[\rho a^2]_{j-\frac{1}{2}}^{n}\left(\tilde{v}_{j}^{n+1} - \tilde{v}_{j-1}^{n+1}\right)$$

and

$$\tilde{v}_{j}^{n+1} = \frac{1}{2}\left(\tilde{v}_{j-\frac{1}{2}} + \tilde{v}_{j+\frac{1}{2}}\right) - \frac{1}{\rho_{j+\frac{1}{2}}^{n}}\frac{\Delta t}{\Delta x}\left(\tilde{p}_{j+\frac{1}{2}} - p_{j}^{n}\right) - \frac{1}{\rho_{j-\frac{1}{2}}^{n}}\frac{\Delta t}{\Delta x}\left(p_{j}^{n} - \tilde{p}_{j-\frac{1}{2}}\right) \quad 3.46$$

where

$$\tilde{v}_{j+\frac{1}{2}} = \frac{1}{2}\left(v_{j}^{n} + v_{j+1}^{n}\right) - \frac{\Delta t}{\Delta x}.v_{j+\frac{1}{2}}^{n}\left(v_{j+1}^{n+1} - v_{j}^{n+1}\right) \quad 3.47$$

$$\tilde{v}_{j-\frac{1}{2}} = \frac{1}{2}\left(v_{j-1}^{n} + v_{j}^{n}\right) - \frac{\Delta t}{\Delta x}.v_{j-\frac{1}{2}}^{n}\left(v_{j}^{n+1} - v_{j-1}^{n+1}\right)$$

And the average values calculated as:

$$v_{j+\frac{1}{2}}^{n} = \frac{1}{2}\left(v_{j}^{n} + v_{j+1}^{n}\right) \quad 3.48$$

$$\rho_{j+\frac{1}{2}}^{n} = \frac{1}{2}\left(\rho_{j}^{n} + \rho_{j+1}^{n}\right) \quad 3.49$$

And in the corrector step we have:

$$\tilde{U}_{j+\frac{1}{2}} = \frac{1}{2}\left(U_{j} + U_{j+1}\right) - \frac{\Delta t}{\Delta x}\left(\tilde{G}_{j+1} - \tilde{G}_{j}\right) \quad 3.50$$

$$U_{j}^{n+1} = \frac{1}{2}\left(\tilde{U}_{j-\frac{1}{2}} + \tilde{U}_{j+\frac{1}{2}}\right) - \frac{\Delta t}{\Delta x}\left(\tilde{H}_{j+\frac{1}{2}} - \tilde{H}_{j-\frac{1}{2}}\right) \quad 3.51$$

where

$$\tilde{G}_{j} = \begin{pmatrix} \tilde{\rho}_{j}^{n+1}\tilde{v}_{j}^{n+1} \\ \tilde{\rho}_{j}^{n+1}\left(\tilde{v}_{j}^{n+1}\right)^2 \end{pmatrix} \quad 3.52$$

$$\widetilde{H}_{j+\frac{1}{2}} = \begin{pmatrix} 0 \\ \tilde{p}_{j+\frac{1}{2}} \end{pmatrix}$$

Now we want to obtain the implicit matrices for solving Isothermal Euler model, defining some new variables to simplify the equation:

$$a = \frac{1}{2}\left(p_j^n + p_{j+1}^n\right) \qquad 3.53$$

$$b = \frac{\Delta t}{\Delta x} v^n_{j+\frac{1}{2}}$$

$$c = \frac{\Delta t}{\Delta x} [\rho a^2]^n_{j+\frac{1}{2}}$$

$$d = \frac{1}{2}\left(p_{j-1}^n + p_j^n\right)$$

$$e = \frac{\Delta t}{\Delta x} v^n_{j-\frac{1}{2}}$$

$$f = \frac{\Delta t}{\Delta x} [\rho a^2]^n_{j-\frac{1}{2}}$$

$$k = \frac{1}{2}\left(v_j^n + v_{j+1}^n\right)$$

$$l = \frac{\Delta t}{\Delta x} v^n_{j+\frac{1}{2}}$$

$$m = \frac{1}{2}\left(v_{j-1}^n + v_j^n\right)$$

$$n = \frac{\Delta t}{\Delta x} v^n_{j-\frac{1}{2}}$$

$$o = \frac{1}{\rho^n_{j+\frac{1}{2}}} \frac{\Delta t}{\Delta x}$$

$$p = \frac{1}{\rho^n_{j-\frac{1}{2}}} \frac{\Delta t}{\Delta x}$$

Then the equations 3.44, 3.45, 3.46 and 3.47 would be rewritten in the form of:

$$p_j^{n+1} = \frac{1}{2}\left(p_{j-\frac{1}{2}}^{n+1} + p_{j+\frac{1}{2}}^{n+1}\right) \tag{3.54}$$

$$p_{j+\frac{1}{2}}^{n+1} = a - b\left(p_{j+1}^{n+1} - p_j^{n+1}\right) - c\left(v_{j+1}^{n+1} - v_j^{n+1}\right)$$

$$p_{j-\frac{1}{2}}^{n+1} = d - e\left(p_j^{n+1} - p_{j-1}^{n+1}\right) - f\left(v_j^{n+1} - v_{j-1}^{n+1}\right)$$

$$v_j^{n+1} = \frac{1}{2}\left(v_{j-\frac{1}{2}}^{n+1} + v_{j+\frac{1}{2}}^{n+1}\right) - o.\left(p_{j+\frac{1}{2}}^{n+1} - p_j^n\right) - p.\left(p_j^n - p_{j-\frac{1}{2}}^{n+1}\right) \tag{3.55}$$

$$v_{j+\frac{1}{2}}^{n+1} = k - l\left(v_{j+1}^{n+1} - v_j^{n+1}\right)$$

$$v_{j-\frac{1}{2}}^{n+1} = m - n\left(v_j^{n+1} - v_{j-1}^{n+1}\right)$$

From equations 3.54 and 3.55 we would have:

$$p_j^{n+1} = \frac{1}{2}\left(p_{j-\frac{1}{2}}^{n+1} + p_{j+\frac{1}{2}}^{n+1}\right) \tag{3.56}$$

$$= \frac{1}{2}\Big(a - b\left(p_{j+1}^{n+1} - p_j^{n+1}\right) - c\left(v_{j+1}^{n+1} - v_j^{n+1}\right) + d - e\left(p_j^{n+1} - p_{j-1}^{n+1}\right) - f\left(v_j^{n+1} - v_{j-1}^{n+1}\right)\Big)$$

$$= \frac{1}{2}\left(a - bp_{j+1}^{n+1} + bp_j^{n+1} - cv_{j+1}^{n+1} + cv_j^{n+1} + d - ep_j^{n+1} + ep_{j-1}^{n+1} - fv_j^{n+1} + fv_{j-1}^{n+1}\right)$$

$$= \frac{1}{2}\left(a - bp_{j+1}^{n+1} + (b-e)p_j^{n+1} + ep_{j-1}^{n+1} - cv_{j+1}^{n+1} + fv_{j-1}^{n+1} + (c-f)v_j^{n+1} + d\right)$$

Reformatting equation 3.56 we obtain the final form of the pressure equation as:

$$-ep_{j-1}^{n+1} + (e - b + 2)p_j^{n+1} + bp_{j+1}^{n+1} - fv_{j-1}^{n+1} + (f-c)v_j^{n+1} + cv_{j+1}^{n+1} = a + d \tag{3.57}$$

Similarly, for velocity equation we have:

$$v_j^{n+1} = \frac{1}{2}\left(v_{j-\frac{1}{2}}^{n+1} + v_{j+\frac{1}{2}}^{n+1}\right) - o\left(p_{j+\frac{1}{2}}^{n+1} - p_j^n\right) - p\left(p_j^n - p_{j-\frac{1}{2}}^{n+1}\right) \quad 3.58$$

$$= \frac{1}{2}\left(k - l\left(v_{j+1}^{n+1} - v_j^{n+1}\right) + m - n\left(v_j^{n+1} - v_{j-1}^{n+1}\right)\right)$$
$$- o\left(a - b\left(p_{j+1}^{n+1} - p_j^{n+1}\right) - c\left(v_{j+1}^{n+1} - v_j^{n+1}\right) - p_j^n\right)$$
$$- p\left(p_j^n - \left(d - e\left(p_j^{n+1} - p_{j-1}^{n+1}\right) - f\left(v_j^{n+1} - v_{j-1}^{n+1}\right)\right)\right)$$

$$= \frac{1}{2}\left(k - lv_{j+1}^{n+1} + lv_j^{n+1} + m - nv_j^{n+1} + nv_{j-1}^{n+1}\right)$$
$$- o\left(a - bp_{j+1}^{n+1} + bp_j^{n+1} - cv_{j+1}^{n+1} + cv_j^{n+1} - p_j^n\right)$$
$$- p\left(p_j^n - d + ep_j^{n+1} - ep_{j-1}^{n+1} + fv_j^{n+1} - fv_{j-1}^{n+1}\right)$$

$$= \left(\frac{1}{2}k - \frac{1}{2}lv_{j+1}^{n+1} + \frac{1}{2}lv_j^{n+1} + \frac{1}{2}m - \frac{1}{2}nv_j^{n+1} + \frac{1}{2}nv_{j-1}^{n+1}\right) - oa + obp_{j+1}^{n+1}$$
$$- obp_j^{n+1} + ocv_{j+1}^{n+1} - ocv_j^{n+1} + op_j^n - pp_j^n + pd - pep_j^{n+1}$$
$$+ pep_{j-1}^{n+1} - pfv_j^{n+1} + pfv_{j-1}^{n+1}$$

$$= \left(-\frac{1}{2}l + oc\right)v_{j+1}^{n+1} + \left(\frac{1}{2}l - \frac{1}{2}n - oc - pf\right)v_j^{n+1} + \left(\frac{1}{2}n + pf\right)v_{j-1}^{n+1}$$
$$+ (-ob - pe)p_j^{n+1} + (ob)p_{j+1}^{n+1} + (pe)p_{j-1}^{n+1} + \frac{1}{2}k + \frac{1}{2}m - oa$$
$$+ pd + op_j^n - pp_j^n$$

Reformatting equation 3.58 we obtain the final form of velocity equation as:

$$\left(-\frac{1}{2}n - pf\right)v_{j-1}^{n+1} + \left(1 - \frac{1}{2}l + \frac{1}{2}n + oc + pf\right)v_j^{n+1} + \left(\frac{1}{2}l - oc\right)v_{j+1}^{n+1} \quad 3.59$$
$$- (pe)p_{j-1}^{n+1} + (ob + pe)p_j^{n+1} - (ob)p_{j+1}^{n+1}$$
$$= \frac{1}{2}k + \frac{1}{2}m - oa + pd + op_j^n - pp_j^n$$

To find the matrices we extend the equations for different grid numbers as:

j=1:

$$(e-b+2)p_1^{n+1}+bp_2^{n+1}+(f-c)v_1^{n+1}+cv_2^{n+1}=ep_0^{n+1}+fv_0^{n+1}+a+d \qquad 3.60a$$
$$+(1-\frac{1}{2}l+\frac{1}{2}n+oc+pf)v_1^{n+1}+(\frac{1}{2}l-oc)v_2^{n+1}+(ob+pe)p_1^{n+1}$$
$$-(ob)p_2^{n+1}$$
$$=\left(\frac{1}{2}n+pf\right)v_0^{n+1}+(pe)p_0^{n+1}+\frac{1}{2}k+\frac{1}{2}m-oa+pd+op_1^n$$
$$-pp_1^n$$

j=2:

$$-ep_1^{n+1}+(e-b+2)p_2^{n+1}+bp_3^{n+1}-fv_1^{n+1}+(f-c)v_2^{n+1}+cv_3^{n+1} \qquad 3.60b$$
$$=a+d$$
$$(-\frac{1}{2}n-pf)v_1^{n+1}+(1-\frac{1}{2}l+\frac{1}{2}n+oc+pf)v_2^{n+1}+(\frac{1}{2}l-oc)v_3^{n+1}$$
$$-(pe)p_1^{n+1}+(ob+pe)p_2^{n+1}-(ob)p_3^{n+1}$$
$$=\frac{1}{2}k+\frac{1}{2}m-oa+pd+op_2^n-pp_2^n$$

j=3:

$$-ep_2^{n+1}+(e-b+2)p_3^{n+1}+bp_4^{n+1}-fv_2^{n+1}+(f-c)v_3^{n+1}+cv_4^{n+1} \qquad 3.60c$$
$$=a+d$$
$$(-\frac{1}{2}n-pf)v_2^{n+1}+(1-\frac{1}{2}l+\frac{1}{2}n+oc+pf)v_3^{n+1}+(\frac{1}{2}l-oc)v_4^{n+1}$$
$$-(pe)p_2^{n+1}+(ob+pe)p_3^{n+1}-(ob)p_4^{n+1}$$
$$=\frac{1}{2}k+\frac{1}{2}m-oa+pd+op_3^n-pp_3^n$$

j=4:

$$-ep_3^{n+1} + (e - b + 2)p_4^{n+1} + bp_5^{n+1} - fv_3^{n+1} + (f - c)v_4^{n+1} + cv_5^{n+1} = a + d \quad 3.60d$$

$$(-\frac{1}{2}n - pf)v_3^{n+1} + (1 - \frac{1}{2}l + \frac{1}{2}n + oc + pf)v_4^{n+1} + (\frac{1}{2}l - oc)v_5^{n+1} - (pe)p_3^{n+1} + (ob + pe)p_4^{n+1} - (ob)p_5^{n+1} = \frac{1}{2}k + \frac{1}{2}m - oa + pd + op_4^n - pp_4^n$$

j=j:

$$-ep_{j-1}^{n+1} + (e - b + 2)p_j^{n+1} + bp_{j+1}^{n+1} - fv_{j-1}^{n+1} + (f - c)v_j^{n+1} + cv_{j+1}^{n+1} = a + d \quad 3.60e$$

$$(-\frac{1}{2}n - pf)v_{j-1}^{n+1} + (1 - \frac{1}{2}l + \frac{1}{2}n + oc + pf)v_j^{n+1} + (\frac{1}{2}l - oc)v_{j+1}^{n+1} - (pe)p_{j-1}^{n+1} + (ob + pe)p_j^{n+1} - (ob)p_{j+1}^{n+1} = \frac{1}{2}k + \frac{1}{2}m - oa + pd + op_j^n - pp_j^n$$

j=N:

$$-ep_{N-1}^{n+1} + (e - b + 2)p_N^{n+1} - fv_{N-1}^{n+1} + (f - c)v_N^{n+1} = -bp_{N+1}^{n+1} - cv_{N+1}^{n+1} + a + d \quad 3.60f$$

$$(-\frac{1}{2}n - pf)v_{N-1}^{n+1} + (1 - \frac{1}{2}l + \frac{1}{2}n + oc + pf)v_N^{n+1} - (pe)p_{N-1}^{n+1} + (ob + pe)p_N^{n+1} = \left(-\frac{1}{2}l + oc\right)v_{N+1}^{n+1} + (ob)p_{N+1}^{n+1} + \frac{1}{2}k + \frac{1}{2}m - oa + pd + op_N^n - pp_N^n$$

Concerning the samples written in 3.66a to 3.66f, we are able to derive the matrices as:

$$A\_up = \begin{bmatrix} e-b+2 & f-c & b & c & & & & & & & & \\ -e & -f & e-b+2 & f-c & b & c & & & & & & \\ & & -e & -f & e-b+2 & f-c & b & c & & & & \\ & & & & -e & -f & e-b+2 & f-c & b & c & & \\ & & & & & & & & \cdots & & & \\ & & & & & & & & -e & -f & e-b+2 & f-c \end{bmatrix} \quad 3.61$$

$$A_{down} = \begin{bmatrix} ob+pe & 1-\frac{1}{2}l+\frac{1}{2}n+oc+pf & -ob & \frac{1}{2}l-oc & & & & & & & & \\ -pe & -\frac{1}{2}n-pf & ob+pe & 1-\frac{1}{2}l+\frac{1}{2}n+oc+pf & -ob & \frac{1}{2}l-oc & & & & & & \\ & & -pe & -\frac{1}{2}n-pf & ob+pe & 1-\frac{1}{2}l+\frac{1}{2}n+oc+pf & -ob & \frac{1}{2}l-oc & & & & \\ & & & & & & & & \cdots & & & \\ & & & & & & -pe & -\frac{1}{2}n-pf & ob+pe & 1-\frac{1}{2}l+\frac{1}{2}n+oc+pf & & \end{bmatrix} \quad 3.62$$

$$A = \begin{bmatrix} A_{up} \\ A_{down} \end{bmatrix} \quad 3.63$$

$$X = \begin{bmatrix} p_1 \\ v_1 \\ p_2 \\ v\_2 \\ p_3 \\ v_3 \\ p_4 \\ v_4 \\ \cdots \\ p_N \\ v_N \end{bmatrix} \quad 3.64$$

$$B = \begin{bmatrix} ep_0^{n+1} + fv_0^{n+1} + a + d \\ a + d \\ a + d \\ \dots \\ bp_{N+1}^{n+1} + cv_{N+1}^{n+1} + a + d \\ \left(\frac{1}{2}n + pf\right)v_0^{n+1} + (pe)p_0^{n+1} + \frac{1}{2}k + \frac{1}{2}m - oa + pd + op_1^n - pp_1^n \\ \frac{1}{2}k + \frac{1}{2}m - oa + qd + op_2^n - pp_2^n \\ \frac{1}{2}k + \frac{1}{2}m - oa + qd + op_3^n - pp_3^n \\ \dots \\ \left(-\frac{1}{2}l + oc\right)v_{N+1}^{n+1} + (ob)p_{N+1}^{n+1} + \frac{1}{2}k + \frac{1}{2}m - oa + pd + op_N^n - pp_N^n \end{bmatrix} \quad 3.65$$

Solving matrix equation $AX = B$ we can calculate pressure and velocity at each grid cell. The result of the X-Force predictor-corrector scheme for the isothermal Euler model is plotted and verified with the exact solution by (Sahebi 2019). We have covered all different cases of two shock waves, two rarefaction waves, left shock and right rarefaction waves, left rarefaction and right shock waves. In addition, we have merged the graphs into a single plot after for a better illustration.

Test no.	v_L	v_R	ρ_L	ρ_R	γ	K
#1	1.5	-1.5	1	1	1.4	1
#2	-1	1	3	3	1.4	1
#3	0	0	2	1	1.4	1
#4	0	0	1	2	1.4	1

Table 1: Input data for validating X-Force predictor-corrector numerical scheme for the isothermal Euler model with the exact solution done by Hamed Sahebi (Sahebi 2019)

Test no.1

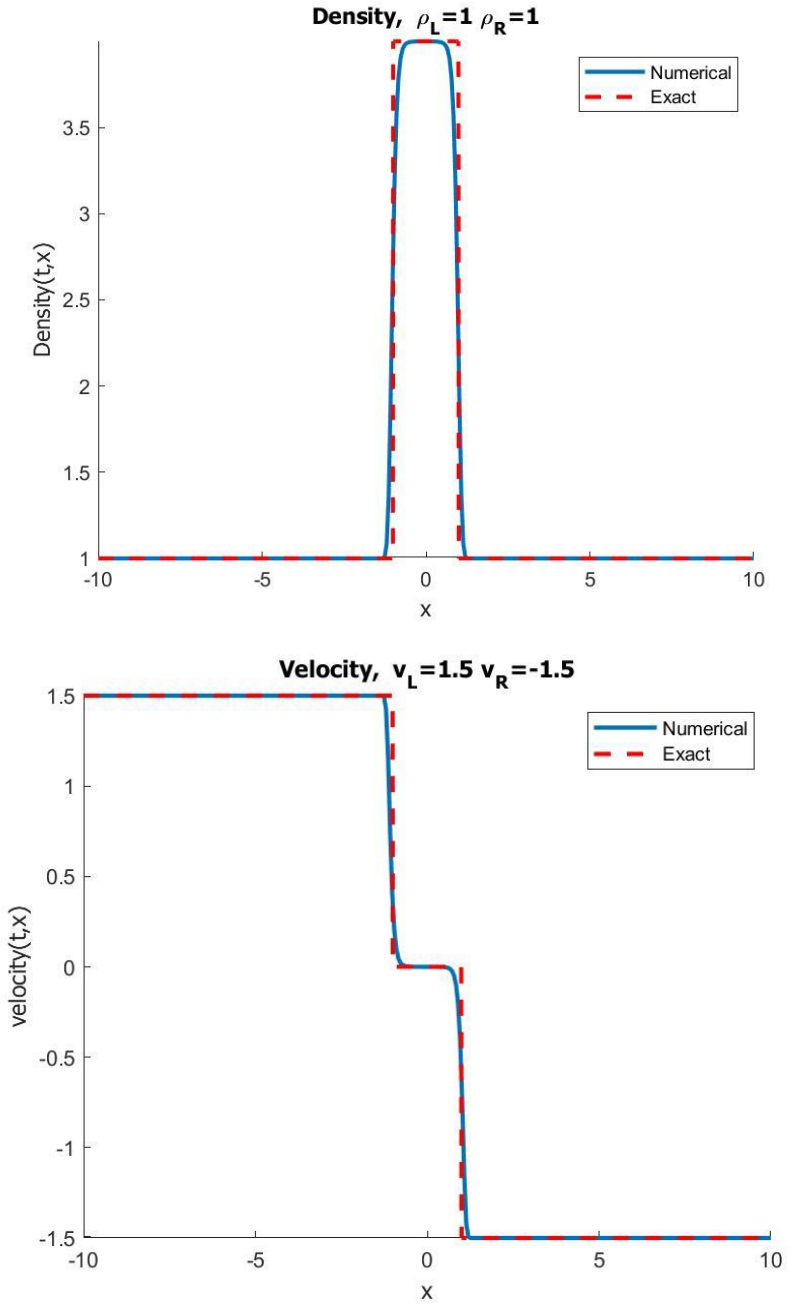

Figure 28: Solution of the Riemann problem for isothermal Euler model, A comparison between X-Force predictor-corrector numerical scheme with the exact solution formulated by (Sahebi 2019) for $\rho_L = 1, \rho_R = 1, v_L = 1.5, v_R = -1.5$, two shock wave case with $\Delta t = 0.01, \Delta x = 0.02$ at t=2

Test no.2

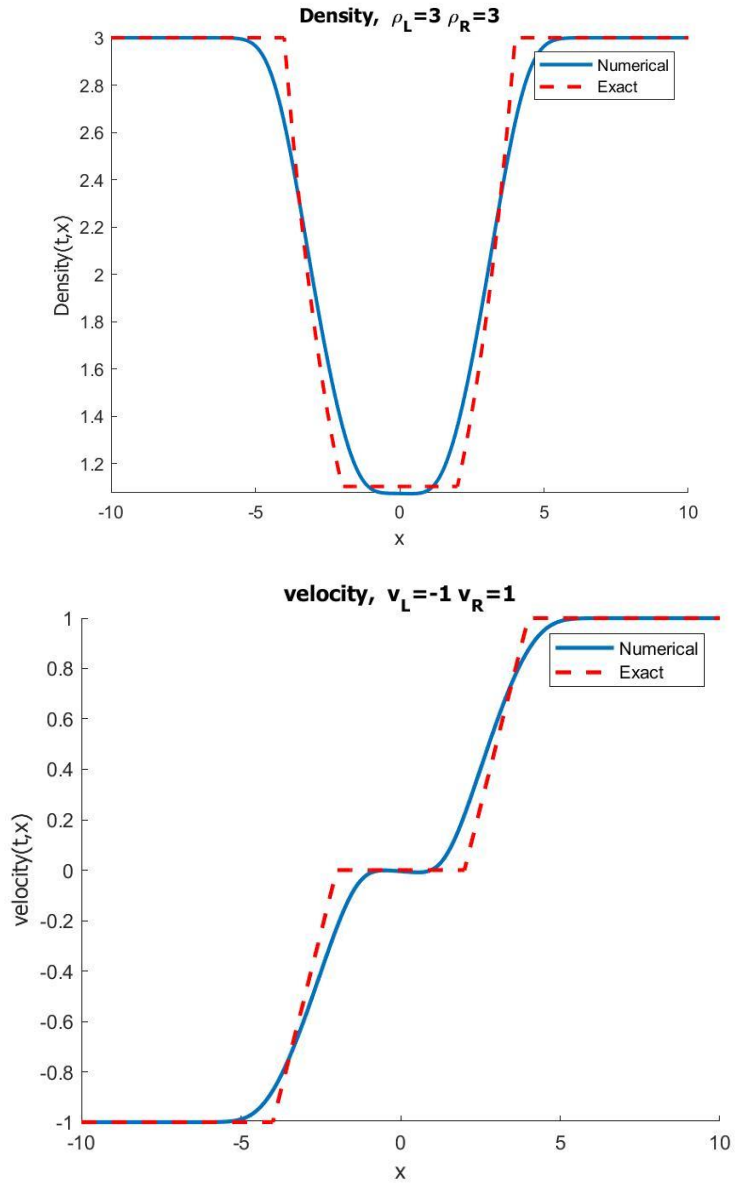

Figure 29: Solution of the Riemann problem for isothermal Euler model, A comparison between X-Force predictor-corrector numerical scheme with the exact solution formulated by (Sahebi 2019) for $\rho_L = 3, \rho_R = 3, v_L = -1, v_R = 1$, *two rarefaction wave case with* $\Delta t = 0.01, \Delta x = 0.02$ *at t=2*

Test no.3

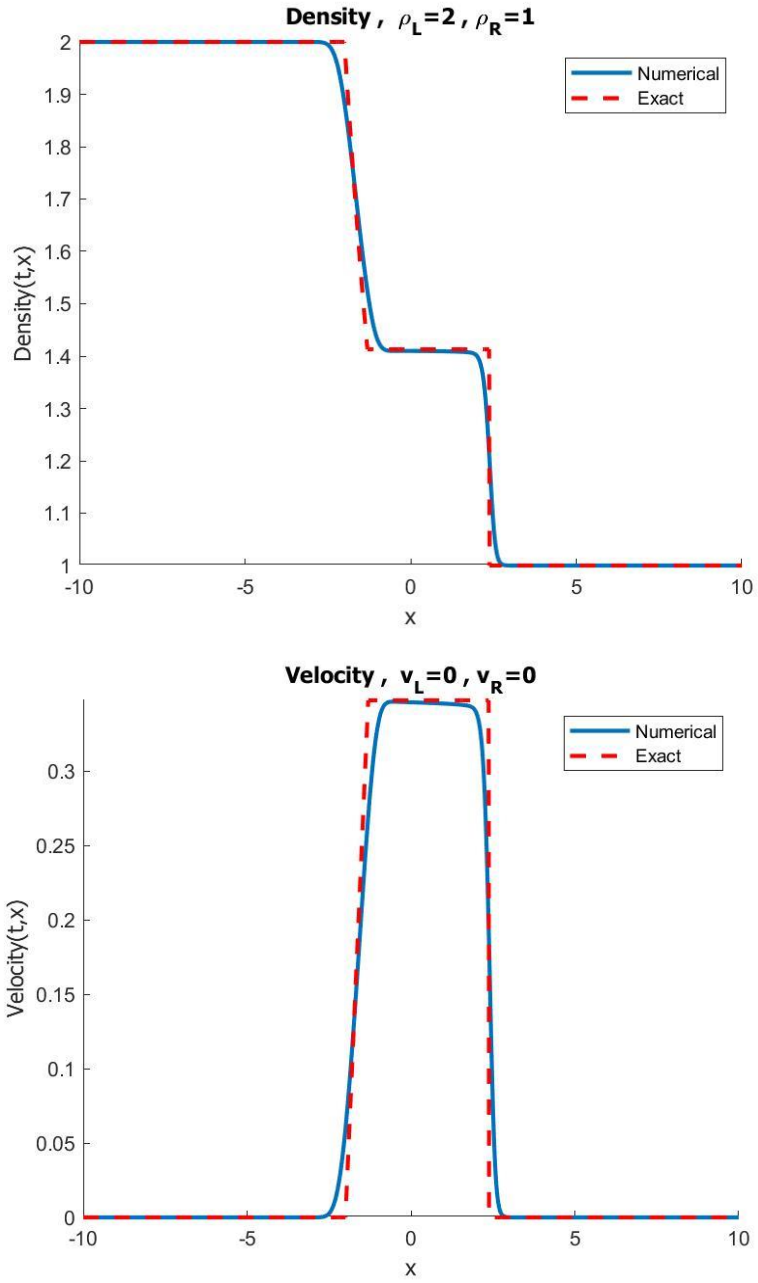

Figure 30: Solution of the Riemann problem for isothermal Euler model, A comparison between X-Force predictor-corrector numerical scheme with the exact solution formulated by (Sahebi 2019) for $\rho_L = 2, \rho_R = 1, v_L = 0, v_R = 0$, left rarefaction wave right shock wave case with $\Delta t = 0.01, \Delta x = 0.02$ at t=2

Test no.4

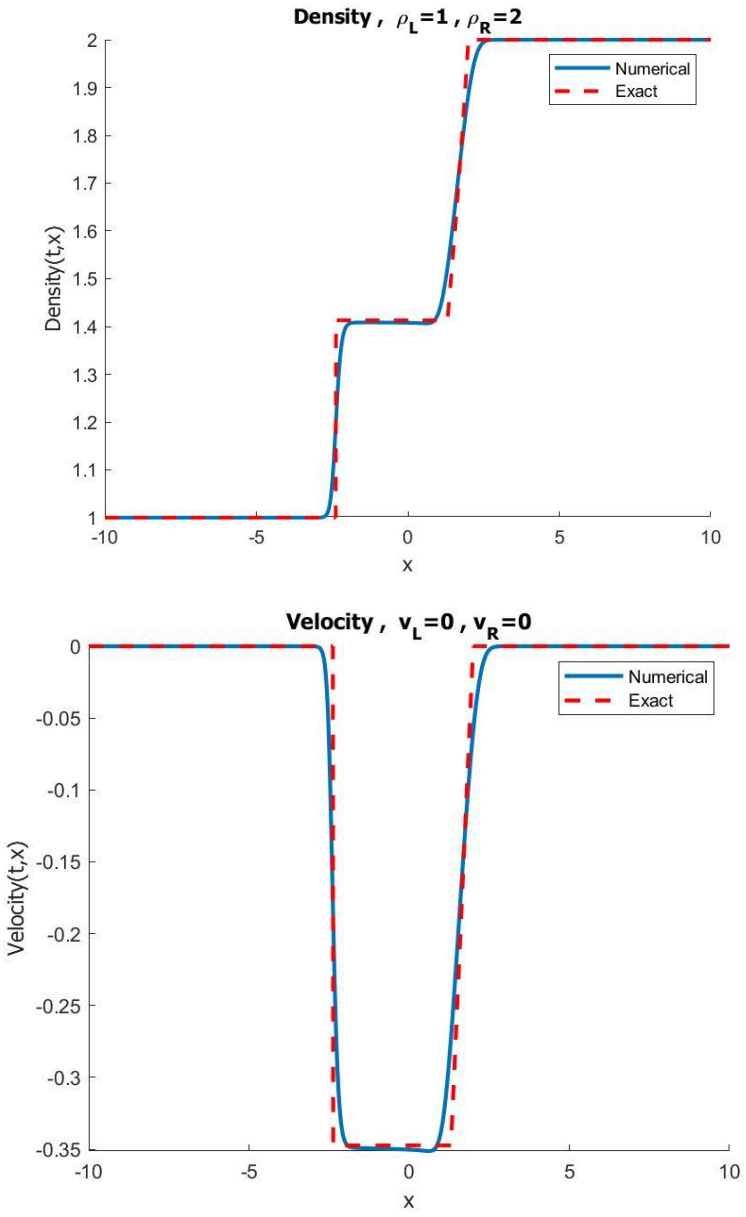

Figure 31: Solution of the Riemann problem for isothermal Euler model, A comparison between X-Force predictor-corrector numerical scheme with the exact solution formulated by (Sahebi 2019) for $\rho_L = 1, \rho_R = 2, v_L = 0, v_R = 0$, left shock wave right rarefaction wave case with $\Delta t = 0.01, \Delta x = 0.02$ at t=2

3.7 Full Euler equation

In this section, we apply the predictor-corrector scheme to full Euler equation. The pressure-velocity coupling will be solved in a matrix same as isothermal Euler model with some specifications as:

$$\tilde{\rho}_j^{n+1} = \rho_j^n + \frac{1}{[c^2]_j^n}\left(\tilde{p}_j^{n+1} - p_j^n\right) \tag{3.66}$$

where c corresponds to sound velocity and would be formulated as:

$$c^2 = \left(\frac{\partial p}{\partial \rho}\right)_s = \gamma \frac{p}{\rho} \tag{3.67}$$

And for the corrector step, the primitive and conserved sets of variables are:

$$\widetilde{W}_j^{n+1} = \begin{pmatrix} \tilde{\rho}_j^{n+1} \\ \tilde{p}_j^{n+1} \\ \tilde{v}_j^{n+1} \end{pmatrix} \tag{3.68}$$

$$\widetilde{U}_j^{n+1} = \begin{pmatrix} \tilde{\rho}_j^{n+1} \\ \tilde{\rho}_j^{n+1}\tilde{v}_j^{n+1} \\ \tilde{\rho}_j^{n+1}\tilde{e}_j^{n+1} + \frac{1}{2}\tilde{\rho}_j^{n+1}\left(\tilde{v}_j^{n+1}\right)^2 \end{pmatrix} \tag{3.69}$$

where

$$p = (\gamma - 1)\rho e \tag{3.70}$$

$$e = \frac{p}{\rho(\gamma - 1)}$$

The conservative update for full Euler equation would be derived as:

$$U_j^{n+1} = \frac{1}{4}\left(U_{j-1}^n + 2U_j^n + U_{j+1}^n\right) - \frac{1}{2}.\frac{\Delta t}{\Delta x}\left(\tilde{v}_{j+1}^{n+1}\tilde{U}_{j+1} - \tilde{v}_{j-1}^{n+1}\tilde{U}_{j-1}\right) - \frac{\Delta t}{\Delta x}\begin{pmatrix} 0 \\ \tilde{p}_{j+\frac{1}{2}} - \tilde{p}_{j-\frac{1}{2}} \\ \bar{v}_{j+\frac{1}{2}}\left(\tilde{p}_{j+\frac{1}{2}} - p_j^n\right) + \bar{v}_{j-\frac{1}{2}}\left(p_j^n - \tilde{p}_{j-\frac{1}{2}}\right) \end{pmatrix} - \frac{1}{2}.\frac{\Delta t}{\Delta x}\begin{pmatrix} 0 \\ 0 \\ \bar{p}_{j-\frac{1}{2}}\left(\tilde{v}_j^{n+1} - \tilde{v}_{j-1}^{n+1}\right) + \bar{p}_{j+\frac{1}{2}}\left(\tilde{v}_{j+1}^{n+1} - \tilde{v}_j^{n+1}\right) \end{pmatrix} \quad 3.71$$

where

$$\bar{v}_{j+\frac{1}{2}} = \frac{1}{2}\left(\tilde{v}_j^{n+1} + \tilde{v}_{j+1}^{n+1}\right) \quad 3.72$$

$$\bar{p}_{j+\frac{1}{2}} = \frac{1}{2}\left(p_j^n + p_{j+1}^n\right) \quad 3.73$$

3.8 Hybridizing with WIMF scheme

As the last part of the research, the aim is to hybridize the formulated predictor-corrector for full Euler equation with an explicit upwind scheme in order to increase the accuracy on the contact wave without interrupting the robust resolution of the pressure waves. Considering equation 3.71 we rewrite the equation and flux matrix as:

$$U_j^{n+1} = U_j^n + \frac{\Delta t}{\Delta x}\left(G_{j-\frac{1}{2}} - G_{j+\frac{1}{2}}\right) + pressure\ terms \quad 3.74$$

where

$$G^I = \frac{1}{2}\left(\tilde{v}_j\tilde{U}_j + \tilde{v}_{j+1}\tilde{U}_{j+1}\right) - \frac{1}{4}\frac{\Delta x}{\Delta t}.\left(U_{j+1}^n - U_j^n\right) \quad 3.75$$

In this section, we want to hybridize the flux G^I with a more accurate flux G^U while keeping stability:

$$G^U = \begin{cases} v_{j+\frac{1}{2}}.U_j & if \quad v_{j+\frac{1}{2}} > 0 \\ v_{j+\frac{1}{2}}.U_{j+1} & if\ v_{j+\frac{1}{2}} \leq 0 \end{cases} \tag{3.76}$$

The final flux would be given as:

$$G = M_1 G^I + M_2 G^U \tag{3.77}$$

where

$$M_1 = \left(\frac{\partial u}{\partial v}\right)_\mu \frac{\partial v}{\partial u} \tag{3.78}$$

$$M_2 = \left(\frac{\partial u}{\partial \mu}\right)_\nu \frac{\partial \mu}{\partial u} \tag{3.79}$$

Note that

$$M_1 + M_2 = I \tag{3.80}$$

As it is thoroughly discussed by (Evje, Flåtten et al. 2006) and (Munkejord, Evje et al. 2009) we split the state into two separate parts named $d\mu$ and dv connected to contact wave and pressure waves respectively.

$$dv = \begin{pmatrix} p \\ v \\ 0 \end{pmatrix} \tag{3.81}$$

$$d\mu = \begin{pmatrix} 0 \\ 0 \\ \rho T ds \end{pmatrix} = \begin{pmatrix} 0 \\ 0 \\ \rho de - \frac{p}{\rho}.d\rho \end{pmatrix} \tag{3.82}$$

Defining

$$h = e + \frac{p}{\rho} \tag{3.83}$$

We get $d\mu$ as:

$$d\mu = \begin{pmatrix} 0 \\ 0 \\ d(\rho e) - h d\rho \end{pmatrix} \quad 3.84$$

In terms of conserved variables, we have:

$$dp = \left(c^2 - \Gamma \frac{p}{\rho}\right) d\rho + \Gamma \rho de \quad 3.85$$

where Γ is the Grüneisen coefficient:

$$\Gamma = \frac{1}{\rho}\left(\frac{\partial \rho}{\partial e}\right)_{\rho} \quad 3.86$$

We have considered ideal gas in the numerical calculation. In this specific we have:

$$\Gamma = \gamma - 1 \quad 3.87$$

where γ is specific heat ratio given by:

$$\gamma = \frac{C_p}{C_v} \quad 3.88$$

where C_p and C_v are specific heat of gas in constant pressure and volume

We can rewrite equation 3.85 to obtain:

$$dp = (c^2 - \Gamma h) d\rho + \Gamma d(\rho e) \quad 3.89$$

As a reminder, we have conserved variables as:

$$u = \begin{pmatrix} u_1 \\ u_2 \\ u_3 \end{pmatrix} = \begin{pmatrix} \rho \\ \rho v \\ \frac{1}{2}\rho v^2 + \rho e \end{pmatrix} \quad 3.90$$

We can write in terms of the matrix u:

$$dv = \frac{1}{\rho}(du_2 - v du_1) \quad 3.91$$

$$d\left(\frac{1}{2}\rho v^2\right) = v du_2 - \frac{1}{2} v^2 du_1 \quad 3.92$$

$$d(\rho e) = \frac{1}{2}v^2 du_1 - v du_2 + du_3 \tag{3.93}$$

$$dp = \left(c^2 - \Gamma\left(h - \frac{1}{2}v^2\right)\right) du_1 - \Gamma v du_2 + \Gamma du_3 \tag{3.94}$$

And eventually we would obtain:

$$\frac{\partial \mu}{\partial u} = \begin{pmatrix} 0 & 0 & 0 \\ 0 & 0 & 0 \\ \frac{1}{2}v^2 & -v & 1 \end{pmatrix} \tag{3.95}$$

$$\frac{\partial \nu}{\partial u} = \begin{pmatrix} c^2 - \Gamma(h - \frac{1}{2}v^2) & -v\Gamma & \Gamma \\ \frac{-v}{\rho} & \frac{1}{\rho} & 0 \\ 0 & 0 & 0 \end{pmatrix} \tag{3.96}$$

$$\left(\frac{\partial \mu}{\partial u}\right)_\nu = \begin{pmatrix} 0 & 0 & -\Gamma c^{-2} \\ 0 & 0 & -v\Gamma c^{-2} \\ 0 & 0 & 1 - \Gamma\left(h + \frac{1}{2}v^2\right)c^{-2} \end{pmatrix} \tag{3.97}$$

$$\left(\frac{\partial \nu}{\partial u}\right)_\mu = \begin{pmatrix} c^{-2} & 0 & 0 \\ vc^{-2} & \rho & 0 \\ \left(h + \frac{1}{2}v^2\right)c^{-2} & \rho v & 0 \end{pmatrix} \tag{3.98}$$

Then we can get the new accurate fluxes as:

$$\left(\frac{\partial u}{\partial \mu}\right)_v \frac{\partial \mu}{\partial u} \qquad 3.99$$

$$= \frac{1}{c^2}\begin{pmatrix} \Gamma(h-\frac{1}{2}v^2) & \Gamma v & -\Gamma \\ v\Gamma(h-\frac{1}{2}v^2) & \Gamma v^2 & -\Gamma v \\ \left(h-\frac{1}{2}v^2\right)\left(\Gamma\left(h+\frac{1}{2}v^2\right)-c^2\right) & v\left(\Gamma\left(h+\frac{1}{2}v^2\right)-c^2\right) & c^2-\Gamma\left(h+\frac{1}{2}v^2\right) \end{pmatrix}$$

$$\left(\frac{\partial u}{\partial v}\right)_\mu \frac{\partial v}{\partial u} \qquad 3.100$$

$$= \frac{1}{c^2}\begin{pmatrix} c^2-\Gamma\left(h-\frac{1}{2}v^2\right) & -\Gamma v & \Gamma \\ -v\Gamma\left(h-\frac{1}{2}v^2\right) & c^2-\Gamma v^2 & \Gamma v \\ \left(c^2-\Gamma\left(h+\frac{1}{2}v^2\right)\right)\left(h-\frac{1}{2}v^2\right) & v\left(c^2-\Gamma\left(h+\frac{1}{2}v^2\right)\right) & \Gamma\left(h+\frac{1}{2}v^2\right) \end{pmatrix}$$

For illustrating the accuracy of the updated flux derived from WIMF method we compare the result of the WIMF scheme with X-Force predictor-corrector scheme over 10 different timesteps showing how the numerical schemes will behave with respect to stability and accuracy. In specific we use constant boundary values for velocity and pressure and a jump in density. As it can be shown by the solution of the WIMF scheme, density will move over timesteps and reach the exact solution in case of $\Delta t = \frac{\Delta x}{v}$. The simulation is done with $\Delta x = 0.12$ at $t = 2$.

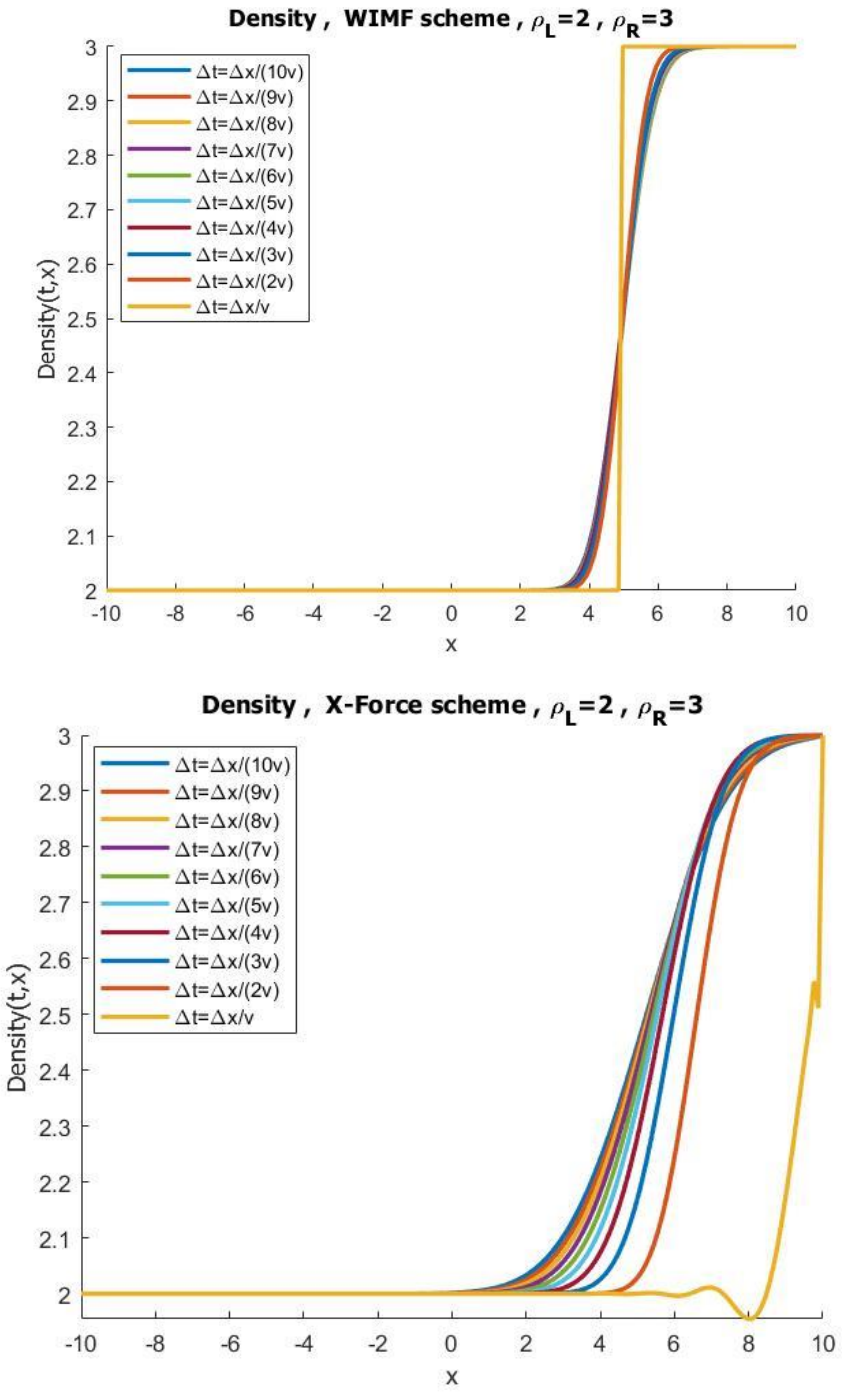

Figure 32: A comparison between WIMF scheme and X-Force scheme over different timesteps with constant velocity $v = 2.5$ and constant pressure $p = 2$ with $\Delta x = 0.12$ at $t = 2$

4 Results and discussion

The work of this thesis is split into several parts to gradually build up the way to formulate the X-Force predictor-corrector numerical scheme. In this section, the result of the numerical scheme is presented and verified with other studies.

4.1 Numerical solution assessment

In this section, we validate the results of X-Force predictor-corrector scheme for full Euler equation with Riemann initial conditions, generated from a computer code written with MATLAB, with two separate studies.

- Analytical exact solution done in a master thesis by Hamed Sahebi (Sahebi 2019).
- Toro's five test problem (Toro 2013).

4.1.1 Validation with an analytical exact solution

To better show the numerical simulation code results, four different tests have been introduced to indicate the solutions of full Euler model for different Riemann initial conditions over a grid system with $\Delta t = 0.025$ and $\Delta x = 0.05$ after 2 seconds. The tests are validated with analytical solution done in a master thesis by H. Sahebi. (Sahebi 2019). The test cases indicate all situations of two shockwaves, two rarefaction waves, left shock wave and right rarefaction wave and right shock wave and left rarefaction wave. Input data are mentioned in the following table:

Test no.	v_L	v_R	p_L	p_R	ρ_L	ρ_R	γ	K
#1	1.5	-1.5	2	2.1	1	1.2	1.4	1
#2	-1	1	2.5	2	3	3.5	1.4	1
#3	0	0	4	2.5	3	2	1.4	1
#4	0	0	2.5	4	2	3	1.4	1

Table 2: Input data for validating numerical scheme for the full Euler model with the exact solution done by Hamed Sahebi (Sahebi 2019)

Test no.1:

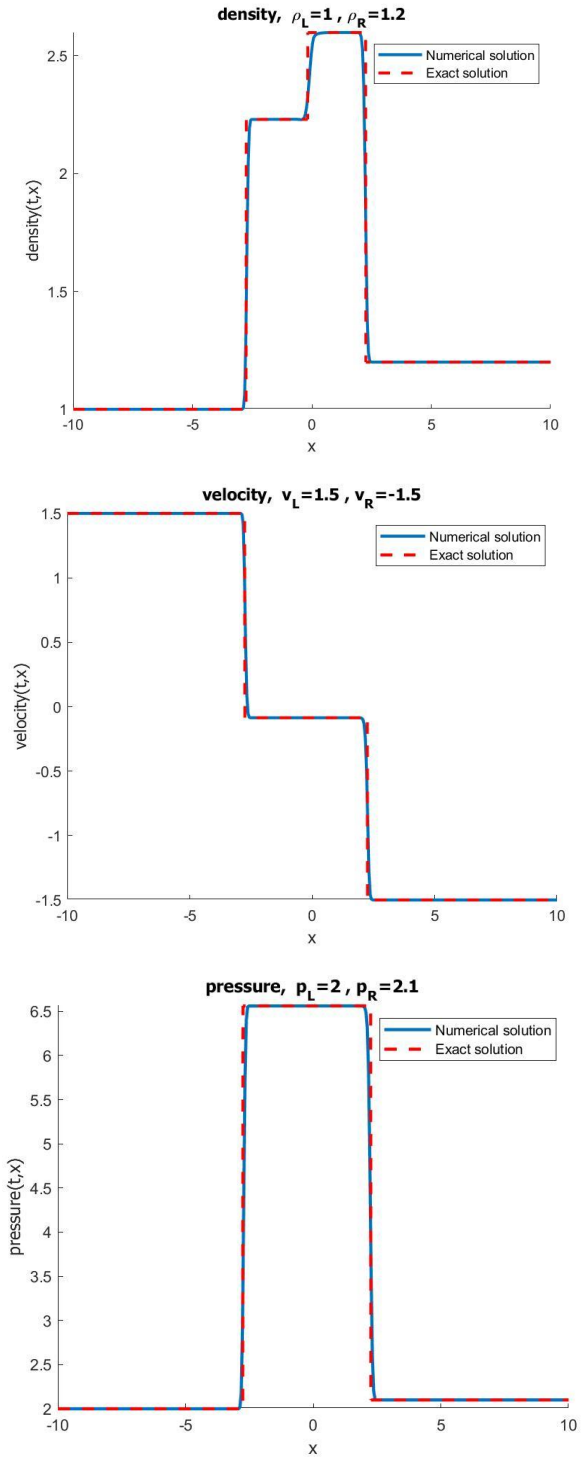

Figure 33: Solution of the Riemann problem for the full Euler model, A comparison between the WIMF numerical scheme with the exact solution formulated by (Sahebi 2019) for $v_L = 1.5, v_R = -1.5, p_L = 2, p_R = 2.1, \rho_L = 1, \rho_R = 1.2$*, two shock waves case with* $\Delta t = 0.005, \Delta x = 0.025$ *at t=2*

Test no.2:

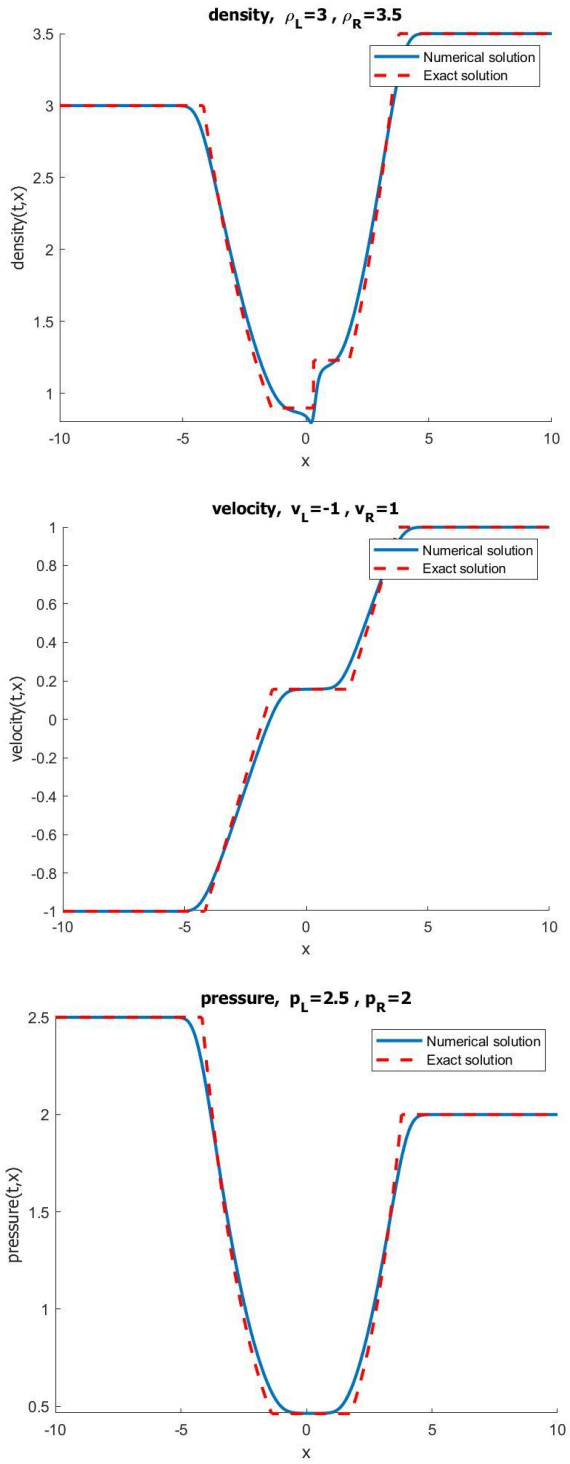

Figure 34: Solution of the Riemann problem for the full Euler model, A comparison between the WIMF numerical scheme with the exact solution formulated by (Sahebi 2019) for $v_L = -1, v_R = 1, p_L = 2.5, p_R = 2, \rho_L = 3, \rho_R = 3.5$*, two rarefaction waves case with* $\Delta t = 0.005, \Delta x = 0.025$ *at t=2*

Test no.3:

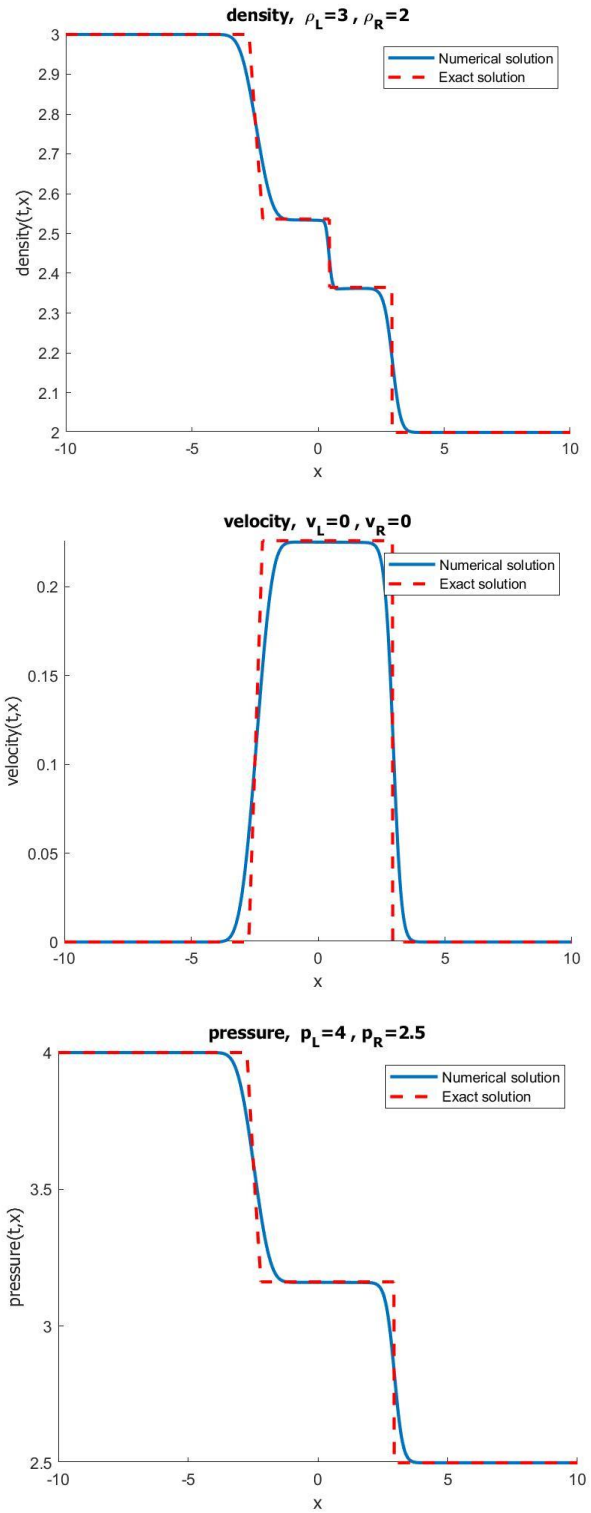

Figure 35: Solution of the Riemann problem for the full Euler model, A comparison between the WIMF numerical scheme with the exact solution formulated by (Sahebi 2019) for $v_L = 0, v_R = 0, p_L = 4, p_R = 2.5, \rho_L = 3, \rho_R = 2$, left rarefaction right shock wave case with $\Delta t = 0.005, \Delta x = 0.025$ at t=2

Test no.4:

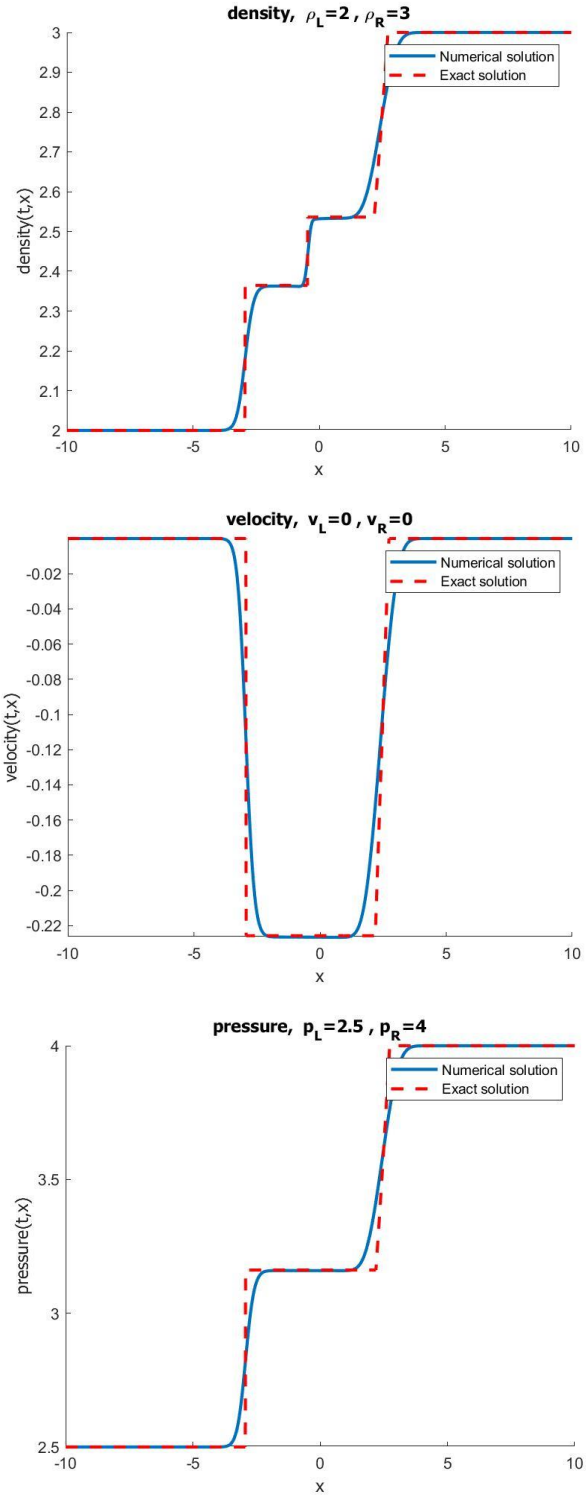

Figure 36: Solution of the Riemann problem for the full Euler model, A comparison between the WIMF numerical scheme with the exact solution formulated by (Sahebi 2019) for $v_L = 0, v_R = 0, p_L = 2.5, p_R = 4, \rho_L = 2, \rho_R = 3$, left shock right rarefaction wave case with $\Delta t = 0.005, \Delta x = 0.025$ at t=2

4.1.2 Validation with Toro's five tests problem

In this section, we investigate Toro's five test problem proposed by (Toro 2013). Toro practiced five different Riemann problems to perform a test of accuracy and robustness. Input parameters are mentioned in the following table.

Test	v_L	v_R	p_L	p_R	ρ_L	ρ_R
#1	0	0	1	0.1	1	0.125
#2	-2	2	0.4	0.4	1	1
#3	0	0	1000	0.01	1	1
#4	0	0	0.01	100	1	1
#5	19.5975	-6.19633	460.894	46.095	5.99924	5.99242

Table 3: input data for Toro's five test problem

Test no.1:

This test is also called Sod test problem (Sod 1978). The solution of this case includes left sonic rarefaction, a contact and right travelling shockwave and the solution show entropy satisfaction. The results indicating density, velocity and pressure are plotted with X-Force predictor-corrector scheme and verified with Toro's analytical solution.

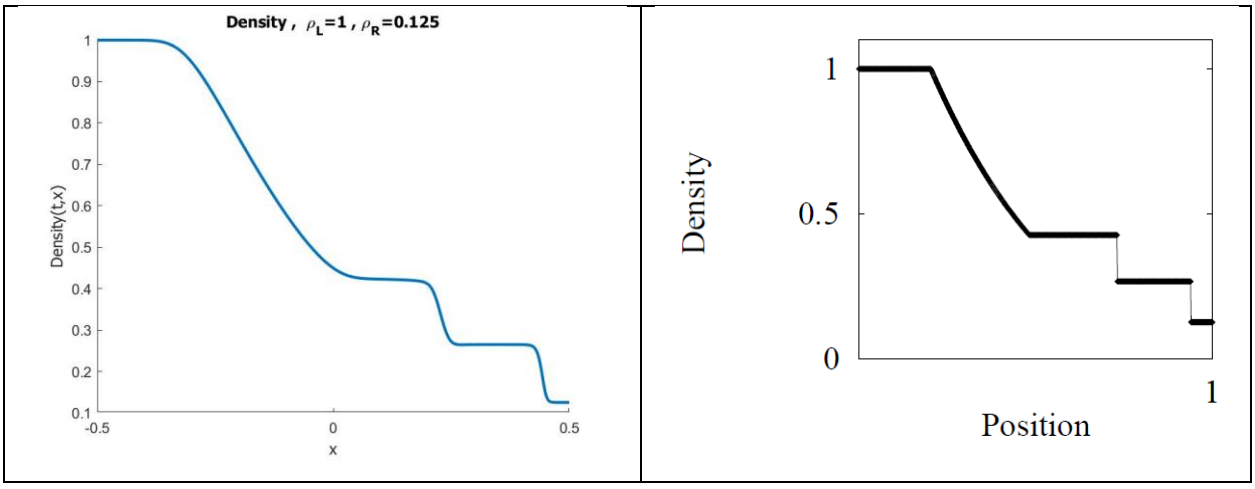

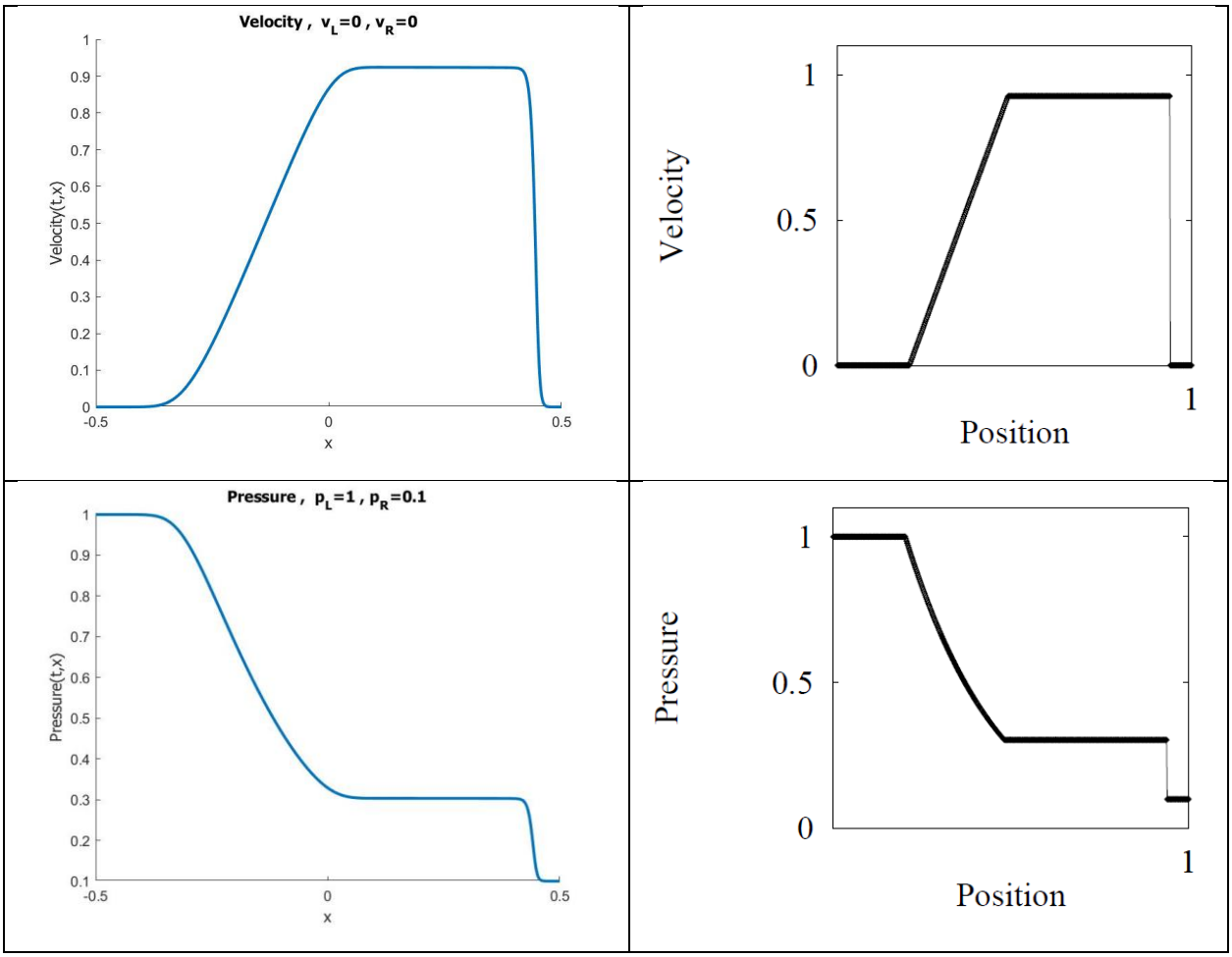

Figure 37: Solution of WIMF scheme (left plots) for $v_L = 0, v_R = 0, p_L = 1, p_R = 0.1, \rho_L = 1, \rho_R = 0.125$ with $\Delta t = 0.0001, \Delta x = 0.001$ after $t = 0.25$ and comparison with Toro's test no.1 (right plots)

Test no.2

This test is called 123 problem, which a near vacuum is created in the middle of the tube. The solution consists of two strong rarefaction waves and a slight contact discontinuity. This test is suitable for entropy violation testing in addition to evaluating the performance of numerical schemes where flow density is relatively low. While this test is quite challenging in the matter of stability the result for density, velocity and pressure is generated using the X-Force predictor-corrector scheme and verified with the analytical solution of Toro. (Toro 2013)

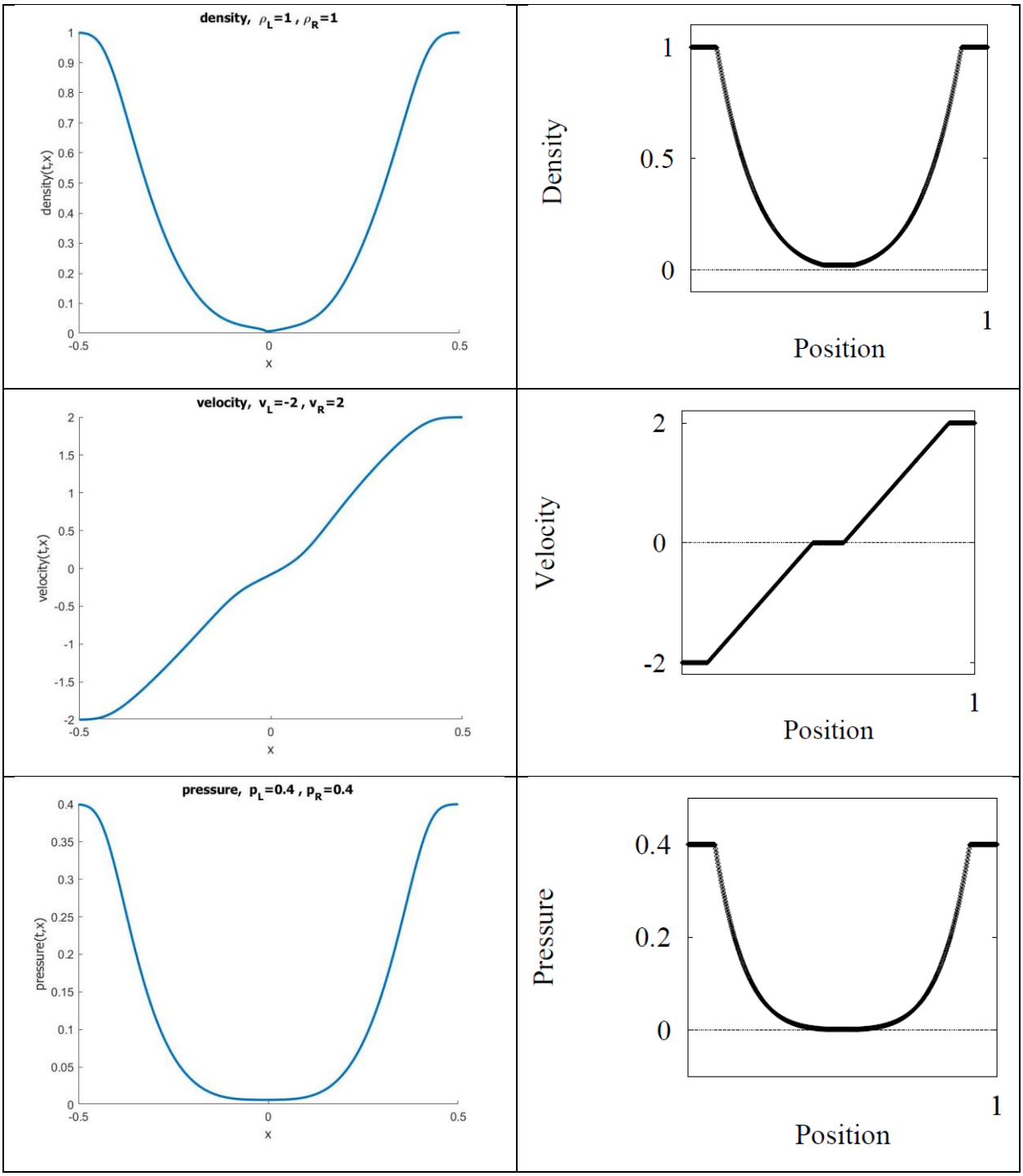

Figure 38: : Solution of WIMF scheme (left plots) for $v_L = -2, v_R = 2, p_L = 0.4, p_R = 0.4, \rho_L = 1, \rho_R = 1$ *with* $\Delta t = 0.0001, \Delta x = 0.001$ *after* $t = 0.15$ *and comparison with Toro's test no.2 (right plots)*

Test no.3:

This test is left half of the blast wave problem investigated by (Woodward and Colella 1984). The solution includes left rarefaction, a contact discontinuity and a right shock wave. The results for density, velocity and pressure are plotted and verified with Toro's solution.

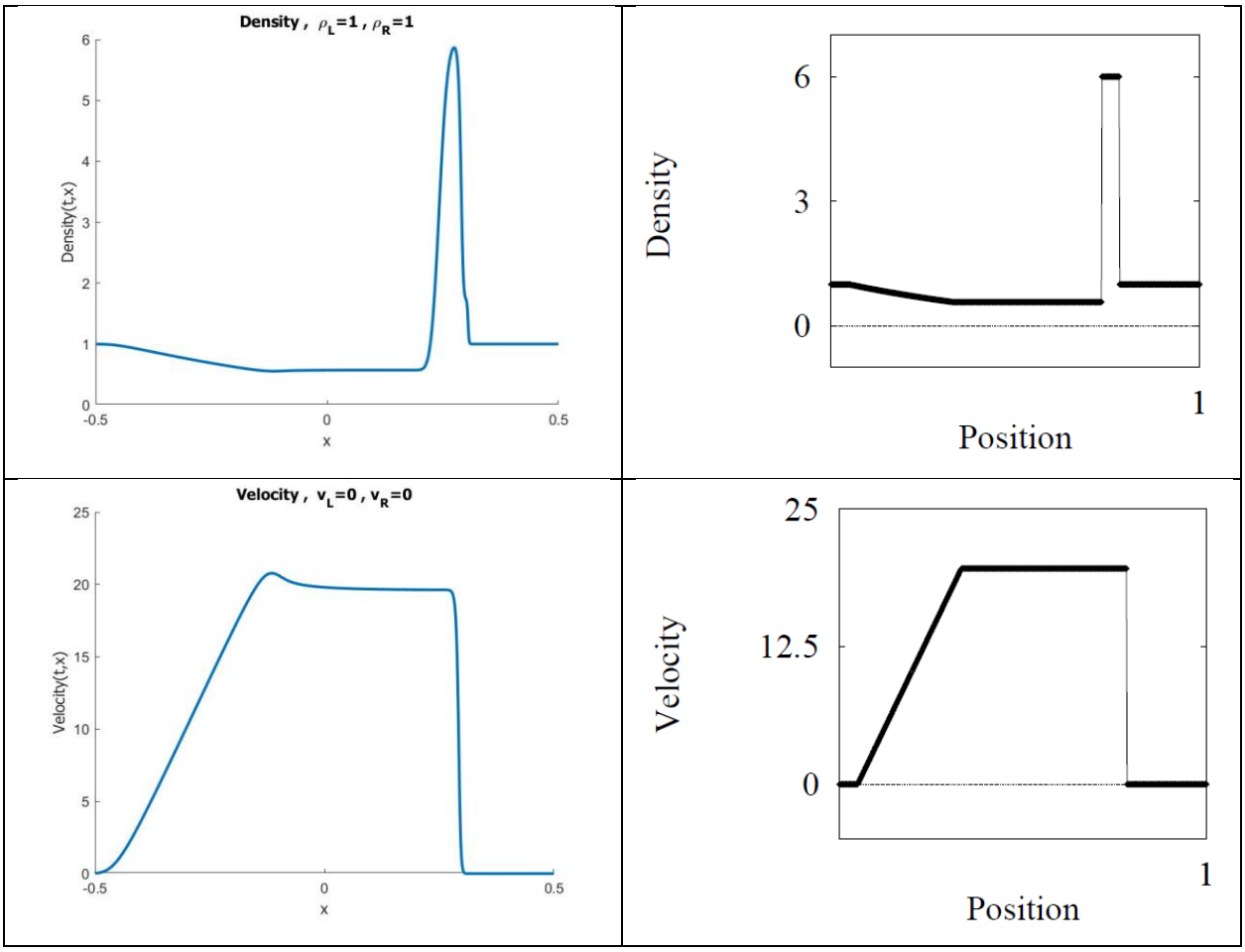

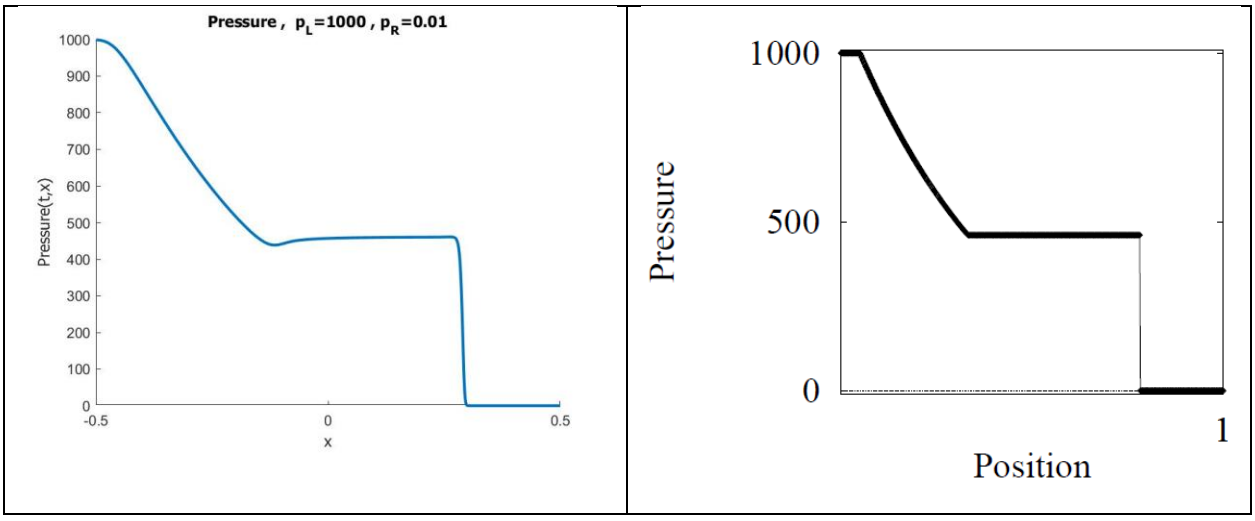

Figure 39: : Solution of WIMF scheme (left plots) for $v_L = 0, v_R = 0, p_L = 1000, p_R = 0.01, \rho_L = 1, \rho_R = 1$ with $\Delta t = 0.00001, \Delta x = 0.001$ after $t = 0.012$ and comparison with Toro's test no.3 (right plots)

Test no.4

This test is the right half of the blast wave problem studied by (Woodward and Colella 1984). The solution includes a left shockwave, a contact and a right rarefaction wave. The result could not be generated as a stable numerical solution.

Test no.5

This test includes strong shock waves in left and right appearing from the solution of tests 3 and 4 respectively. Left facing shock moves to the right with a very slow speed. The solution demonstrates the collision of these two waves. The solution for density, velocity and pressure is plotted using the X-Force predictor-corrector scheme and verified with Toro's solution.

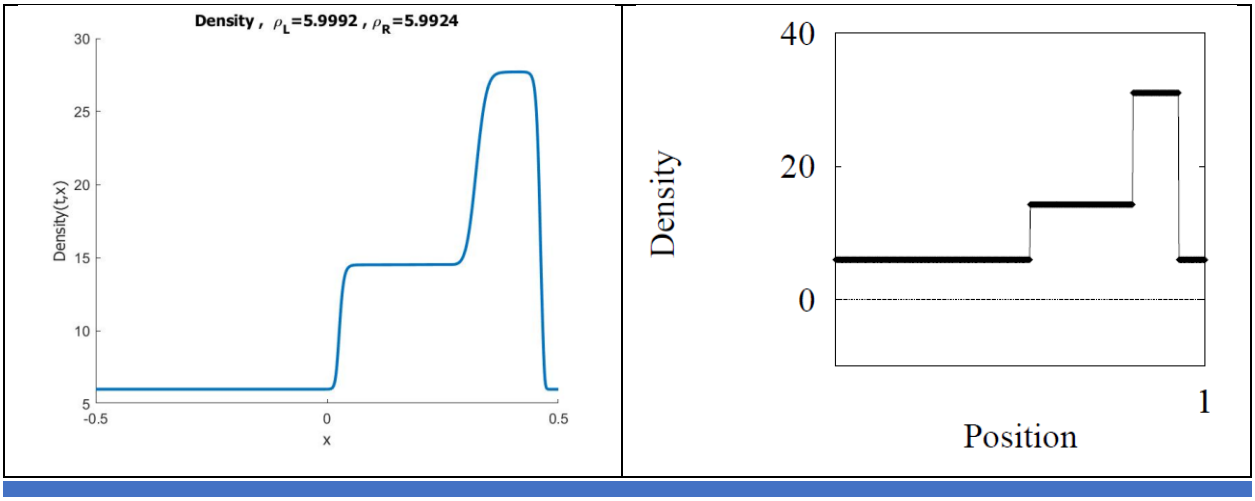

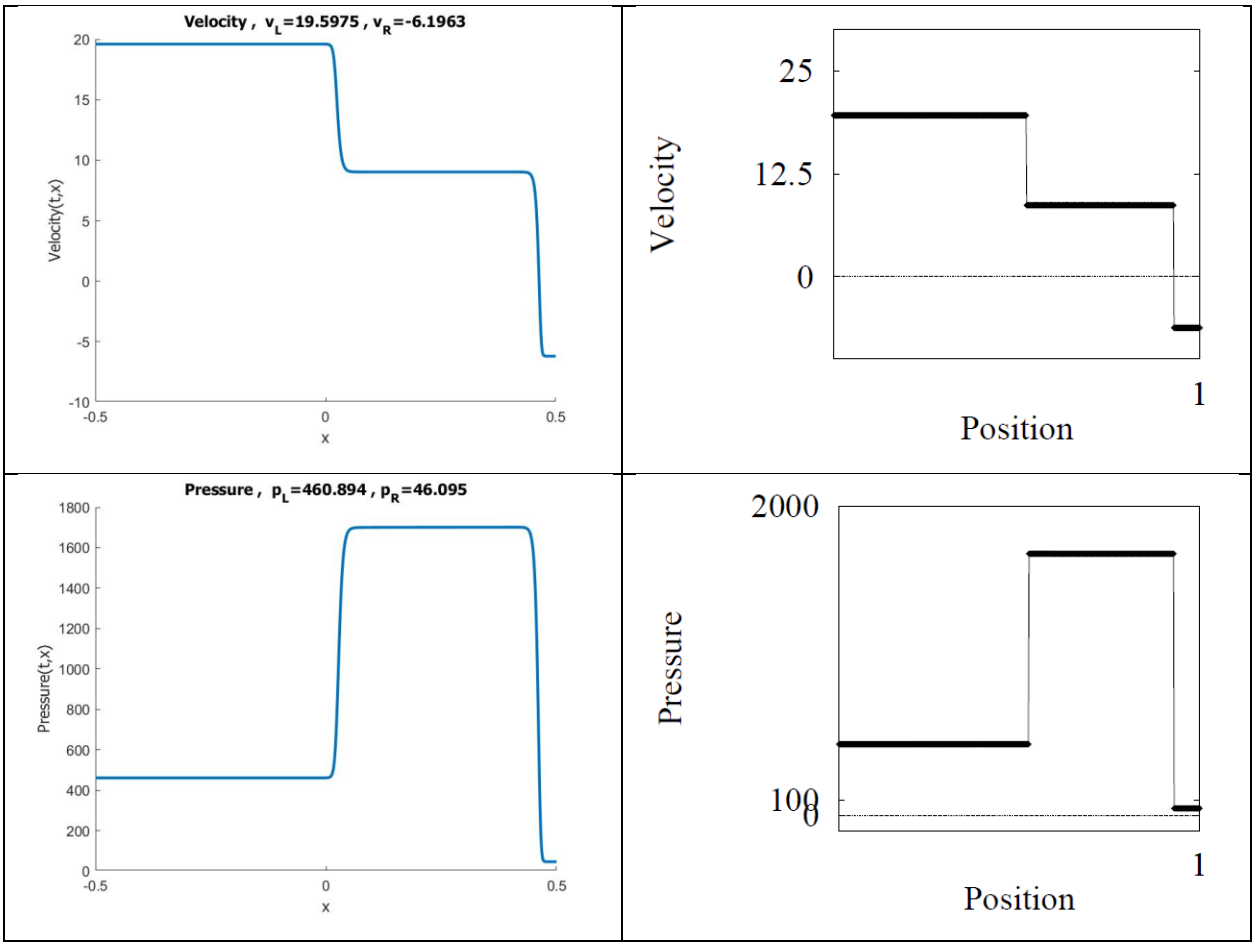

Figure 40: Solution of WIMF scheme (left plots) for $v_L = 19.5975, v_R = -6.19633, p_L = 460.894, p_R = 46.095, \rho_L = 5.99924, \rho_R = 5.99242$ *with* $\Delta t = 0.00001, \Delta x = 0.0001$ *after* $t = 0.035$ *and comparison with Toro's test no.5 (right plots)*

4.2 Conclusions and future prospects

In this thesis, we have formulated and coded the numerical scheme named X-Force predictor-corrector proposed by Tore Flåtten and Trygve Wangensteen as an unpublished work in collaboration with TechnipFMC. The important achievement of the thesis is a fundamental understanding of the characteristic behaviour of flow dynamics and the numerical analysis as well as coding challenges. The scheme is developed to solve any problem, but in the thesis, we have focused on the Riemann initial condition for better representation of the solution. The way of developing X-Force predictor-corrector scheme has been built up gradually from linear hyperbolic equations, nonlinear hyperbolic equations and isothermal and full Euler equations as a set of nonlinear hyperbolic conservation laws. The gradual buildup of the problem will help the reader obtain a better viewpoint and understand the problem more easily in both mathematics and

computer vision. All the steps are formulated and coded with MATLAB as part of the thesis. The numerical solution of the full Euler model as the final result of the thesis is generated through the computer code and verified with an analytical exact solution by Hamed Sahebi (Sahebi 2019) and Toro's five test problem (Toro 2013).

The contents of this thesis are dedicated to a contribution to previous studies on Weakly Implicit Mixture Flux model developed by Evje and Flåtten (Evje and Flåtten 2005) in order to extend the study to full Euler model by incorporating conservation of energy equations. We have formulated the numerical model with two considerations:

- We have only one phase flow as an ideal gas
- The numerical scheme is formulated in one dimension

However the current study is applicable in the simulation of gas dynamics in well and pipelines, concerning the considerations mentioned above, we have formulated the model as the first step of more complex research on multiphase-phase flow modelling and further extension could be pursued on drift-flux model.

5 References

Andrianov, N. and G. Warnecke (2004). "The Riemann problem for the Baer–Nunziato two-phase flow model." Journal of Computational Physics **195**(2): 434-464.

Bressan, A. (2013). Hyperbolic conservation laws: an illustrated tutorial. Modelling and optimisation of flows on networks, Springer**:** 157-245.

Evje, S. and T. Flåtten (2005). "CFL-Violating Numerical Schemes for a Two-Fluid Model." Journal of Scientific Computing **29**(1): 83-114.

Evje, S. and T. Flåtten (2005). "Weakly Implicit Numerical Schemes for a Two-Fluid Model." SIAM Journal on Scientific Computing **26**(5): 1449-1484.

Evje, S., et al. (2008). "On a relation between pressure-based schemes and central schemes for hyperbolic conservation laws." Numerical Methods for Partial Differential Equations **24**(2): 605-645.

Evje, S., et al. (2006). "A WIMF scheme for the drift-flux two-phase flow model."

Faille, I. and E. Heintzé (1999). "A rough finite volume scheme for modeling two-phase flow in a pipeline." Computers & Fluids **28**(2): 213-241.

Flåtten, T. (2019). "personal communication."

Harlow, F. H. and J. E. Welch (1965). "Numerical Calculation of Time-Dependent Viscous Incompressible Flow of Fluid with Free Surface." Physics of Fluids **8**(12).

Khouider, B. (2008). "Finite difference and finite volume methods for transport and conservation laws." PIMS summer school on stochastic and probabilistic methods for athmosphere, ocean, and dynamics.

LeVeque, R. J. (2002). Finite volume methods for hyperbolic problems, Cambridge university press.

Masella, J., et al. (1998). "Transient simulation of two-phase flows in pipes." International Journal of Multiphase Flow **24**(5): 739-755.

Meier, H., et al. (1999). "Comparison between staggered and collocated grids in the finite-volume method performance for single and multi-phase flows." Computers & chemical engineering **23**(3): 247-262.

Meyers, R. A. (2011). Mathematics of complexity and dynamical systems, Springer Science & Business Media.

Munkejord, S. T., et al. (2009). "A MUSTA Scheme for a Nonconservative Two-Fluid Model." SIAM Journal on Scientific Computing **31**(4): 2587-2622.

Novozhilov, A. S. "The linear transport equation." University lecture, North Dakota State University.

Ransom, V. and D. Hicks (1988). "Hyperbolic two-pressure models for two-phase flow revisited." Journal of Computational Physics **75**(2): 498-504.

Reis, G., et al. (2015). "A compact finite differences exact projection method for the Navier–Stokes equations on a staggered grid with fourth-order spatial precision." Computers & Fluids **118**: 19-31.

Sahebi, H. (2019). "Riemann problem for two-phase flow drift flux model." A master thesis project, University of Stavanger, UiS.

Salih, A. (2015). "Inviscid Burgers' Equation." A university lecture, Indian Institute of Space Science and Technology.

Sod, G. A. (1978). "A survey of several finite difference methods for systems of nonlinear hyperbolic conservation laws." Journal of Computational Physics **27**(1): 1-31.

Tadmor, E. (1984). "Numerical viscosity and the entropy condition for conservative difference schemes." Mathematics of Computation **43**(168): 369-381.

Toro, E. F. (2013). Riemann solvers and numerical methods for fluid dynamics: a practical introduction, Springer Science & Business Media.

Van Leer, B. (1979). "Towards the ultimate conservative difference scheme. V. A second-order sequel to Godunov's method." Journal of Computational Physics **32**(1): 101-136.

Wallis, G. B. (1969). "One-dimensional two-phase flow."

Woodward, P. and P. Colella (1984). "The numerical simulation of two-dimensional fluid flow with strong shocks." Journal of Computational Physics **54**(1): 115-173.

Zeidan, D. (2011). "The Riemann problem for a hyperbolic model of two-phase flow in conservative form." International Journal of Computational Fluid Dynamics **25**(6): 299-318.

Zeidan, D., et al. (2007). "Numerical study of wave propagation in compressible two-phase flow." International Journal for Numerical Methods in Fluids **54**(4): 393-417.

Годунов, С. К. (1959). "Разностный метод численного расчета разрывных решений уравнений гидродинамики." Математический сборник **47**(3): 271-306.